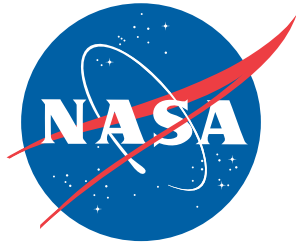


NASA/TM-2013-217995/Volume I  
NESC-RP-12-00822



# Probing Aircraft Flight Test Hazard Mitigation for the Alternative Fuel Effects on Contrails & Cruise Emissions (ACCESS) Research Team

*Michael J. Kelly/NESC  
Langley Research Center, Hampton, Virginia*

## NASA STI Program . . . in Profile

Since its founding, NASA has been dedicated to the advancement of aeronautics and space science. The NASA scientific and technical information (STI) program plays a key part in helping NASA maintain this important role.

The NASA STI program operates under the auspices of the Agency Chief Information Officer. It collects, organizes, provides for archiving, and disseminates NASA's STI. The NASA STI program provides access to the NASA Aeronautics and Space Database and its public interface, the NASA Technical Report Server, thus providing one of the largest collections of aeronautical and space science STI in the world. Results are published in both non-NASA channels and by NASA in the NASA STI Report Series, which includes the following report types:

- **TECHNICAL PUBLICATION.** Reports of completed research or a major significant phase of research that present the results of NASA Programs and include extensive data or theoretical analysis. Includes compilations of significant scientific and technical data and information deemed to be of continuing reference value. NASA counterpart of peer-reviewed formal professional papers, but having less stringent limitations on manuscript length and extent of graphic presentations.
- **TECHNICAL MEMORANDUM.** Scientific and technical findings that are preliminary or of specialized interest, e.g., quick release reports, working papers, and bibliographies that contain minimal annotation. Does not contain extensive analysis.
- **CONTRACTOR REPORT.** Scientific and technical findings by NASA-sponsored contractors and grantees.

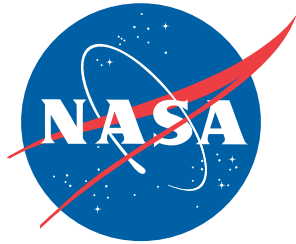
- **CONFERENCE PUBLICATION.** Collected papers from scientific and technical conferences, symposia, seminars, or other meetings sponsored or co-sponsored by NASA.
- **SPECIAL PUBLICATION.** Scientific, technical, or historical information from NASA programs, projects, and missions, often concerned with subjects having substantial public interest.
- **TECHNICAL TRANSLATION.** English-language translations of foreign scientific and technical material pertinent to NASA's mission.

Specialized services also include organizing and publishing research results, distributing specialized research announcements and feeds, providing information desk and personal search support, and enabling data exchange services.

For more information about the NASA STI program, see the following:

- Access the NASA STI program home page at <http://www.sti.nasa.gov>
- E-mail your question to [help@sti.nasa.gov](mailto:help@sti.nasa.gov)
- Fax your question to the NASA STI Information Desk at 443-757-5803
- Phone the NASA STI Information Desk at 443-757-5802
- Write to:  
STI Information Desk  
NASA Center for AeroSpace Information  
7115 Standard Drive  
Hanover, MD 21076-1320

NASA/TM-2013-217995/Volume I  
NESC-RP-12-00822



# Probing Aircraft Flight Test Hazard Mitigation for the Alternative Fuel Effects on Contrails & Cruise Emissions (ACCESS) Research Team

*Michael J. Kelly/NESC  
Langley Research Center, Hampton, Virginia*

National Aeronautics and  
Space Administration

Langley Research Center  
Hampton, Virginia 23681-2199

May 2013

## Acknowledgments

Nielsen Engineering and Research, Inc., contractors Mr. Stanley C. Perkins, Jr., and Mr. Omar Quijano conducted aerodynamic analyses in support of this assessment.

Michael Sean Walsh provided excellent graphic artist support.


The following team members were significant contributors to the contents of this document.

| Name               | Discipline                    | Organization                           |
|--------------------|-------------------------------|--|
| <b>Core Team</b>   |                               |  |
| Joseph Roche       | NESC Deputy Lead              | GRC                                    |
| Robert Clarke      | Flight Test Hazard Mitigation | DFRC                                   |
| Fletcher Hartshorn | Loads and Dynamics            | Tybrin Corporation                     |
| Steve Lilley       | Safety and Mission Assurance  | GRC                                    |
| Michael Mendenhall | Aerodynamics Subteam Lead     | Nielsen Engineering and Research, Inc. |
| Anthony Pototzky   | Loads and Dynamics            | LaRC                                   |
| William Rose       | Flight Test Hazard Mitigation | Rose Engineering and Research, Inc.    |
| <b>Consultants</b> |                               |  |
| Wayne Bryant       | Wake Turbulence Expert        | Retired FAA                            |

The use of trademarks or names of manufacturers in the report is for accurate reporting and does not constitute an official endorsement, either expressed or implied, of such products or manufacturers by the National Aeronautics and Space Administration.

Available from:


NASA Center for AeroSpace Information  
7115 Standard Drive  
Hanover, MD 21076-1320  
443-757-5802

|  |   |   |                        |
|--|---|---|------------------------|
|                 | <b>NASA Engineering and Safety Center<br/>Technical Assessment Report</b> | Document #:<br><b>NESC-RP-<br/>12-00822</b> | Version:<br><b>1.0</b> |
| Title:<br><b>Probing Aircraft Flight Test Hazard Mitigation<br/>for the ACCESS Research Team</b> |   | Page #:<br>1 of 118                         |                        |

## Volume I

# Probing Aircraft Flight Test Hazard Mitigation for the Alternative Fuel Effects on Contrails & Cruise Emissions (ACCESS) Research Team

**April 18, 2013**


|  |   |  |                        |
|--|---|--|------------------------|
|                 | <b>NASA Engineering and Safety Center<br/>Technical Assessment Report</b> | Document #:<br><b>NESC-RP-12-00822</b> | Version:<br><b>1.0</b> |
| Title:<br><b>Probing Aircraft Flight Test Hazard Mitigation<br/>for the ACCESS Research Team</b> |   | Page #:<br>2 of 118                    |                        |

## Report Approval and Revision History

NOTE: This document was approved at the April 18, 2013, NRB. This document was submitted to the NESC Director on April 30, 2013, for configuration control.

|           |                                   |        |
|-----------|-----------------------------------|--------|
| Approved: | <i>Original Signature on File</i> | 5/1/13 |
|           | NESC Director                     | Date   |


| Version | Description of Revision | Office of Primary Responsibility                                       | Effective Date |
|---------|-------------------------|--|----------------|
| 1.0     | Initial Release         | Mr. Michael J. Kelly,<br>NESC Associate<br>Principal Engineer,<br>LaRC | 4/18/13        |

|  |   |                         |            |
|--|---|-------------------------|------------|
|       | <b>NASA Engineering and Safety Center<br/>Technical Assessment Report</b> | Document #:             | Version:   |
|  |   | <b>NESC-RP-12-00822</b> | <b>1.0</b> |
| Title:   |   | Page #:                 |            |
| <b>Probing Aircraft Flight Test Hazard Mitigation<br/>for the ACCESS Research Team</b> |   | <b>3 of 118</b>         |            |

## Table of Contents

### Technical Assessment Report

|            |  |           |
|------------|--|-----------|
| <b>1.0</b> | <b>Notification and Authorization</b> .....                    | <b>7</b>  |
| <b>2.0</b> | <b>Signature Page</b> .....                                    | <b>8</b>  |
| <b>3.0</b> | <b>Team List</b> .....   | <b>9</b>  |
| 3.1        | Acknowledgements.....  | 9         |
| <b>4.0</b> | <b>Executive Summary</b> .....                                 | <b>10</b> |
| <b>5.0</b> | <b>Assessment Plan</b> .....                                   | <b>13</b> |
| <b>6.0</b> | <b>Background and Problem Description</b> .....                | <b>13</b> |
| 6.1        | ACCESS Flight Tests.....                                       | 13        |
| 6.1.1      | Experiment Background and Aircraft Descriptions.....           | 13        |
| 6.1.2      | DC-8 Description.....  | 16        |
| 6.1.3      | Falcon 20 Description.....                                     | 17        |
| 6.2        | Previous Flight Tests with Leader/Follower Aircraft.....       | 23        |
| 6.2.1      | NASA Flight Tests.....   | 24        |
| 6.2.2      | Canadian National Research Council (NRC) Flight Tests.....     | 24        |
| 6.2.3      | German Aerospace Agency Flight Tests.....                      | 26        |
| 6.3        | Falcon Flight Test Hazards.....                                | 29        |
| 6.3.1      | Aircraft Structural Failure.....                               | 29        |
| 6.3.2      | Engine Flameout due to Ingestion of Distorted Flow.....        | 29        |
| 6.3.3      | Aircraft Controllability/Operability at Unusual Attitudes..... | 30        |
| 6.4        | Project Analyses.....  | 30        |
| 6.4.1      | Wake Model.....  | 30        |
| 6.4.2      | Aerodynamic Analysis.....                                      | 31        |
| 6.4.3      | Structural Assessment.....                                     | 31        |
| <b>7.0</b> | <b>Data Analyses</b> .....                                     | <b>32</b> |
| 7.1        | Wake Vortex Behavior.....                                      | 32        |
| 7.1.1      | Fundamental Behavior and Evolution.....                        | 32        |
| 7.1.2      | Near-Field Behavior.....                                       | 35        |
| 7.1.3      | Far-Field Behavior.....  | 50        |
| 7.1.4      | Mid-Field Behavior.....  | 57        |
| 7.2        | Vortex Encounter Loads.....                                    | 58        |
| 7.2.1      | Assessment of Project Loads Analyses.....                      | 58        |
| 7.2.2      | Independent Loads Analyses.....                                | 59        |
| 7.2.3      | Core Size Sensitivity Analysis.....                            | 72        |
| 7.2.4      | Dynamic Simulations.....                                       | 74        |
| 7.3        | Flight Test Hazards Mitigation.....                            | 91        |
| 7.3.1      | Structural Failure Hazard.....                                 | 91        |
| 7.3.2      | Engine Flameout Hazard.....                                    | 102       |
| 7.3.3      | Loss of Control Hazard.....                                    | 104       |


|  |   |                         |            |
|--|---|-------------------------|------------|
|       | <b>NASA Engineering and Safety Center<br/>Technical Assessment Report</b> | Document #:             | Version:   |
|  |   | <b>NESC-RP-12-00822</b> | <b>1.0</b> |
| Title:   |   | Page #:                 |            |
| <b>Probing Aircraft Flight Test Hazard Mitigation<br/>for the ACCESS Research Team</b> |   | 4 of 118                |            |

|             |   |            |
|-------------|---|------------|
| <b>8.0</b>  | <b>Findings, Observations, and NESC Recommendations.....</b>      | <b>106</b> |
| 8.1         | Findings .....  | 106        |
| 8.2         | Observations .....  | 108        |
| 8.3         | NESC Recommendations .....  | 109        |
| <b>9.0</b>  | <b>Alternate Viewpoint.....</b>                                   | <b>110</b> |
| <b>10.0</b> | <b>Other Deliverables .....</b>                                   | <b>110</b> |
| <b>11.0</b> | <b>Lessons Learned.....</b>                                       | <b>110</b> |
| <b>12.0</b> | <b>Recommendations for NASA Standards and Specifications.....</b> | <b>110</b> |
| <b>13.0</b> | <b>Definition of Terms.....</b>                                   | <b>110</b> |
| <b>14.0</b> | <b>Acronyms List .....</b>  | <b>111</b> |
| <b>15.0</b> | <b>References.....</b>  | <b>113</b> |
| <b>16.0</b> | <b>Volume II. Appendices (separate volume).....</b>               | <b>118</b> |


### List of Figures

|                |  |    |
|----------------|--|----|
| Figure 6.1-1.  | R-2508 Complex Restricted Area.....  | 15 |
| Figure 6.1-2.  | DC-8-72 Aircraft.....  | 16 |
| Figure 6.1-3.  | NASA DC-8-72 .....   | 17 |
| Figure 6.1-4.  | Falcon 20G Aircraft .....  | 18 |
| Figure 6.1-5.  | General Layout of Falcon 20 ACCESS Experiment Instrumentation .....  | 19 |
| Figure 6.1-6.  | General View of NASA Falcon 20 .....   | 20 |
| Figure 6.1-7.  | Front View of NASA Falcon 20 .....   | 20 |
| Figure 6.1-8.  | Falcon 20 Cruciform Tail, Left Side with Access Panels Installed .....   | 21 |
| Figure 6.1-9.  | Falcon 20 Cruciform Tail, Left Side with Access Panels Removed.....  | 21 |
| Figure 6.1-10. | Falcon 20, Right-side Horizontal Tail Aft Connection.....  | 22 |
| Figure 6.1-11. | Falcon 20, Right-side Horizontal Tail Forward Connection.....  | 22 |
| Figure 6.1-12. | Falcon 20 Visually Inspected Fuselage Frame Showing Greasy Residue .....   | 23 |
| Figure 6.2-1.  | NASA T-39 Sabreliner .....   | 24 |
| Figure 6.2-2.  | Canadian NRC T-33 .....  | 25 |
| Figure 6.2-3.  | Canadian NRC Falcon 20 .....   | 26 |
| Figure 6.2-4.  | DLR Falcon 20.....   | 27 |
| Figure 6.2-5.  | General Layout of Falcon 20 DLR Experiment Instrumentation.....  | 28 |
| Figure 7.1-1.  | The Rolling-up Process.....  | 32 |
| Figure 7.1-2.  | Photograph of Merging Exhaust and Vortex Pair from Transport Airplane in Landing Configuration at Unknown Speed and Altitude.....      | 37 |
| Figure 7.1-3.  | Photograph of Merging Exhaust and Vortex Pair from an A-3 Airplane in Cruise Configuration at $M = 0.5$ and Altitude of 20,000 ft..... | 38 |
| Figure 7.1-4.  | Contours of Total Temperature Fluctuation 98 ft (30 m) Behind an A-3 .....   | 39 |



|  |   |  |                        |
|--|---|--|------------------------|
|                 | <b>NASA Engineering and Safety Center<br/>Technical Assessment Report</b> | Document #:<br><b>NESC-RP-12-00822</b> | Version:<br><b>1.0</b> |
| Title:<br><b>Probing Aircraft Flight Test Hazard Mitigation<br/>for the ACCESS Research Team</b> |   | Page #:<br>5 of 118                    |                        |


|                |  |    |
|----------------|--|----|
| Figure 7.1-5.  | Contours of Total Temperature Fluctuation 330 ft (100 m) Behind an A-3 .....   | 40 |
| Figure 7.1-6.  | Contours of Total Temperature Fluctuation 980 ft (300 m) Behind an A-3 .....   | 41 |
| Figure 7.1-7.  | Contours of Total Temperature Fluctuation 3,300 ft (1 km) Behind an A-3 .....  | 42 |
| Figure 7.1-8.  | DLR Falcon 20 Flying behind an A-340 .....   | 44 |
| Figure 7.1-9.  | Approximately Scaled Depiction of Lateral Clearance between Falcon Wingtip and Leader Aircraft Wingtip Vortices of 1-, 2- and 3.5-Percent Core Size.....                 | 46 |
| Figure 7.1-10. | Notional Depiction of Three-Dimensional Near-Field Sample-Area Geometry .....  | 50 |
| Figure 7.1-11. | B-737 Approaching C-130 Vortex Pair in Far Field.....  | 51 |
| Figure 7.1-12. | DLR Video Screen Grab showing Far-Field Separation: Diffuse Exhaust Contrail above Wake Vortices .....   | 52 |
| Figure 7.1-13. | DLR Video Screen Grab showing Diffuse Exhaust Contrail above A-380 Wake Vortices.....  | 52 |
| Figure 7.1-14. | DLR Video Screen Grab showing Diffuse Exhaust Contrail above A-340 Wake Vortices.....  | 53 |
| Figure 7.1-15. | NRC Image of Diffuse Exhaust Contrail above B-727 Wake Vortices Far Field .....  | 55 |
| Figure 7.1-16. | Qualitative Computation of Formation of Shield Composed of Engine-exhaust Products (open circles) around Vortex Wake (filled circles) when Engine Thrust is Robust ..... | 56 |
| Figure 7.2-1.  | Comparison of Lamb-Oseen and Burnham-Hallock Tangential Velocity Distributions..   | 59 |
| Figure 7.2-2.  | Panel Layout for DC-8 Wing and Horizontal Tail (left) and Strip Theory Model of DC-8 Wing (right) .....  | 61 |
| Figure 7.2-3.  | Predicted Span-Load Distributions for DC-8 Wing and Horizontal Tail .....  | 62 |
| Figure 7.2-4.  | DC-8 Model Wake Vortices .....   | 63 |
| Figure 7.2-5.  | Velocity Flow Field Depiction behind Model DC-8 .....  | 64 |
| Figure 7.2-6.  | Induced Rolling Moment Coefficient ( $C_l$ ) .....   | 65 |
| Figure 7.2-7.  | Induced Normal Force Coefficient ( $\Delta C_N$ ) .....  | 66 |
| Figure 7.2-8.  | Induced Pitching Moment Coefficient ( $C_m$ ).....   | 66 |
| Figure 7.2-9.  | Near-Field Map of Falcon Right Horizontal Tail Normal Force Coefficient ( $C_{NF22}$ ) .....   | 67 |
| Figure 7.2-10. | Near-Field Map of Falcon Right Horizontal Tail Bending Moment Coefficient ( $C_{BM22}$ ) .....   | 68 |
| Figure 7.2-11. | Near-Field Map of Falcon Left Horizontal Tail Normal Force Coefficient ( $C_{NF23}$ ) .....  | 68 |
| Figure 7.2-12. | Near-Field Map of Falcon Left Horizontal Tail Bending Moment Coefficient ( $C_{BM23}$ ) .....  | 69 |
| Figure 7.2-13. | Near-Field Map of Falcon Vertical Tail Alone Normal Force Coefficient ( $C_{NF21}$ ) .....   | 69 |
| Figure 7.2-14. | Near-Field Map of Falcon Vertical Tail (Alone) Bending Moment Coefficient ( $C_{BM21}$ )..   | 70 |
| Figure 7.2-15. | Core Radius Effect on Vortex-Induced Tangential Velocity .....   | 73 |
| Figure 7.2-16. | Cessna 550 .....   | 76 |
| Figure 7.2-17. | Simulation Depiction for Light Falcon Beginning in the Vortex .....  | 78 |
| Figure 7.2-18. | Response Data for Light Falcon Beginning in the Vortex .....   | 79 |
| Figure 7.2-19. | Force Data for Light Falcon Beginning in the Vortex .....  | 80 |

|  |   |                         |            |
|--|---|-------------------------|------------|
|       | <b>NASA Engineering and Safety Center<br/>Technical Assessment Report</b> | Document #:             | Version:   |
|  |   | <b>NESC-RP-12-00822</b> | <b>1.0</b> |
| Title:   |   | Page #:                 |            |
| <b>Probing Aircraft Flight Test Hazard Mitigation<br/>for the ACCESS Research Team</b> |   | 6 of 118                |            |

|                |   |     |
|----------------|---|-----|
| Figure 7.2-20. | Simulation Depiction for Heavy Falcon Released in the Wingtip Vortex.....       | 80  |
| Figure 7.2-21. | Response Data for Heavy Falcon Beginning in the Vortex .....                    | 81  |
| Figure 7.2-22. | Force Data for Heavy Falcon Beginning in the Vortex .....                       | 82  |
| Figure 7.2-23. | Simulation Depiction for Light Falcon Released Behind Inboard Engine .....      | 83  |
| Figure 7.2-24. | Response Data for Light Falcon Released Behind Inboard Engine .....             | 84  |
| Figure 7.2-25. | Force Data for Light Falcon Released Behind Inboard Engine .....                | 84  |
| Figure 7.2-26. | Simulation Depiction for Heavy Falcon Released Behind Inboard Engine.....       | 85  |
| Figure 7.2-27. | Response Data for Heavy Falcon Released Behind Inboard Engine .....             | 86  |
| Figure 7.2-28. | Force Data for Heavy Falcon Released Behind Inboard Engine .....                | 86  |
| Figure 7.2-29. | Simulation Depiction for Light Falcon Released with Wingtip in Vortex .....     | 87  |
| Figure 7.2-30. | Response Data for Light Falcon Released with Wingtip in Vortex.....             | 88  |
| Figure 7.2-31. | Force Data for Light Falcon Released with Wingtip in Vortex .....               | 88  |
| Figure 7.2-32. | Simulation Depiction for Heavy Falcon Released with Wingtip in Vortex.....      | 89  |
| Figure 7.2-33. | Response Data for Heavy Falcon Released with Wingtip in Vortex.....             | 90  |
| Figure 7.2-34. | Force Data for Heavy Falcon Released with Wingtip in Vortex .....               | 90  |
| Figure 7.3-1.  | Vane Directions and Velocity Vectors .....                                      | 98  |
| Figure 7.3-2.  | Approximately Scaled Comparison of A-10 and Falcon 20 showing Engine Layout.... | 103 |

### List of Tables

|              |  |    |
|--------------|--|----|
| Table 6.1-1. | Falcon 20 ACCESS Experiment Instrumentation.....   | 18 |
| Table 6.2-1. | DLR Flight Experiments with Falcon 20 as the Follower Aircraft.....  | 27 |
| Table 7.1-1. | Bounding Weights for Aircraft in the Photometric Analysis.....   | 35 |
| Table 7.1-2. | Lateral Vortex Clearance for Falcon 20 behind Different Leader Aircraft .....                                  | 45 |
| Table 7.2-1. | Key Aircraft Model Parameters Used in the NESC Aerodynamic Analyses .....                                      | 60 |
| Table 7.2-2. | Key Assumptions Used for NESC and Project Models.....  | 63 |
| Table 7.2-3. | Falcon 20 Presumed DLL Conditions.....   | 71 |
| Table 7.2-4. | Computed Vortex-induced Loads for a 1-percent Vortex Core.....   | 72 |
| Table 7.2-5. | Falcon Maximum Forces and Bending Moments for Three Vortex Core Sizes.....                                     | 74 |
| Table 7.2-6. | Basic Comparison Between Cessna 550 and Falcon 20 .....  | 76 |
| Table 7.2-7. | Falcon 20 Inertial Properties, Empty and at MTOW .....   | 77 |
| Table 7.2-8. | Falcon 6-DOF Simulations .....   | 77 |
| Table 7.3-1. | Candidate Instrumentation Items for Vortex Avoidance, Structural Health<br>Monitoring, or Engine Flameout..... | 99 |

|  |   |  |                        |
|--|---|--|------------------------|
|                 | <b>NASA Engineering and Safety Center<br/>Technical Assessment Report</b> | Document #:<br><b>NESC-RP-12-00822</b> | Version:<br><b>1.0</b> |
| Title:<br><b>Probing Aircraft Flight Test Hazard Mitigation<br/>for the ACCESS Research Team</b> |   | Page #:<br>7 of 118                    |                        |


## Technical Assessment Report

### 1.0 Notification and Authorization

The Alternative Fuel Effects on Contrails & Cruise Emissions (ACCESS) Project Integration Manager, Mr. Brian F. Beaton, requested in July 2012 that the NASA Engineering and Safety Center (NESC) form a team to independently assess aircraft structural failure hazards associated with the ACCESS experiment and to identify potential flight test hazard mitigations to ensure flight safety. Mr. Beaton subsequently requested that the assessment scope be focused predominantly on structural failure risks to the aircraft empennage (horizontal and vertical tail).

Mr. Michael Kelly, NESC Associate Principal Engineer at NASA Langley Research Center (LaRC), was selected to lead the assessment. The assessment plan was approved by the NESC Review Board (NRB) on August 2, 2012. A preliminary stakeholder summary with preliminary NESC recommendations was approved by the NRB on October 4, 2012.



|   |   |  |                        |
|---|---|--|------------------------|
|  | <b>NASA Engineering and Safety Center<br/>Technical Assessment Report</b> | Document #:<br><b>NESC-RP-<br/>12-00822</b>  | Version:<br><b>1.0</b> |
|   |   | <b>Probing Aircraft Flight Test Hazard Mitigation<br/>for the ACCESS Research Team</b> |                        |


### 3.0 Team List

| Name                          | Discipline                    | Organization                           |
|-------------------------------|-------------------------------|--|
| <b>Core Team</b>              |                               |  |
| Michael Kelly                 | NESC Lead                     | LaRC                                   |
| Joseph Roche                  | NESC Deputy Lead              | GRC                                    |
| Patricia Pahlavani            | MTSO Program Analyst          | LaRC                                   |
| Robert Clarke                 | Flight Test Hazard Mitigation | DFRC                                   |
| Josue Cruz                    | Loads and Dynamics            | DFRC                                   |
| Fletcher Hartshorn            | Loads and Dynamics            | Tybrin Corporation                     |
| Daniel Lesieutre              | Aerodynamics Analyst          | Nielsen Engineering and Research, Inc. |
| Steve Lilley                  | Safety and Mission Assurance  | GRC                                    |
| Michael Mendenhall            | Aerodynamics Subteam Lead     | Nielsen Engineering and Research, Inc. |
| Clarence Modlin               | Loads and Dynamics            | Retired NASA                           |
| Shishir Pandya                | Aerodynamics Analyst          | ARC                                    |
| Anthony Pototzky              | Loads and Dynamics            | LaRC                                   |
| William Rose                  | Flight Test Hazard Mitigation | Rose Engineering and Research, Inc.    |
| Thomas Yechout                | Flight Test Hazard Mitigation | USAF Academy                           |
| <b>Consultants</b>            |                               |  |
| Wayne Bryant                  | Wake Turbulence Expert        | Retired FAA                            |
| James Stewart                 | NESC DFRC Chief Engineer      | DFRC                                   |
| <b>Administrative Support</b> |                               |  |
| Linda Burgess                 | Planning and Control Analyst  | LaRC/AMA                               |
| Jonay Campbell                | Technical Writer              | LaRC/NG                                |
| Terri Derby                   | Project Coordinator           | LaRC/AMA                               |

### 3.1 Acknowledgements

Nielsen Engineering and Research, Inc., contractors Mr. Stanley C. Perkins, Jr., and Mr. Omar Quijano conducted aerodynamic analyses in support of this assessment.

Michael Sean Walsh for his excellent graphic artist support.

|  |   |  |                        |
|--|---|--|------------------------|
|                 | <b>NASA Engineering and Safety Center<br/>Technical Assessment Report</b> | Document #:<br><b>NESC-RP-12-00822</b> | Version:<br><b>1.0</b> |
| Title:<br><b>Probing Aircraft Flight Test Hazard Mitigation<br/>for the ACCESS Research Team</b> |   | Page #:<br>10 of 118                   |                        |

## 4.0 Executive Summary

The Alternative Fuel Effects on Contrails & Cruise Emissions (ACCESS) Project Integration Manager, Mr. Brian F. Beaton, requested in July 2012 that the NASA Engineering and Safety Center (NESC) form a team to independently assess aircraft structural failure hazards associated with the ACCESS experiment and identify potential flight test hazard mitigations to ensure flight safety. Mr. Beaton requested results prior to a review scheduled for early October 2012. The ACCESS Project Manager, Dr. Ruben Del Rosario from the NASA Glenn Research Center (GRC), was a secondary stakeholder. Dr. Bruce Anderson, also from the NASA GRC, was the ACCESS principal investigator. The NASA Aeronautics Research Mission Directorate (ARM D) chartered the ACCESS research team to conduct experimental flight tests to investigate the potential for alternative fuels to reduce the impact of aviation on air quality and climate.


The NESC Initial Evaluation was approved to proceed by the NESC Review Board (NRB) on July 12, 2012 (Appendix A). The project team planned to fly a series of flights between February 18 and March 31, 2013, using two NASA aircraft assets to obtain on-the-ground and in-flight emission measurements of alternative fuels engine exhaust at high altitude and cruise speed. The test team planned to fly a NASA Falcon 20 business jet at distances behind a NASA DC-8-72 jet transport aircraft on the order of a few wingspans (near field) and at distances on the order of a few miles (far field). The project team provided to the NESC material from a June 2012 Systems Requirements Review (SRR) (Appendix B).

The NESC formed a team of experts in wake vortex science, aerodynamic flight loads, structural analysis, aircraft flight testing and operations, and safety and mission assurance, and kicked off its work on August 10, 2012 (Appendix C). On August 14, 2012, the project team briefed the NESC team about the analyses it had already completed to address the structural hazard (Appendix D).

During the next 6 weeks, the NESC team focused its efforts on the most value-adding work that could be accomplished in the short time available. By September 26, 2012, the team had accomplished the following:

- Researched and discussed the state of knowledge of the strength and behavior of wake vortices generated by heavy transport aircraft with flaps and slats retracted, flying at high altitudes and cruise speeds.
- Researched and discussed the evolution of engine exhaust plumes and wake vortices in the near field and in the far field.
- Researched and discussed pilots' lessons learned from previous similar experiments.
- Considered and discussed the ACCESS project's loads assessment.
- Conducted an independent loads assessment.



|  |   |  |                        |
|--|---|--|------------------------|
|                 | <b>NASA Engineering and Safety Center<br/>Technical Assessment Report</b> | Document #:<br><b>NESC-RP-12-00822</b> | Version:<br><b>1.0</b> |
| Title:<br><b>Probing Aircraft Flight Test Hazard Mitigation<br/>for the ACCESS Research Team</b> |   | Page #:<br>11 of 118                   |                        |

- Conducted independent aircraft trajectory simulations.
- Developed flight test hazard mitigations and formulated recommendations.

Summaries of the team’s analyses deliverables can be found in Appendices E and F. A summary of test pilot lessons learned from the German Aerospace Center (Deutsches Zentrum für Luft- und Raumfahrt (DLR)) can be found in Appendix G.

The NESC team drafted findings, observations, and NESC recommendations on October 1, 2012. The NRB approved a preliminary stakeholder briefing with findings, observations, and NESC recommendations on October 4, 2012, and the NESC team provided the briefing to the ACCESS stakeholders on October 5, 2012 (Appendix H).


The top NESC recommendation was that for all ACCESS flight test experiments the test team enforce as a *mission rule* that wake vortices must be made visible by rolled up exhaust contrails. This was assessed to be necessary to mitigate the risk of the Falcon inadvertently encountering the dangerous flow field around the vortices.

Of near equal importance, the NESC team recommended that prior to any flight tests to gather science data, the test team conduct practice flight tests dedicated to developing pilot proficiency in avoiding wake vortices. Various lessons were learned from pilots who conducted similar experiments, but the NESC team concluded that proficiency in visualizing and avoiding vortices could only be achieved through practice.

The NESC team recommended aircraft instrumentation that could offer additional means to detect and avoid inadvertent wake vortex encounters and identify whether structural damage had occurred following an inadvertent wake vortex encounter.

The NESC team provided independent peak static loads calculated with a tool of higher fidelity than those used by the project team and showed improved margins when compared with conservative manufacturer design conditions. Definitive empennage margins of safety could not be determined because Falcon 20 strength capability information was not available from the manufacturer. The NESC team computed coefficients and peak loads for three vortex strengths, to provide project analysts with data that would allow them to assess risk using their own assumptions about vortex decay rates. The NESC team also conducted 6-degree-of-freedom (DOF) independent simulations of the Falcon 20 dynamic response when beginning at various locations in the flow field behind the DC-8. The Falcon response in some cases mimicked reports from pilots who had conducted similar experiments.

The NESC team recommended as a hazard mitigation that ACCESS pilots minimize control inputs if an inadvertent wake vortex encounter appeared imminent or was indicated to be imminent by instrumentation (if any). This recommendation was to allow the vortex flow field to move the Falcon 20 naturally away from the vortex core. The NESC team recommended that once clear of the vortex, ACCESS pilots should stabilize the aircraft by performing a rapid and


|  |   |   |                        |
|--|---|---|------------------------|
|                 | <b>NASA Engineering and Safety Center<br/>Technical Assessment Report</b> | Document #:<br><b>NESC-RP-<br/>12-00822</b> | Version:<br><b>1.0</b> |
| Title:<br><b>Probing Aircraft Flight Test Hazard Mitigation<br/>for the ACCESS Research Team</b> |   | Page #:<br>12 of 118                        |                        |

positive centering of its flight controls. This was to minimize excursions in sideslip and angle of attack and thereby reduce the likelihood of spin entry through inertial coupling.

This NESC technical assessment report provides a detailed description of the team's assessment activities and supporting narrative in support of the findings, observations, and NESC recommendations.

On February 8, 2013, NESC team members participated in a project technical briefing of their flight test plan to an Independent Review Team (Appendix I). During the last week of February 2013, ACCESS pilots conducted proficiency practice flight tests in accordance with the top two NESC recommendations. On March 1, 2013, the project team provided a briefing of lessons learned to the NESC team. Images from test videos and team notes from this meeting can be found in Appendix J.



|  |   |  |                        |
|--|---|--|------------------------|
|                 | <b>NASA Engineering and Safety Center<br/>Technical Assessment Report</b> | Document #:<br><b>NESC-RP-12-00822</b> | Version:<br><b>1.0</b> |
| Title:<br><b>Probing Aircraft Flight Test Hazard Mitigation<br/>for the ACCESS Research Team</b> |   | Page #:<br>13 of 118                   |                        |

## 5.0 Assessment Plan

The ACCESS flight test could expose the Falcon 20 test aircraft to distorted flow and other adverse conditions that could result in structural failure. The ACCESS project conducted aerodynamic and structural analyses and researched flight test mitigation lessons learned. They asked the NESC team to conduct independent aerodynamic and structural analyses, to assess the Falcon 20 structural failure hazard, and to provide hazard mitigation strategy recommendations that could provide independent insight and ensure flight safety.

The NESC team's plan was to characterize the wake of the DC-8-72 and produce wake flow field aerodynamic models, to conduct Falcon 20 vertical and horizontal tail loads analyses, and to compare these tail loads against Falcon 20 design certification load envelopes (if they could be acquired).

If the available data allowed, then a safe operating envelope was to be identified behind the DC-8-72 within which load limits would not be exceeded. If the identified safe operating envelope had large uncertainty because of poor DC-8 wake characterization or lack of Falcon 20 design data, then the plan included a contingency to assess the merits of collecting new DC-8 wake data using a Dryden Flight Research Center (DFRC) fighter aircraft asset. The plan also included a contingency to evaluate wing dynamic loads because of possible asymmetric effects from jet efflux.

Finally, the plan included the creation of structural failure hazard mitigation recommendations for the ACCESS test team and for its operational flight crews. A contingency was included to create recommendations to mitigate the other two identified Falcon 20 hazards—engine flameout and loss of control—if these were incidentally developed as an integral part of developing the structural hazard mitigations.

## 6.0 Background and Problem Description


### 6.1 ACCESS Flight Tests

#### 6.1.1 Experiment Background and Aircraft Descriptions

This section provides a description of the ACCESS experiment and of the two aircraft involved.

The ARMD Fundamental Aeronautics Program's Subsonic Fixed Wing project chartered the ACCESS project team to conduct experimental tests to investigate the potential for alternative fuels to reduce the impact of aviation on air quality and climate. The benefits of jet aircraft using alternative fuels include reduced particulate emissions, reduced carbon dioxide and other gaseous emissions, and reduced or eliminated contrails.

The ACCESS project team planned a series of ground and flight tests in February and March 2013, using a NASA DC-8-72 transport jet aircraft and a NASA Falcon 20 business jet aircraft that was specially instrumented to collect engine exhaust emission data.

|  |   |   |                        |
|--|---|---|------------------------|
|                 | <b>NASA Engineering and Safety Center<br/>Technical Assessment Report</b> | Document #:<br><b>NESC-RP-<br/>12-00822</b> | Version:<br><b>1.0</b> |
| Title:<br><b>Probing Aircraft Flight Test Hazard Mitigation<br/>for the ACCESS Research Team</b> |   | Page #:<br>14 of 118                        |                        |

The ACCESS project plan was to conduct approximately one-hour static ground tests with the DC-8 burning a 50:50 blend of JP-8 and biofuel in some engines with the instrumented Falcon 20 parked behind it. The project team also planned to conduct a series of 4-hour flight tests with the DC-8 flying as a “leader aircraft” burning the biofuel blend in some engines and the instrumented Falcon 20 flying at various distances behind it as a “follower aircraft.”

The Falcon 20 was to collect data to characterize aspects of DC-8 exhaust emissions including exhaust plume chemistry, thermal stability, chemical kinetics, and ignition energy. The data would also characterize aspects of contrail formation including number densities of ice particles and soot. Research questions were to identify how alternative fuels affect the number and physical characteristics of soot emissions; how they affect nitrogen oxide, nitrogen dioxide, carbon monoxide, and total hydrocarbon emissions; how fuel properties affect downstream volatile aerosol formation; how alternative fuels affect the formation temperature and initial characteristics of contrails; whether there are links between exhaust particulate matter number/properties and contrail ice number and properties; whether contrail formation is to be suppressed by burning sulfur-free alternative fuel in a modern low-particulate matter emitting engine; and how cruise-altitude emission values relate to ground-based measurements.

The Falcon 20 was to collect data behind the DC-8 within two experimental zones referred to as the near field and the far field. Near-field distances were measured as multiples of leader aircraft wingspan lengths behind the leader aircraft. Far-field distances were usually measured in miles behind the leader aircraft.

The flight test experiments were to originate and terminate at the NASA DFRC in Edwards, CA, and were to be conducted in airspace between altitudes of 27,000 and 39,000 ft, along 10- to 20-mile-long tracks aligned with the wind direction, “well away from flight corridors.” Airspace regions of large-scale uniformity where contrails would be likely to form were to be sought within the R-2508 airspace complex comprised of Edwards Air Force Base, Fort Irwin National Training Center, and Naval Air Weapons Station China Lake.

The R-2508 Complex, shown in Figure 6.1-1, could support the planned flight tests for both near and far operations. The dimensions of this restricted area were roughly 140 (N-S) by 100 (E-W) nautical miles (nm). This large restricted area would allow flights aligned with winds aloft in any direction. It also contained numerous suitable airport runways to which the Falcon 20 could glide in the event of a dual engine flameout.



Title:

Probing Aircraft Flight Test Hazard Mitigation  
for the ACCESS Research Team

Page #:

15 of 118



Figure 6.1-1. R-2508 Complex Restricted Area


A project ACCESS hazard review in summer 2012 identified three hazards associated with flying the Falcon 20 in proximity to the wake vortices that trail behind the DC-8:

1. Falcon 20 structural failure
2. Falcon 20 engine flameout due to ingestion of distorted flow
3. Falcon 20 loss of controllability/operability at unusual attitudes

The risk likelihoods for these hazards were not identified, but the potential consequences for all three were identified as loss of mission, damage to asset, loss of asset, and loss of personnel.

The stakeholder requested Falcon 20 empennage structural design data, drawings, and certification load limit envelopes from the aircraft's manufacturer, the Dassault Falcon Jet Corporation. These proprietary data, if acquired, would allow comparison of loads calculated from wake vortex encounters with aircraft strength capability and computation of margins of



|  |   |  |                        |
|--|---|--|------------------------|
|                 | <b>NASA Engineering and Safety Center<br/>Technical Assessment Report</b> | Document #:<br><b>NESC-RP-12-00822</b> | Version:<br><b>1.0</b> |
| Title:<br><b>Probing Aircraft Flight Test Hazard Mitigation<br/>for the ACCESS Research Team</b> |   | Page #:<br>16 of 118                   |                        |

safety. The stakeholder also explored the possibility of NASA leveraging an existing contract between the U.S. Coast Guard and Dassault to submit project loads analyses results to Dassault for pass/fail evaluation against design envelopes.

### 6.1.2 DC-8 Description

NASA has owned a DC-8-72 aircraft (tail number N817NA, serial number 46082) since 1987; the aircraft is operated for earth, atmospheric, and space sciences research activities. This modified flying laboratory was manufactured by the Douglas Aircraft Company and is based at DFRC.


The aircraft, shown in Figure 6.1-2, is a four-engine jet transport aircraft with a range in excess of 5,000 nm and a flight ceiling of 41,000 ft. Its normal cruise speed at altitudes above 30,000 ft is 450 knots true airspeed (KTAS). Its empty weight is 150,000 lb, and its maximum takeoff weight (MTOW) is 350,000 lb. It can carry 30,000 lb of scientific instruments and equipment and seat up to 45 experimenters and flight crew. The aircraft is powered by four CFM International CFM56-2-C1 high-bypass-ratio turbofan engines that develop a maximum thrust of 22,000 lb each.

The aircraft is 157 ft long with a 148-ft wingspan. It has special viewports, power systems, and instruments. Removable wing pylons near each wingtip can accommodate 100 lb of experimenter equipment. Each pylon has power and signal cables and is designed to hold a laser aerosol probe but could accommodate other instruments of comparable size and weight.

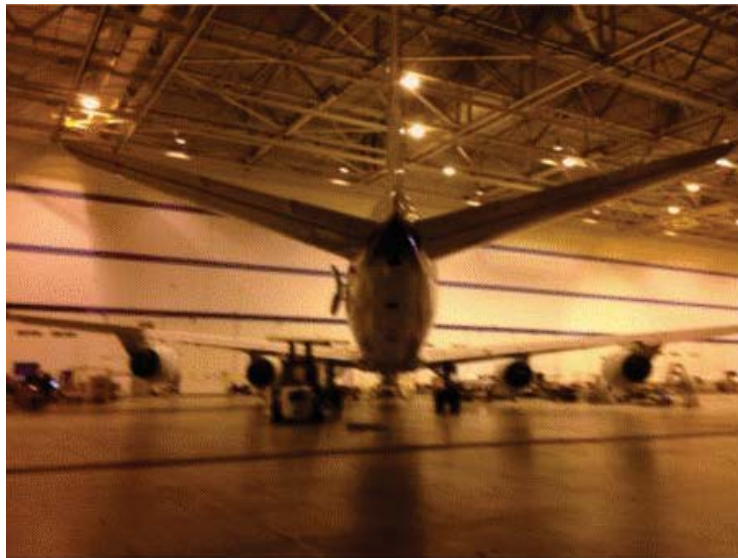


*Figure 6.1-2. DC-8-72 Aircraft*

The NASA DC-8-72 was examined by NESC team members at DFRC (Figure 6.1-3). To get a sense of scale, the NESC team walked beneath the aircraft's wings and engines and stood behind

|  |   |   |                        |
|--|---|---|------------------------|
|                 | <b>NASA Engineering and Safety Center<br/>Technical Assessment Report</b> | Document #:<br><b>NESC-RP-<br/>12-00822</b> | Version:<br><b>1.0</b> |
| Title:<br><b>Probing Aircraft Flight Test Hazard Mitigation<br/>for the ACCESS Research Team</b> |   | Page #:<br>17 of 118                        |                        |

the aircraft at short distances comparable to the planned following distance. The aircraft's removable wingtip pylons were visually examined.



*Figure 6.1-3. NASA DC-8-72*


The aircraft crew chief made available to the NESC team the DC-8 maintenance manual [ref. 1].

### **6.1.3 Falcon 20 Description**

NASA acquired a Falcon 20G (tail number N525NA, serial number 447) in November 2011 from the U.S. Coast Guard. The Coast Guard used the aircraft as a search and rescue platform based in Cape Cod, MA. It was manufactured in 1981 by the French Dassault Falcon Jet Corporation as a military version of its Falcon 20 business jet. This variant is called an HU-25C Guardian but will be referred to throughout this report as a Falcon 20. The aircraft is based at the NASA Langley Research Center (LaRC) in Hampton, VA.

The twin-engine Falcon 20, shown in Figure 6.1-4, has a range of about 1,900 nm and a maximum altitude of 42,000 ft. Its maximum speed is 495 KTAS and cruising speed is 405 KTAS. Its empty weight is 16,600 lb, and its MTOW is 32,000 lb with a useful payload of 3,000 lb. The aircraft is powered by two Garrett AiResearch ATF3-6-2C turbofan engines.

The aircraft is 55 ft long with a 54-ft wingspan. The aircraft was modified by the Coast Guard to include a nadir camera port, large side-looking search window ports, side-looking radar hard points, and a drop hatch.

|  |   |                         |            |
|--|---|-------------------------|------------|
|       | <b>NASA Engineering and Safety Center<br/>Technical Assessment Report</b> | Document #:             | Version:   |
|  |   | <b>NESC-RP-12-00822</b> | <b>1.0</b> |
| Title:   |   | Page #:                 |            |
| <b>Probing Aircraft Flight Test Hazard Mitigation<br/>for the ACCESS Research Team</b> |   | 18 of 118               |            |



*Figure 6.1-4. Falcon 20G Aircraft*


The Falcon 20 primary flight controls have been hydraulically boosted. Each boost actuator functions with pressure from either of the aircraft’s two hydraulic systems. Each flight control has an artificial feel unit in combination with a variable length bell crank Dassault called “Arthur Q units.” As the aircraft hydraulics systems moves the aircraft control surfaces, these artificial feel units give pilots control sensations proportional with control deflections, adjusting the sensitivity of the controls as the airspeed changes. This provides a low-speed feel that is similar to that at high speed.

Modifications for the ACCESS experiment included installation of an aerosol/gas inlet probe and a cloud droplet probe on top of the aircraft’s fuselage, a diode laser hygrometer (DLH) mounted in a fuselage side window, an angle-of-attack sensor (Rosemount 858Y) mounted on its left side, and a humidity sensor inlet (dew-/frost-point hygrometer) and a fast-response temperature sensor mounted on the aircraft’s nose. A descriptive list of instrumentation installed on the Falcon 20 for the ACCESS experiment is included in Table 6.1-1, and a drawing reproduction showing the general layout of some key instruments is shown in Figure 6.1-5.

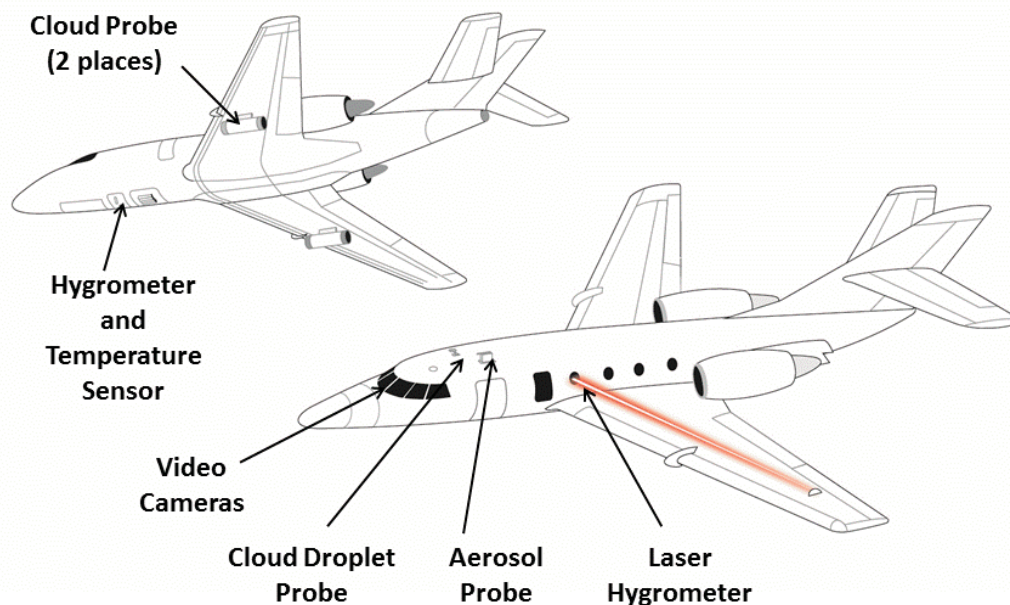
*Table 6.1-1. Falcon 20 ACCESS Experiment Instrumentation*

| Parameter                             | Instrument                                  | Operating Principle          |
|---------------------------------------|---|------------------------------|
| Carbon dioxide (CO <sub>2</sub> )     | LiCor 7000                                  | Non-dispersive infrared (IR) |
| Carbon Monoxide (CO), CO <sub>2</sub> | Cavity ring-down (CRD) Los Gatos            | CRD absorption               |
| Water (H <sub>2</sub> O)              | LaRC -- DLH                                 | Long-path IR                 |
|                                       | Edgetech 137                                | Chilled mirror               |
| Nitric Oxide (NO)                     | Teledyne T200UP                             | Chemiluminescence            |
| Nitrogen Dioxide (NO <sub>2</sub> )   | Los Gatos Research                          | Cavity ring-down absorption  |
| Ozone (O <sub>3</sub> )               | 2B Technologies                             | Chemiluminescence            |
| Ultrafine aerosol                     | TSI3025 Condensation Particle Counter (CPC) | Condensation growth/optical  |



|   |   |   |                        |
|---|---|---|------------------------|
|  | <b>NASA Engineering and Safety Center<br/>Technical Assessment Report</b> | Document #:<br><b>NESC-RP-<br/>12-00822</b>   | Version:<br><b>1.0</b> |
|   |   | <b>Title:</b><br><br><b>Probing Aircraft Flight Test Hazard Mitigation<br/>for the ACCESS Research Team</b> |                        |

| Parameter                  | Instrument  | Operating Principle         |
|----------------------------|---|-----------------------------|
| Fine aerosol               | TSI3010 CPC   | Condensation growth/optical |
| Nonvolatile aerosol        | TSI3010 CPC   | Condensation growth/optical |
| Size: 10 to 300 nm         | TSI SMPS  | Condensation growth/optical |
| Size 80 to 1000 nm         | DMT Ultra-High Sensitivity Aerosol Spectrometer (UHSAS)                   | Optical scattering          |
| Soot size/mass             | DMT Single Particle Soot Photometer (SP2)                                 | Laser Incandescence         |
| Cloud particle size        | DMT Cloud Droplet Probe (CDP)   | Optical scattering          |
| Cloud particle images      | DMT Cloud, Aerosol and Precipitation Spectrometer (CAPS)                  | Optical Scattering/imaging  |
| Temperature                | Rosemount T sensor  | Hot wire                    |
| Position and accelerations | Applanix Inertial Navigation System (INS)/Global Positioning System (GPS) | GPS, accelerometers         |
| U, V, W                    | Rosemount 558 probes or Radome Mods                                       | Differential pressure       |



*Figure 6.1-5. General Layout of Falcon 20 ACCESS Experiment Instrumentation*

The Falcon 20 was examined on two separate occasions by NESC team members at the LaRC. Aircraft general and front views are shown in Figures 6.1-6 and 6.1-7. No skin dents or warping



# NASA Engineering and Safety Center Technical Assessment Report

Document #:  
**NESC-RP-  
12-00822**

Version:  
**1.0**

Title:

## **Probing Aircraft Flight Test Hazard Mitigation for the ACCESS Research Team**

Page #:  
20 of 118

that could have indicated prior yielding load events were apparent. No skin doublers that could have indicated prior damage repair were apparent on the Falcon. Areas of minor skin roughness that may have been indicative of corrosion or repair were visible through the paint on some skin surfaces.




*Figure 6.1-6. General View of NASA Falcon 20*



*Figure 6.1-7. Front View of NASA Falcon 20*



|  |   |  |                        |
|--|---|--|------------------------|
|                 | <b>NASA Engineering and Safety Center<br/>Technical Assessment Report</b> | Document #:<br><b>NESC-RP-12-00822</b> | Version:<br><b>1.0</b> |
| Title:<br><b>Probing Aircraft Flight Test Hazard Mitigation<br/>for the ACCESS Research Team</b> |   | Page #:<br>21 of 118                   |                        |

On one examination occasion, maintenance access panels had been removed. The aircraft's cruciform tail configuration is apparent in Figures 6.1-8 and 6.1-9. The removed access panels allowed examination of internal primary structure and attachment fittings. Figures 6.1-10 and 6.1-11 show the horizontal tail attachment fittings to the vertical tail. No evidence of corrosion was observed in the aircraft interior structure.



*Figure 6.1-8. Falcon 20 Cruciform Tail, Left Side with Access Panels Installed*



*Figure 6.1-9. Falcon 20 Cruciform Tail, Left Side with Access Panels Removed*



**NASA Engineering and Safety Center  
Technical Assessment Report**

Document #:  
**NESC-RP-  
12-00822**

Version:  
**1.0**

Title:

**Probing Aircraft Flight Test Hazard Mitigation  
for the ACCESS Research Team**

Page #:  
22 of 118




*Figure 6.1-10. Falcon 20, Right-side Horizontal Tail Aft Connection*



*Figure 6.1-11. Falcon 20, Right-side Horizontal Tail Forward Connection*

The aft fuselage ring spar (Figure 6.1-12), to which the vertical tail forward spar was attached, was visually inspected. No corrosion was present, but it was greasy with hydraulic fluid residue in a manner considered consistent with the age of the aircraft.

|  |   |  |                        |
|--|---|--|------------------------|
|                 | <b>NASA Engineering and Safety Center<br/>Technical Assessment Report</b> | Document #:<br><b>NESC-RP-12-00822</b> | Version:<br><b>1.0</b> |
| Title:<br><b>Probing Aircraft Flight Test Hazard Mitigation<br/>for the ACCESS Research Team</b> |   | Page #:<br>23 of 118                   |                        |



*Figure 6.1-12. Falcon 20 Visually Inspected Fuselage Frame Showing Greasy Residue*

The Falcon 20 aircraft crew chief made available to the NESC team the following documents to facilitate this assessment:


- *HU-25 Weight and Balance Manual* [ref. 2].
- *Flight Manual: U.S. Coast Guard Series HU-25 Aircraft* [ref. 3].
- *Maintenance Manual: U.S. Coast Guard Model HU-25A Falcon Jet* [ref. 4].
- *Structural Repair Manual: U.S. Coast Guard Model HU-25 Falcon Jet* [ref. 5].

The NESC team reviewed the repair records and confirmed that no significant repairs had been made to the airplane's primary structure.

## **6.2 Previous Flight Tests with Leader/Follower Aircraft**

Research teams from NASA, Canada, and Germany conducted previous flight test research experiments similar to those planned by the ACCESS project team. Aspects of these tests pertinent to the ACCESS experiment are described. The NESC team's analyses and conclusions regarding the relevance of these tests are found in Section 7.0.



|  |   |  |                        |
|--|---|--|------------------------|
|                 | <b>NASA Engineering and Safety Center<br/>Technical Assessment Report</b> | Document #:<br><b>NESC-RP-12-00822</b> | Version:<br><b>1.0</b> |
| Title:<br><b>Probing Aircraft Flight Test Hazard Mitigation<br/>for the ACCESS Research Team</b> |   | Page #:<br>24 of 118                   |                        |

### 6.2.1 NASA Flight Tests

NASA conducted leader/follower aircraft flight tests as part of research experiments, called Subsonic Assessment of Near-Field Flight Interactions (SNIF), in 1995 (SNIF-I), 1996 (SNIF-II), and 1997 (SNIF-III), and as part of Subsonic Assessment of Cloud and Contrail Effects Special Study (SUCCESS) in 1996.

The follower aircraft for all these tests was the NASA Wallops Flight Facility (WFF) asset, a twin-engine Rockwell T-39 Sabreliner (registered N425NA, shown in Figure 6.2-1). The T-39 followed a variety of leader aircraft: NASA B-737, P-3B, and C-130 (SNIF-1); MD-80, B-757, and B-747 (SNIF-II); NASA DC-8 and B-757 (SUCCESS); and Air National Guard F-16 (SNIF-III). Videos of T-39 interaction in wake vortices were reviewed by the team.




*Figure 6.2-1. NASA T-39 Sabreliner*

### 6.2.2 Canadian National Research Council (NRC) Flight Tests

The Canadian NRC conducted leader/follower aircraft flight tests as part of research experiments to measure biofuels exhaust and wake vortex dynamics.

For some of these tests, the NRC employed a 1960s vintage Lockheed T-33 (registered N303FS, shown in Figure 6.2-2) as a follower aircraft behind various military and commercial leader aircraft. The T-33 was capable of high-speed and high-altitude maneuvers from +7.33 to -3.0 g with two pilots. The NRC T-33 was instrumented to measure three-axis rigid body response, allowing the evaluation of aircraft response to turbulence or control maneuver inputs.

|  |   |   |                        |
|--|---|---|------------------------|
|                 | <b>NASA Engineering and Safety Center<br/>Technical Assessment Report</b> | Document #:<br><b>NESC-RP-<br/>12-00822</b> | Version:<br><b>1.0</b> |
| Title:<br><b>Probing Aircraft Flight Test Hazard Mitigation<br/>for the ACCESS Research Team</b> |   | Page #:<br>25 of 118                        |                        |




*Figure 6.2-2. Canadian NRC T-33*

The NRC T-33's sensors included:

- Three-axis accelerations, attitudes, and rates
- Flight and engine control positions
- Longitudinal and lateral stick forces (rear cockpit)
- Angle of attack and sideslip
- Static and dynamic pressures
- Temperature probe
- Provisions for additional sensors

Since 1991, the NRC operated a Falcon 20 (registered C-FIGD, serial number 109, shown in Figure 6.2-3). This Falcon 20 was employed as a follower aircraft by researchers investigating wake vortex development and far-field stability behind a B-727 transport leader aircraft.

|  |   |   |                        |
|--|---|---|------------------------|
|                 | <b>NASA Engineering and Safety Center<br/>Technical Assessment Report</b> | Document #:<br><b>NESC-RP-<br/>12-00822</b> | Version:<br><b>1.0</b> |
| Title:<br><b>Probing Aircraft Flight Test Hazard Mitigation<br/>for the ACCESS Research Team</b> |   | Page #:<br>26 of 118                        |                        |



*Figure 6.2-3. Canadian NRC Falcon 20*

NRC conducted far-field experiments in the 1990s flying their Falcon 20 between 1 and 6 nm behind the B-727. NRC Falcon 20 instrumentation included an inertial measurement system, a global positioning system, and a five-hole flush air data system. With these data, the NRC computed cross-plane wake-induced velocity and deduced shear structures and wake characteristics.


The team noted that because the B-727 MTOW was less than 300,000 lb and the DC-8-72 MTOW was 350,000 lb, the International Civil Aviation Organization (ICAO) classified the B-727 as a “medium” category wake-generating aircraft and the DC-8-72 as a “heavy” category aircraft.

The NESC team observed that NRC required atmospheric conditions that made contrails visible (cited as a relative humidity greater than 70 percent and an air temperature below  $-56$  degrees C) before launching the aircraft for these experiments. The NRC pilots’ practice was to never intentionally enter a visible wake vortex.

In more recent experiments, the NESC team noted that the structural robustness of the NRC Falcon 20 was qualitatively demonstrated by its use in microgravity experiments that required parabolic flight trajectories and recoveries. Of interest, the NRC has also used its Falcon 20 as a *leader* aircraft burning unblended biofuel [ref. 6].

### **6.2.3 German Aerospace Agency Flight Tests**

The German Aerospace Center (DLR), located in Oberpfaffenhofen, Bavaria, Germany, since 1976 has owned and operated a Falcon 20E (registered D-CMET SN 329 and manufactured in 1975 (Figure 6.2-4)). This aircraft is similar to the NASA Falcon 20 but with a lower certified

|  |   |                         |            |
|--|---|-------------------------|------------|
|       | <b>NASA Engineering and Safety Center<br/>Technical Assessment Report</b> | Document #:             | Version:   |
|  |   | <b>NESC-RP-12-00822</b> | <b>1.0</b> |
| Title:   |   | Page #:                 |            |
| <b>Probing Aircraft Flight Test Hazard Mitigation<br/>for the ACCESS Research Team</b> |   | 27 of 118               |            |

MTOW of 29,100 lb. The aircraft had two Garrett Turbojet Triebwerke TFE 731-5BR-2C engines. The aircraft is 59 ft long including its nose boom, with a 54-ft wingspan.



*Figure 6.2-4. DLR Falcon 20*


The NESC team learned that for approximately 20 years DLR has conducted exhaust plume sampling and wake encounter flight tests using this Falcon 20 as a follower aircraft behind many different leader aircraft, including ICAO heavy wake turbulence category leader aircraft with four engines. Summary information of DLR flight experiments involving the Falcon 20 as the follower aircraft is shown in Table 6.2-1.

*Table 6.2-1. DLR Flight Experiments with Falcon 20 as the Follower Aircraft*

| <b>DLR EXPERIMENT</b>   | <b>YEAR(S)</b> | <b>LEADER AIRCRAFT</b>                                |
|---|----------------|---|
| SULFUR, series 1-7  | 1994-1997      | ATTAS, A-310, A-340, B-707, B-747, B-737, DC-8, DC-10 |
| Pollution from Aircraft Emissions in the North Atlantic Flight Corridor (POLINAT) | 1997           | Several aircraft, including NASA DC-8                 |
| Contrail and Cirrus Experiment (CONCERT)  | 2009-2011      | Various aircraft                                      |
| Lufthansa flight experiment   | 2012           | A-380   |

For these tests, the DLR Falcon 20 was modified to allow on-board atmospheric research teams to measure trace gases and aerosols and to collect air samples for subsequent laboratory analysis. The top and bottom of the aircraft's fuselage were modified to include optical windows for

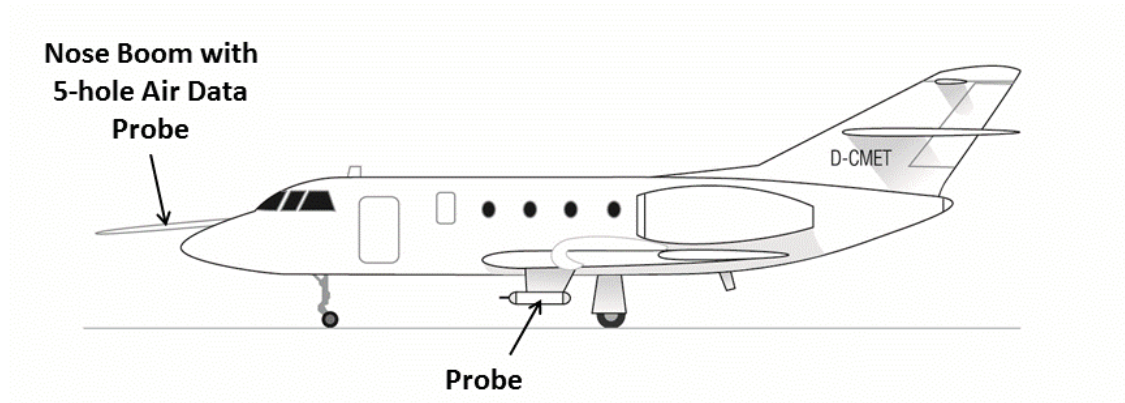


|  |   |   |                        |
|--|---|---|------------------------|
|                 | <b>NASA Engineering and Safety Center<br/>Technical Assessment Report</b> | Document #:<br><b>NESC-RP-<br/>12-00822</b> | Version:<br><b>1.0</b> |
| Title:<br><b>Probing Aircraft Flight Test Hazard Mitigation<br/>for the ACCESS Research Team</b> |   | Page #:<br>28 of 118                        |                        |

cameras and Laser Imaging Detection and Ranging (LIDAR) atmospheric measurement systems. The following is a summary of modifications and additions made to the DLR Falcon 20:

- Nose boom with integrated flow probe for measuring inflow velocity and direction of inflow.
- A total of three special windows in the roof and the floor of the fuselage, which can be used, for instance, for the deployment of LIDAR instruments for atmospheric measurements. The lower special windows can be protected against debris damage during takeoff and landing by a roller door.
- New engines with additional power generators for supplying power to experiments (2×300 amperes at 28 volts).
- Four small openings (with a diameter of 8 cm) in the top of the fuselage.
- Four underwing hard points for carrying particle measurement systems (PMS).
- Central hard point on the bottom of the fuselage for carrying various measuring containers.
- Side windows for IR and radar antennas, so-called microwave measuring equipment.
- Hard points on the lower aft section of the fuselage for carrying radiometers.


Figure 6.2-5 shows the general layout of some key instruments on the DLR Falcon 20.



**Figure 6.2-5. General Layout of Falcon 20 DLR Experiment Instrumentation**

After outreach efforts by the NESC team, two DLR Falcon 20 flight test pilots made themselves available by teleconference on September 18, 2012, to answer questions from both the project and the NESC team. The DLR pilots provided numerous comments from their experiences flying exhaust plume sampling missions using their Falcon 20 (Appendix G). These were discussed at length by the NESC team and evaluated with other available information.



|  |   |  |                        |
|--|---|--|------------------------|
|                 | <b>NASA Engineering and Safety Center<br/>Technical Assessment Report</b> | Document #:<br><b>NESC-RP-12-00822</b> | Version:<br><b>1.0</b> |
| Title:<br><b>Probing Aircraft Flight Test Hazard Mitigation<br/>for the ACCESS Research Team</b> |   | Page #:<br>29 of 118                   |                        |

Descriptions and team assessment of DLR lessons learned are described at pertinent locations throughout Section 7.0.

### 6.3 Falcon Flight Test Hazards

Prior to the NESC team's involvement, the ACCESS project team conducted an SRR in June 2012 (Appendix B). One of the SRR's 12 success criteria was that the review board members conclude that major risks had been identified and technically assessed and that viable mitigation strategies had been defined.

Three safety hazards were identified in the SRR that could result in loss of personnel, loss or damage to asset, or loss of mission: structural failure, engine flameout, and loss of control. The structural failure hazard was the specific focus of this NESC assessment. The engine flameout and loss-of-control hazards were in scope inasmuch as they were systemically involved with the structural failure hazard. For example, recovery from loss of control could result in structural failure. This section describes the three hazards. The team's analyses and assessments are given in Section 7.0.

#### 6.3.1 Aircraft Structural Failure

This hazard was described in the SRR charts as follows: "The probing aircraft will see significantly different flow conditions in the wake of the heavy lead aircraft than in normal planned operation resulting in a risk of overloading or failure of aircraft structural components." Possible mitigations described included:


- Determine the wake flow conditions for the area to be probed.
- Compare certification loads for probing aircraft to expected loading from above and determine safe operating envelope.
- Examine additional instrumentation for structural health.
- Evaluate crew safety/egress.
- Utilize a build-up test approach, to include envelope expansion testing.

This hazard was the principal focus of the NESC assessment team. All of the proposed mitigations were assessed except evaluating crew egress.

#### 6.3.2 Engine Flameout due to Ingestion of Distorted Flow

This hazard was described as follows: "Ingestion of distorted flow in the wake of the heavy lead aircraft could cause engine distress up to and including flameout on the probing aircraft with potentially limited ability to restart." Possible mitigations described included:

- Determine/examine engine distorted flow tolerance.
- Determine/examine wake distortion in the area to be probed.

|  |   |  |                        |
|--|---|--|------------------------|
|                 | <b>NASA Engineering and Safety Center<br/>Technical Assessment Report</b> | Document #:<br><b>NESC-RP-12-00822</b> | Version:<br><b>1.0</b> |
| Title:<br><b>Probing Aircraft Flight Test Hazard Mitigation<br/>for the ACCESS Research Team</b> |   | Page #:<br>30 of 118                   |                        |

- Determine and account for engine restart envelope.
- Evaluate probing aircraft state instrumentation capabilities.
- Use the above to determine safe operating limits and plan for recovery altitude for abnormal aircraft attitudes.
- Evaluate crew safety/egress.

This hazard was discussed by the NESC assessment team in the course of its investigation of the aerodynamic flow fields behind the DC-8.

### 6.3.3 Aircraft Controllability/Operability at Unusual Attitudes

This hazard was described as follows: “The lighter probing aircraft flying in the wake of the heavy lead aircraft will likely encounter significant drastic attitude and rate changes resulting in potential difficulties in fuel system function or controllability for a platform not rated for acrobatics.” Possible mitigations described included:

- Determine/examine engine distorted flow tolerance.
- Determine/examine wake distortion in the area to be probed.
- Determine and account for engine restart envelope.
- Evaluate probing aircraft state instrumentation capabilities.
- Use the above to determine safe operating limits and plan for recovery altitude for abnormal aircraft attitudes.
- Evaluate crew safety/egress.


This hazard was discussed by the NESC team in the course of its evaluation of Falcon 20 trajectory simulations.

## 6.4 Project Analyses

The ACCESS project team provided a briefing to the NESC team on August 14, 2012, to describe the wake modeling, aerodynamic analyses, and structural assessment they had completed to date. These project charts are included in Appendix D. This section describes the information conveyed in that meeting. The team’s analyses and assessment are given in Section 7.0.

### 6.4.1 Wake Model

A DC-8 vortex pair wake model, referred to here as the Proctor model, was described by the ACCESS project team [ref. 7]. This model employed the Burnham-Hallock model of vortex-induced tangential velocity. The modeler assumed an elliptic DC-8 wing loading, a DC-8 weight of 280,000 lb, and a vortex core radius of 1 percent of the DC-8 wingspan. A three-phase model of vortex strength decay as a function of distance behind the DC-8 (weak decay in the near field,

|  |   |   |                        |
|--|---|---|------------------------|
|                 | <b>NASA Engineering and Safety Center<br/>Technical Assessment Report</b> | Document #:<br><b>NESC-RP-<br/>12-00822</b> | Version:<br><b>1.0</b> |
| Title:<br><b>Probing Aircraft Flight Test Hazard Mitigation<br/>for the ACCESS Research Team</b> |   | Page #:<br>31 of 118                        |                        |

followed by rapid decay as the vortices rolled up, followed by gradual decay in the mid and far field) was based on the results described in reference 8.

#### **6.4.2 Aerodynamic Analysis**

The ACCESS project team described an analysis of Falcon aerodynamic loads induced by the DC-8 trailing vortex wake that employed the Proctor vortex model [ref. 9]. In this spreadsheet analysis, aerodynamic surfaces were modeled using strip theory, which is a simplified vortex lattice panel method that would be expected to predict higher loads than a panel method or a computational fluid dynamics (CFD) model.

The analyst assumed a worst-case load condition, where a DC-8 trailing vortex was centered on the cruciform intersection of the Falcon horizontal tail and vertical tail. Loading distributions were estimated on both surfaces, and the resulting bending moments were computed. This information was used in the structural analysis described in Section 6.4.3.

#### **6.4.3 Structural Assessment**


The ACCESS project team described the Falcon horizontal and vertical tail structural analysis that had been conducted [ref. 10]. This assessment included both vortex-induced and gust-induced loads. The analyst indicated three stated objectives:

- Determine if vortex-induced loads on the Falcon horizontal and vertical tail drove the design of those components.
- Evaluate the horizontal and vertical tail structures for vortex-induced loads combined with level flight loads, and evaluate gust-induced loads.
- Determine horizontal and vertical tail structural integrity by comparing computed loads against best available information of the Falcon's maximum design loads.

In this analysis, the Falcon 20 was assumed to be about 1.24 miles (2.0 km) behind the DC-8 with its horizontal and vertical tail intersection centered on the primary DC-8 trailing vortex.

The analyst investigated whether it would be necessary to superimpose gust-induced loads along with vortex-induced loads on top of normal flight loads. It was concluded that horizontal tail vortex-induced loads and interface moments were sufficiently in excess of maximum flight loads and moments so as to envelop gust-induced load conditions. The ACCESS project team also concluded that vertical tail vortex-induced loads were generally lower than flight loads if maximum gust loads were not included and that vertical tail vortex-induced interface moments were well in excess of rudder flight loads.

The ACCESS project team acknowledged the uncertainty in the results associated with limited and incomplete tail design loads information from the aircraft manufacturer. The ACCESS team concluded that unless the margins of safety for the horizontal and vertical tails and the rudder were definitively known, vortex-induced loads could be assumed to adversely affect the structural integrity of the aircraft.

|  |   |  |                        |
|--|---|--|------------------------|
|                 | <b>NASA Engineering and Safety Center<br/>Technical Assessment Report</b> | Document #:<br><b>NESC-RP-12-00822</b> | Version:<br><b>1.0</b> |
| Title:<br><b>Probing Aircraft Flight Test Hazard Mitigation<br/>for the ACCESS Research Team</b> |   | Page #:<br>32 of 118                   |                        |

## 7.0 Data Analyses

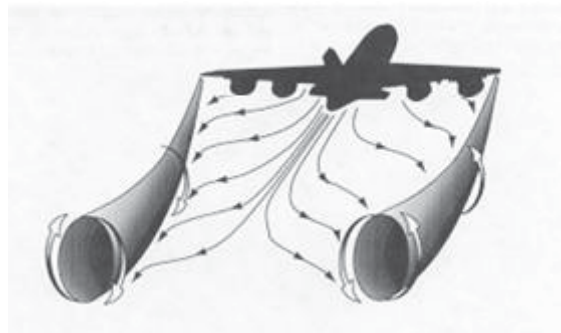
### 7.1 Wake Vortex Behavior

For the cross-discipline NESC team to effectively conduct this assessment, it was necessary for the members to achieve a sufficient understanding of the physics of wake vortex behavior in general and, more specifically, in the near and far field behind a four-engine jet aircraft. This was achieved by research and discussion, facilitated by the NESC team’s wake vortex expert consultant.

#### 7.1.1 Fundamental Behavior and Evolution


When an aircraft travels through the atmosphere, wake vortices associated with lift forces are left behind in its atmospheric wake. Separate vortices emanate (i.e., are shed) from principal external surface features, including but not limited to wingtips, aileron surface edges, engines, flap edges, wing roots, horizontal tail tips, and elevator edges.

When an aircraft is configured for cruise (referred to as a “clean wing” configuration) with its wing flaps and slats retracted and landing gear retracted, the largest two vortices are typically shed from its wingtips. These wingtip vortices are dependent on aircraft weight, geometry, altitude, and atmospheric conditions [ref. 11]. Smaller vortices are shed from other features. At increasing distances behind the aircraft (i.e., at increased elapsed time since shed), these smaller vortices will merge or “roll up” with the larger wingtip vortices. The process of smaller vortices rolling up with a wingtip vortex typically occurs sequentially from those nearest the wingtip vortex to those farthest (i.e., from outboard to inboard), as illustrated in Figure 7.1-1.



*Figure 7.1-1. The Rolling-up Process (reprinted from ref. 12)*

Since ACCESS flight tests were to be conducted at cruise altitudes with the DC-8 in a clean wing configuration, the NESC team’s vortex analyses was focused primarily on wingtip vortices. The NESC team discovered that in academic literature wake vortex behavior is better characterized for landing configurations than for clean wing configurations because of wake safety implications for aircraft operated near airports where airspace density is greater and the severity of an inadvertent wake encounter can be catastrophic. When an aircraft is configured for landing (i.e., with wing flaps and slats and landing gear deployed), its center of lift typically

|  |   |   |                        |
|--|---|---|------------------------|
|                 | <b>NASA Engineering and Safety Center<br/>Technical Assessment Report</b> | Document #:<br><b>NESC-RP-<br/>12-00822</b> | Version:<br><b>1.0</b> |
| Title:<br><b>Probing Aircraft Flight Test Hazard Mitigation<br/>for the ACCESS Research Team</b> |   | Page #:<br>33 of 118                        |                        |

moves inboard; in this condition, flap vortices dominate rather than wingtip vortices. Much of the available information was for wings with flaps and slats deployed and for wake vortex generation, roll up, behavior, and dissipation at altitudes near the ground [ref. 13]. A relative dearth of clean wing wake vortex data forced the NESC team to consider fundamental principles.

An aircraft wing's aerodynamic lift distribution affects the strength, span location, and behavior of its wingtip vortices. The distribution is determined not only by configuration but also by wing shape. Theory predicts that for an elliptical wing loading distribution (as would be associated with a clean wing configuration), shed wingtip vortices will quickly migrate inboard from the wingtips, toward a location approximately  $l^{1/4} \approx 78$ -percent wingspan [ref. 14].

A wake vortex core size (core radius) is defined as the radial distance from a vortex center to a point of maximum tangential velocity. In this report, core sizes are expressed in terms of percent wingspan. Field tests have shown that core sizes in the immediate wake of transport aircraft are consistently on the order of 1 percent of the aircraft's wingspan [ref. 15].

A 1-percent wake vortex core size for a DC-8 with a 148-ft wingspan would have a radius of approximately 1.5 ft.

Core sizes are typically 1 to 3 percent of an aircraft's geometric wingspan [ref. 14]. Core sizes grow and vortex strengths decay with time after they have been shed. Numerous decay models are used by discipline analysts, but all share the fundamental feature that wake vortex strengths grow larger in the far field than in the near field [refs. 16-18]. Vortex decay and dissipation depends on atmospheric conditions and may also depend on instabilities caused by rolled-up exhaust plumes [ref. 19].


A wing's aerodynamic lift distribution impacts vortex strength and the span location behind which the vortex will trail. The distribution may also affect decay behavior [ref. 14]. As stated previously, wake vortex decay research has mostly been focused on takeoff and landing configurations at low altitudes [ref. 13].

Engine exhaust plumes roll up around wingtip vortices in a manner similar to smaller shed vortices. Outboard engine plumes can be expected to roll up with wingtip vortices early [ref. 19]. Vortices shed from the horizontal tail and from inboard engine plumes (if any) can be expected to roll up after.


Under certain atmospheric conditions, engine exhaust plumes are made visible as ice particle contrails. Wake vortices can then become visible if engine contrails become rolled up around them. Contrails and wake vortices can remain visible for tens of miles [ref. 19].

Based on review of references 11, 13, 14, and 16–27, the team compiled seven summary research findings applicable to the formation, decay, and demise of high-altitude, clean wing wake vortices and to wake vortex interactions with both aircraft components and the atmosphere. Some of these will be described in more detail in the following sections in the context of the planned ACCESS flight experiments.



|  |   |  |                        |
|--|---|--|------------------------|
|                 | <b>NASA Engineering and Safety Center<br/>Technical Assessment Report</b> | Document #:<br><b>NESC-RP-12-00822</b> | Version:<br><b>1.0</b> |
| Title:<br><b>Probing Aircraft Flight Test Hazard Mitigation<br/>for the ACCESS Research Team</b> |   | Page #:<br>34 of 118                   |                        |

1. Wake vortex formation and demise are complex processes that depend on many variables, including the generating aircraft type, design and configuration; operational conditions such as density altitude and true airspeed; and atmospheric conditions of turbulence and stratification.
2. The dominant vortex in cruise configuration (landing gear retracted, flaps and slats retracted) is the wingtip vortex, which quickly migrates to a position about 78 percent of the geometric wingspan for elliptic wing loadings. In the absence of data to the contrary regarding a specific airplane, elliptic loading is a reasonable assumption.
3. Wake vortex creation and demise is characterized in two clearly defined regions and a less clearly defined third region. Note that researchers have defined these regions differently than the project team:
  - Near field: distances up to approximately 20 wingspans aft of the generating aircraft (the project team defines the near field as up to approximately 5 wingspans aft of the DC-8 for the purposes of their experiment).
  - Far field: the effects of atmospheric and other factors cause the vortices to begin to be unstable and break up (the project team defines the far field as approximately 2 to 20 miles aft of the DC-8).
  - Mid field: the region between the mid field and the far field (the project team defines the mid field as approximately between 5 wingspans and 2 miles aft of the DC-8).
4. Jet engine exhaust plumes are quickly entrained by, or rolled up, around the wingtip vortex. Outboard engine exhaust, being physically closer to the wingtip vortex, is entrained first; inboard engine exhaust is entrained later.
5. Jet engine exhaust separates from the wingtip vortices in mid- and far-field regions. This separation is thought to be caused by buoyancy effects of the heated gases. The extent of this separation is dependent on the degree of jet turbine and jet bypass mixing that takes place at the engine exhaust.
6. Condensation trails (contrails) can appear behind aircraft when they fly in atmospheric conditions above about 40-percent relative humidity and below about -40 degrees C (some cite lower temperatures). These conditions cause the water vapor in engine exhaust gases to condense and freeze into ice crystals before they have time to evaporate or sublime.
7. An aircraft that encounters a wake vortex from above or below at a shallow angle (interpreted as below 5 degrees, but as small as 1 degree) of flight path with respect to the vortex core axis (grazing angle) may deflect off the vortex. At such angles, it may be difficult or impossible to penetrate the core because the vortical flow forces may overpower the airplane's control authority. At grazing angles greater than 30 degrees,

|  |   |                         |            |
|--|---|-------------------------|------------|
|       | <b>NASA Engineering and Safety Center<br/>Technical Assessment Report</b> | Document #:             | Version:   |
|  |   | <b>NESC-RP-12-00822</b> | <b>1.0</b> |
| Title:   |   | Page #:                 |            |
| <b>Probing Aircraft Flight Test Hazard Mitigation<br/>for the ACCESS Research Team</b> |   | 35 of 118               |            |

an encountering aircraft is likely to transit the vortex core quickly, so that it would primarily experience longitudinal axis acceleration.

### 7.1.2 Near-Field Behavior

The NESC team considered other data that could characterize the near-field geometry and behavior of high-altitude, clean wing wingtip vortices and exhaust plumes. Understanding this geometry could facilitate developing pilot entry, sampling, and exit techniques and test hazard mitigations.

The NESC team conducted a basic photometric analysis of aircraft contrail photographs, considered and discussed current capabilities of CFD tools, reviewed roll-up evolution research data, reviewed mission rules from a 2003 NASA Sky Surfing for Fuel Economy (SURF) near-field flight experiment, and reviewed experiential comments from DLR pilots who had performed near-field flight experiments.

#### Photometric Analyses


The NESC team conducted a basic photometric analysis of 12 photographs of four-engine heavy transport aircraft flying at high altitudes in clean wing configurations in atmospheric conditions suitable to create exhaust contrails. The images were publically available [ref. 28] but copyrighted so are not reproduced here. The photographed aircraft surveyed were Boeing 747-400, Airbus 340-500 and 340-600, and Antonov 124-100 aircraft. The aircraft weights, altitudes, and airspeeds were not known, but bounding aircraft design weights were publically available for these aircraft types (see Table 7.1-1).

*Table 7.1-1. Bounding Weights for Aircraft in the Photometric Analysis*

| Aircraft Type                   | MTOW, lb | Max Zero Fuel Weight, lb |
|---------------------------------|----------|--------------------------|
| <b>Boeing 747-400</b> [ref. 29] | 875,000  | 542,500                  |
| <b>Airbus 340-600</b> [ref. 30] | 811,300  | 540,000                  |
| <b>Antonov An-124</b> [ref. 31] | 893,000  | 385,000                  |
| <b>Airbus 340-500</b> [ref. 30] | 820,100  | 506,900                  |

This photographic data did not represent a statistically significant sample. The data did not include full knowledge of the conditions, and the photographers' perspectives were not known. The NESC team only considered the data useful as representative information regarding contrail and vortex near-field behavior that may corroborate other information. The analyses included measurements of the distance where the exhaust contrails appeared to roll up and the distance where the inboard exhaust plumes had sunk to their minimum elevation relative to the outboard plumes. Both could have implications on sampling technique for the ACCESS Falcon crew. In its analysis, the NESC team superimposed rulers of approximate wingspan length, aligned with the fuselage and positioned to bisect the space between the two inboard contrails.

In the photographs analyzed, contrails were observed to become more diffuse with distance aft of the aircraft, consistent with theory but highly dependent on atmospheric conditions. Outboard

|  |   |   |                        |
|--|---|---|------------------------|
|                 | <b>NASA Engineering and Safety Center<br/>Technical Assessment Report</b> | Document #:<br><b>NESC-RP-<br/>12-00822</b> | Version:<br><b>1.0</b> |
| Title:<br><b>Probing Aircraft Flight Test Hazard Mitigation<br/>for the ACCESS Research Team</b> |   | Page #:<br>36 of 118                        |                        |

contrails were seen to migrate outboard away from each other, consistent with theory as they are drawn toward the initially invisible wingtip vortices that trail the wing at around 78-percent span. Outboard contrails exhibited rotation indicative of having rolled up around the port-side wingtip vortex beyond 2 wingspans aft of the aircraft. Consistent with theory, inboard contrails were seen to physically sink below the altitude of the outboard contrails, affected by the aerodynamic downwash of the wing. At about 4 wingspans aft, inboard contrail vertical sinking relative to outboard contrails was observed to have reached a maximum. These phenomena were observed in all of the images analyzed.

Summary findings from the basic photometric analysis were that outboard contrails rolled up between 1 and 9 wingspan lengths aft; inboard contrails reached maximum vertical descent relative to outboard contrails at no less than 4 to 5 wingspans aft; and inboard contrails did not roll up with wingtip vortices until beyond 9 wingspan lengths aft. If translated to the DC-8, this would infer a near-field aft boundary of more than 1,300 ft (more than 0.25 miles).

The NESC team examined two contrail photographs of a four-engine aircraft at cruise condition in a 2011 paper by Rossow (Figures 3 and 4 in ref. 23). The estimated distance where exhaust plumes were no longer clearly distinct and identifiable (suggesting exhaust/vortex mixing) was about 1,000 ft (300 m), which is consistent with the previously identified value.

### **CFD Simulation of Near-Field Flow Field**


The NESC team reviewed CFD studies and current capabilities for modeling near-field flow and wake vortex roll-up. National laboratories, universities, and airframe companies engaged in wake vortex research and development and in wake vortex separation standards activities have robust CFD capabilities for detailed flow-field studies. But developing models for such CFD studies would require significant resources (both time and money) and would require wind tunnel and probably flight test data to calibrate the CFD predictions and validate the model. Because of the short time allocated for this assessment, the team agreed not to pursue development of a comprehensive CFD near-field flow behavior model. The team instead used the validated numerical model described in Section 7.2.

### **Exhaust Plume and Wake Vortex Roll-up**

The team reviewed the limited research information that was available to better understand the evolution and behavior of exhaust plume roll-up around wake vortices in the near-field and mid-field regions. The results from NESC photometric analysis indicated the DC-8 outboard engine exhaust plumes could become entwined or rolled up with the lifting vortices as quickly as 150 ft (1 wingspan) aft of the aircraft, and the inboard engine exhaust plumes could roll up between 5 and 9 wingspans (750 to 1350 ft) aft of the aircraft. Additional resources were discussed to better understand the roll-up phenomenon.

Figure 7.1-2 is a useful representative of ubiquitous photographs of aircraft wake vortices. It shows an unidentified twin engine jet transport airplane in a landing configuration (looking aft from below), at an unknown speed and altitude, with a vortex pair behind it made visible by




|  |   |  |                        |
|--|---|--|------------------------|
|                 | <b>NASA Engineering and Safety Center<br/>Technical Assessment Report</b> | Document #:<br><b>NESC-RP-12-00822</b> | Version:<br><b>1.0</b> |
| Title:<br><b>Probing Aircraft Flight Test Hazard Mitigation<br/>for the ACCESS Research Team</b> |   | Page #:<br>37 of 118                   |                        |

clouds and fog at an unknown distance. The relative size of the evident rolled up exhaust plumes and vortices can be seen to be about twice as wide as high.



*Figure 7.1-2. Photograph of Merging Exhaust and Vortex Pair from Transport Airplane in Landing Configuration at Unknown Speed and Altitude*

The NESC team reviewed reference 24, which described experimental data from a U.S. Air Force (USAF) study of a twin-engine Douglas Aircraft Company A-3 jet bomber aircraft (with a wingspan of 72.5 ft) flying in a clean wing configuration in the near- and mid-field regions and photographed using temperature-measuring instrumentation onboard another A-3 aircraft. Wing loading distribution is assumed to be elliptical. The NESC team first examined the optically active portions of engine exhaust and its interaction with wingtip vortex flow [ref. 24].

|  |   |   |                        |
|--|---|---|------------------------|
|                 | <b>NASA Engineering and Safety Center<br/>Technical Assessment Report</b> | Document #:<br><b>NESC-RP-<br/>12-00822</b> | Version:<br><b>1.0</b> |
| Title:<br><b>Probing Aircraft Flight Test Hazard Mitigation<br/>for the ACCESS Research Team</b> |   | Page #:<br>38 of 118                        |                        |

The photograph in Figure 7.1-3 shows an A-3 aircraft in cruise configuration (looking aft from above), at  $M = 0.5$  and an altitude of 20,000 ft, with visible exhaust rolled up around a vortex pair about 330 ft (100 m, or about 5 wingspan lengths) behind it [ref. 24]. The image quality is poor because it was captured from a limited resolution video, but it shows features sufficient for this purpose. Dark exhaust plumes are visible behind both engines. The merged exhaust/vortices are visible beneath the timestamp. The merged vortex width-to-height ratio is approximately 2:1 for the total rolled-up flow field.



*Figure 7.1-3. Photograph of Merging Exhaust and Vortex Pair from an A-3 Airplane in Cruise Configuration at  $M = 0.5$  and Altitude of 20,000 ft*



# NASA Engineering and Safety Center Technical Assessment Report

Document #:  
**NESC-RP-  
12-00822**

Version:  
**1.0**

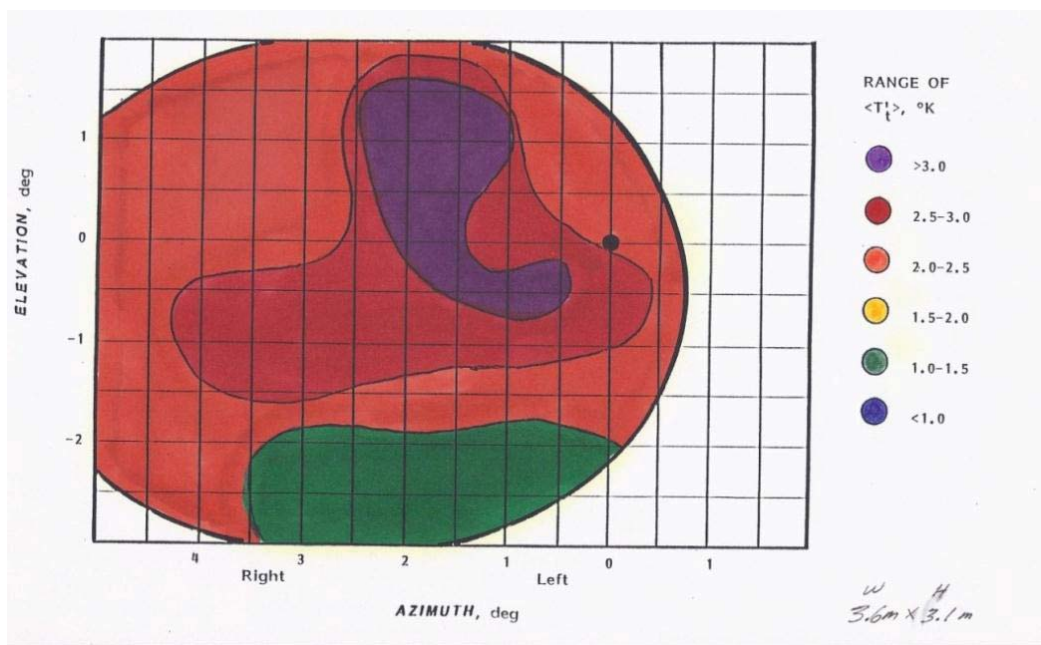
Title:

## Probing Aircraft Flight Test Hazard Mitigation for the ACCESS Research Team

Page #:  
39 of 118

The NESC team reviewed Figures 7.1-4 through 7.1-7 (reprinted here from ref. 24) and examined the locations in trail of exhaust features as they were entrained into the wingtip vortices. These four figures show a series of interpreted spatial total temperature data, taken at distances of about 98, 330, 980, and 3300 ft (30, 100, 300, and 1000 m, respectively) behind an A-3 aircraft. Total temperature data were considered as markers to locate exhaust gases. The camera was mounted just outboard the port engine on a lead airplane, looking aft along a line of sight that is depicted by the black dot in each figure. All scales are in degrees off of the bore sight.

Figure 7.1-4 shows a single exhaust that at 98 ft (30 m, or about 1.4 wingspan lengths) behind the aircraft has spread to about 12 by 10 ft (3.6 by 3.1 m). This result is consistent with one team member's A-3 formation flying experience that the initial exhaust plume spreading angle was about 5 degrees.



**Figure 7.1-4. Contours of Total Temperature Fluctuation 98 ft (30 m) Behind an A-3 (scale: 1.69 ft per degree (width), 2.03 ft per degree (height))**



# NASA Engineering and Safety Center Technical Assessment Report

Document #:  
**NESC-RP-  
12-00822**

Version:  
**1.0**

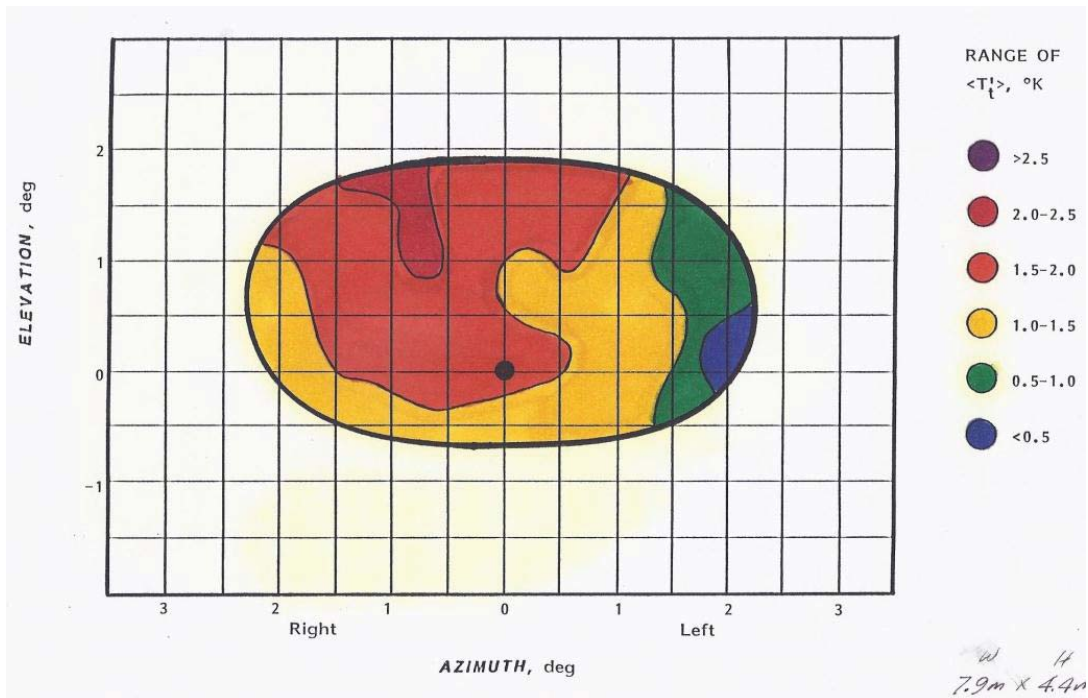
Title:

## Probing Aircraft Flight Test Hazard Mitigation for the ACCESS Research Team

Page #:

40 of 118

At 330 ft (100 m, or about 5 wingspan lengths) behind the aircraft (Figure 7.1-5), a single exhaust plume is still apparent nearly centered on the bore sight. It has been flattened by the vortex interaction. Further significant spreading of the exhaust is due to the mechanical forced mixing of the vortex flow rather than circular shear layer entrainment. At this distance the jet velocity has diminished to less than 10 percent of its initial value.



**Figure 7.1-5. Contours of Total Temperature Fluctuation 330 ft (100 m) Behind an A-3 (scale: 3.70 ft per degree (width), 2.89 ft per degree (height))**





# NASA Engineering and Safety Center Technical Assessment Report

Document #:  
**NESC-RP-  
12-00822**

Version:  
**1.0**

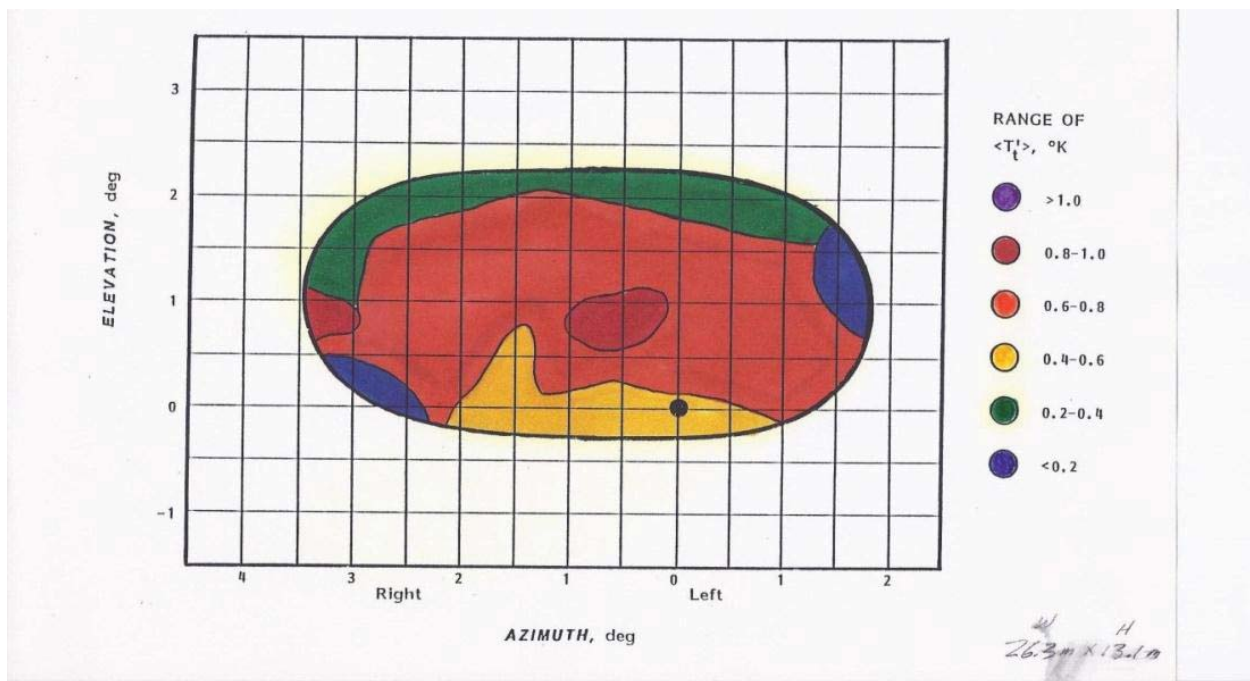
Title:

## Probing Aircraft Flight Test Hazard Mitigation for the ACCESS Research Team

Page #:


41 of 118

At 980 ft (300 m, about 14 wingspan lengths) behind the aircraft, this single-exhaust situation has changed completely (Figure 7.1-6). The center of the total exhaust has moved to the starboard side of the bore sight, indicating that the two exhaust and vortex combinations are contiguous. The contours of temperature fluctuation have lost most of their structure, indicating a forced mixing from the encroaching vortex flow. This is just as in the qualitative portrayal in Figure 7.1-3. For the specific A-3 aircraft and flight conditions being discussed here, the search for the exhaust at 980 ft (300 m) and beyond would put the trail airplane in a vortex flow field.

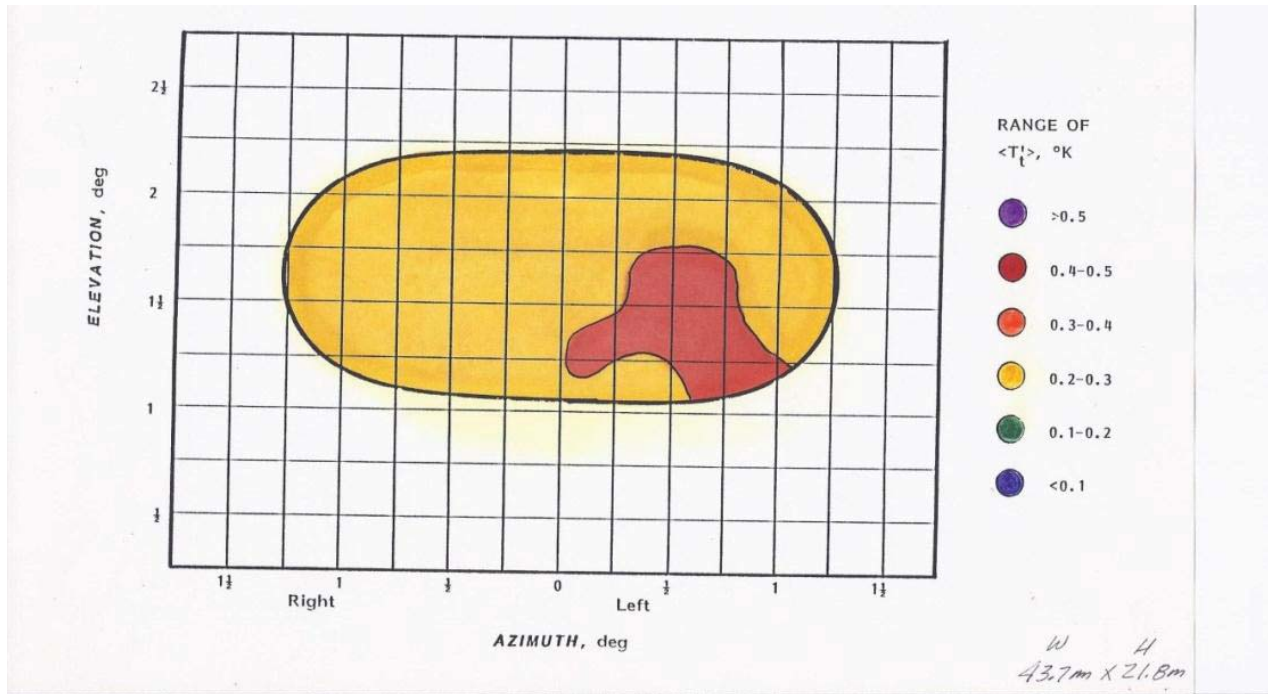


**Figure 7.1-6. Contours of Total Temperature Fluctuation 980 ft (300 m) Behind an A-3  
(scale: 12.3 ft per degree (width), 8.60 ft per degree (height))**



|  |   |                         |            |
|--|---|-------------------------|------------|
|       | <b>NASA Engineering and Safety Center<br/>Technical Assessment Report</b> | Document #:             | Version:   |
|  |   | <b>NESC-RP-12-00822</b> | <b>1.0</b> |
| Title:   |   | Page #:                 |            |
| <b>Probing Aircraft Flight Test Hazard Mitigation<br/>for the ACCESS Research Team</b> |   | 42 of 118               |            |

At 3,300 ft (1 km, about 50 wingspan lengths) behind the aircraft (Figure 7.1-7), the entire combination flow has merged, temperature fluctuations have died off, and the whole flow field containing the exhaust is about 144 by 72 ft (44 by 22 m). Again, the rolled-up flow field is about twice as wide as it is high.




**Figure 7.1-7. Contours of Total Temperature Fluctuation 3,300 ft (1 km) Behind an A-3 (scale: 20.5 ft per degree (width), 14.3 ft per degree (height))**

Beyond 3,300 ft (1 km), few significant changes occur, other than dissipation of the vortex flow into the far field [ref. 24].

There is evidence that exhaust gases remain around the perimeter of the rotating vortex in the mid field in the photographic observations and numerical modeling treatment presented by Rossow and Brown [ref. 19].

Of final note, the sensory experience of the A-3 flight test pilot was that this merged exhaust/vortex region was dangerous. The A-3 survived being “spit out” of vortex flows undamaged, as it was designed for high-vertical-load-factor (high-g) maneuvers. Seasoned pilots were able to recover from these events.

The NESC team concluded from this analysis that for aircraft in a clean wing configuration a practical range aft of where all engines exhaust plumes would likely be rolled up would be between 15 and 50 wingspans. For the DC-8 aircraft, this translates to 2,000 to 7,400 ft. The low-end result of 2,000 ft was generally consistent with the team’s other estimates.

|  |   |  |                        |
|--|---|--|------------------------|
|                 | <b>NASA Engineering and Safety Center<br/>Technical Assessment Report</b> | Document #:<br><b>NESC-RP-12-00822</b> | Version:<br><b>1.0</b> |
| Title:<br><b>Probing Aircraft Flight Test Hazard Mitigation<br/>for the ACCESS Research Team</b> |   | Page #:<br>43 of 118                   |                        |

### NASA Sky SURF Near-Field Observations


The NESC team reviewed mission rules and pilot observations from a 2003 NASA near-field flight test of an F-18 aircraft flying near the NASA DC-8 aircraft to assess fuel savings effects. This was an exploratory investigation at DFRC of large aircraft vortex-induced performance benefits on a fighter aircraft. The F-18 aircraft joined formation aft and outboard of the DC-8 wingtip in the aerodynamic upwash flow field associated with the DC-8's wingtip vortex and slowly moved in laterally to explore the vortex effects. The tests were conducted at 25,000 ft with a separation of about 200 ft nose to tail.

All SURF tests were conducted at 25,000 ft at  $M = 0.56$ . Mission rules required the test F-18 to maintain at least 100 ft nose-to-tail clearance behind the DC-8, and a chase aircraft monitored the nose-to-tail clearance. The DC-8 was required to maintain straight and level flight while the F-18 test aircraft was in formation in the wingtip vortex.

SURF pilots were required to be proficient with formation flight from the DFRC Autonomous Formation Flight (AFF) (F/A-18) project or from SURF flight simulation. Flight simulation showed vortex encounters generating vertical acceleration excursions of less than 2.5 g's. Project documents referenced vortex interaction testing [ref. 32] from the 1970s, which showed vertical acceleration excursions of less than 2.5 g's regardless of aircraft combination. Participant pilot observations of near-field DC-8 exhaust plume and vortex behavior were not captured. An F-18 research pilot remarked that "the overall effect of entering the (DC-8) vortex core was much milder than expected."

### DLR Near Field Observations

The NESC team reviewed DLR Falcon pilot experiential comments that were shared in a September 2012 teleconference with the ACCESS and NESC teams. DLR experimenters conducted flight experiments for 20 years using a Falcon 20 aircraft similar to the NASA asset, following in the near-field behind numerous twin- and four-engine transport aircraft. The four-engine lead aircraft in the DLR experiments were reported to have included six passenger and freight aircraft types: Airbus 380-800, 340-500, and 340-600; Boeing 707-320; and Douglas DC-8-62 and DC-8-72. Figure 7.1-8 shows the view from the DLR Falcon 20 following in the near-field behind an A-340 aircraft. It was not clear how long ago the DC-8 flight experiments occurred or if those were reflected in their experiential comments. It was deduced from photographic images provided by DLR that the B-707 and A-340 flight experiments were contemporaneous. The A-380 experiments were necessarily recent, as that type was certified in 2006.

|  |   |  |                        |
|--|---|--|------------------------|
|                 | <b>NASA Engineering and Safety Center<br/>Technical Assessment Report</b> | Document #:<br><b>NESC-RP-12-00822</b> | Version:<br><b>1.0</b> |
| Title:<br><b>Probing Aircraft Flight Test Hazard Mitigation<br/>for the ACCESS Research Team</b> |   | Page #:<br>44 of 118                   |                        |




*Figure 7.1-8. DLR Falcon 20 Flying behind an A-340*

The DLR Falcon pilots observed that outboard engine exhaust plumes from four-engine aircraft could roll up around clean wing wingtip vortices as near as 1 wingspan aft of the aircraft's tail cone. They described a practicable near-field sample area as between 1 and 5 wingspans behind four-engine aircraft, depending on atmospheric conditions. A 5-wingspan aft limit would be approximately 750 ft for the DC-8.

The DLR aft limit of 5 wingspan lengths was based on their experience seeing the contrail-wrapped vortices and "feeling" the Falcon 20 wingtip interaction with the flow field near the vortex. However, the DLR pilots were not specific about to which lead aircraft this comment applied. The NESC team observed that A-380s and A-340s were considerably larger than B-707s and DC-8s. Wingtip wake vortices from larger (assumed heavier) aircraft would be stronger than for smaller aircraft. The vortices would also logically be further apart laterally for larger aircraft (with assumed longer wingspans).

For any aircraft, the near-field sample area width could be practically defined as the distance between the two wingtip wake vortices, and their theoretical locations could be generally assumed to be at about 78-percent wingspan in the near field beyond 1 wingspan aft [ref. 14]. The team compiled a table of distances between inboard engine centerline and the 78-percent wingspan location. Table 7.1-2 shows the computed lateral clearance between a Falcon 20 wingtip and a leader aircraft vortex for each of the four-engine leader aircraft said to have been chased by the DLR experimenters.


|   |   |  |                        |
|---|---|--|------------------------|
|  | <b>NASA Engineering and Safety Center<br/>Technical Assessment Report</b> | Document #:<br><b>NESC-RP-<br/>12-00822</b>  | Version:<br><b>1.0</b> |
|   |   | <b>Probing Aircraft Flight Test Hazard Mitigation<br/>for the ACCESS Research Team</b> |                        |

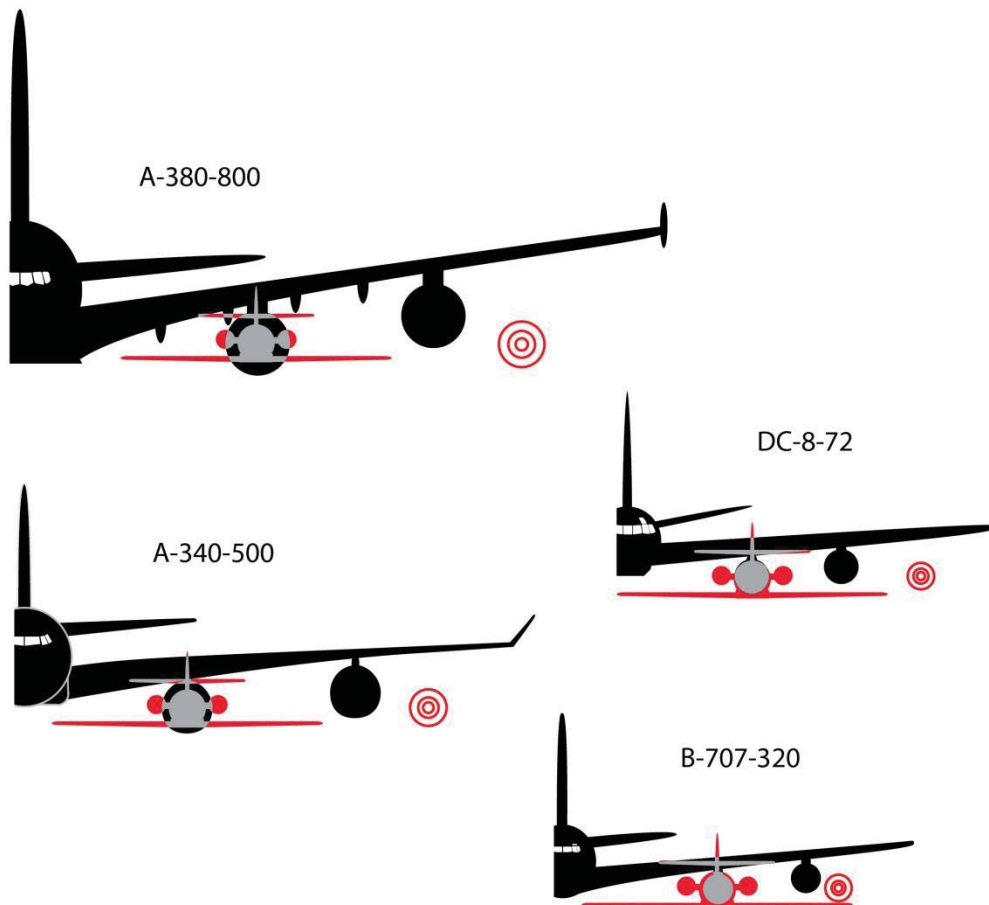
*Table 7.1-2. Lateral Vortex Clearance for Falcon 20 behind Different Leader Aircraft*

| Lead Aircraft<br>(minimum size<br>type reported<br>chased) | Distance Between Inboard<br>Engine Centerline and 78%<br>Wingspan Location<br>(ft) | Lateral clearance Between Falcon<br>Wingtip (when sampling inboard<br>engine plume) and Lead Aircraft<br>Wingtip Vortex (1% core size)<br>(ft) |
|--|--|--|
| <b>A-380-800</b>   | 60.05  | 32   |
| <b>A-340-500</b>   | 50.44  | 22   |
| <b>DC-8-72</b>   | 32.18  | 4  |
| <b>B-707-320</b>   | 24.39  | -4   |

The Falcon 20 half-wingspan length is about 27 ft. In the near field, the radius of a DC-8 wingtip vortex with an assumed 1-percent core radius (the radial location of peak tangential velocity) would be about 1.5 feet and would possibly grow slightly larger as the distance aft of the DC-8 increased.

The compiled data showed that the *lateral* distance between a Falcon 20 wingtip and a DC-8 wingtip vortex with a 1-percent core radius would be approximately 4 ft when sampling directly on the centerline in the near field behind an inboard engine plume. The A-340 provided approximately a 22-ft tip-to-vortex clearance by a similar calculation, and the A-380 provided about a 32-ft clearance. The B-707 provided no clearance; if inboard engine plume sampling was attempted in the near field using a Falcon 20, its wingtip would be immersed in or just beneath the B-707 vortex core. These results are graphically depicted to approximate scale for all four leader aircraft in Figure 7.1-9, with 1-, 2-, and 3.5-percent vortex cores also depicted.

|  |   |  |                        |
|--|---|--|------------------------|
|                 | <b>NASA Engineering and Safety Center<br/>Technical Assessment Report</b> | Document #:<br><b>NESC-RP-12-00822</b> | Version:<br><b>1.0</b> |
| Title:<br><b>Probing Aircraft Flight Test Hazard Mitigation<br/>for the ACCESS Research Team</b> |   |  | Page #:<br>46 of 118   |




**Figure 7.1-9. Approximately Scaled Depiction of Lateral Clearance between Falcon Wingtip and Leader Aircraft Wingtip Vortices of 1-, 2- and 3.5-Percent Core Size**

This analysis accounted for the near-field migration of the wingtip vortex from the wingtip to the 78-percent span location, but it did not account for the uncharacterized near-field sinking of the vortices. An arbitrary vortex vertical location—in lateral line with the inboard engine—is depicted in Figure 7.1-9. This analysis also did not account for the additional sinking of the inboard engine exhaust plumes relative to the outboard plumes and wingtip vortices. The Falcon has been depicted in line with the inboard engine in the figure. These effects could *increase* the vertical clearance between the Falcon wingtip and the DC-8 wingtip vortex.

On the other hand, this analysis did not account for the uncharacterized inboard exhaust plume spreading or outboard migration toward the wake vortex, and this effect could *decrease* the lateral clearance between the Falcon wingtip and the DC-8 wingtip vortex.



|  |   |  |                        |
|--|---|--|------------------------|
|                 | <b>NASA Engineering and Safety Center<br/>Technical Assessment Report</b> | Document #:<br><b>NESC-RP-12-00822</b> | Version:<br><b>1.0</b> |
| Title:<br><b>Probing Aircraft Flight Test Hazard Mitigation<br/>for the ACCESS Research Team</b> |   | Page #:<br>47 of 118                   |                        |

The NESC team concluded that these phenomena could not be reliably predicted except by using CFD simulations. Unfortunately, the limited time available for this assessment prohibited CFD analysis.

The NESC team discussed that the DLR comments regarding near-field wingtip vortex behavior and the ease of vortex avoidance, while valuable, may have been based to some degree on presumably more recent experience with aircraft with larger clearance margins than the DC-8 will provide the ACCESS crew.


During the September 2012 teleconference, the DLR pilots indicated that in the near field they had approached leader aircraft as close as 330 ft (100 m) by their estimate using visual reference. They said they were able to visually identify the point at which inboard engine exhaust plumes began to mix with the wingtip vortex and that this defined their near-field aft limit. The team presumed they had learned to recognize plume/vortex roll-up by visual changes in plume behavior. The NESC team discussed that the ACCESS pilots will only be able to acquire this skill through personal experience and practice.

The DLR Falcon pilots observed a flight rule to only conduct sampling flight experiments in the near field if local atmospheric conditions were such that contrails made engine exhaust plumes visible. The Falcon pilots would ensure visual contrails prior to joining formation with the lead aircraft for a plume sampling experiment. The NESC team noted that this was the same rule observed by NRC Falcon 20 pilots.

The DLR pilots reported nonspecifically that the elevation and position of the sun affected contrail visibility. They suggested planning flight paths for optimal visibility depending on the sun's position. The NESC team noted the ACCESS plan to align their long sampling runs with the direction of prevailing winds and that that this constraint may hinder their ability to adjust for best contrail visibility.

The NESC team noted in one photograph provided by DLR (of an A-340 and a B-707 flying side by side in the near field in front of the DLR Falcon 20 at an unstated altitude in unstated atmospheric conditions) that the A-340 high-bypass engines were producing visible exhaust contrails while the low-bypass B-707 engines were not. This suggested one other variable associated with the formation of visible contrails. The NESC team noted that the NASA DC-8-72 aircraft has favorable high-bypass engines.

The DLR pilots reported the closest distance they had ever operated behind a lead aircraft was 330 ft (100 m). They indicated that staying on condition while sampling an exhaust plume was not difficult because wake turbulence levels remained low in the near field. Yet they described sampling engine exhaust plumes closer than 5 wingspans as "like flying on a washboard." They indicated this was easy to handle and the washboard "feel" provided positive feedback that they were in the right sampling position. The DLR pilots reported no inadvertent wake vortex core encounters in near-field flying. This was because, in the near field, they could feel the weak downwash of a wingtip vortex on their outboard wingtip well before encountering the core.

|  |   |  |                        |
|--|---|--|------------------------|
|                 | <b>NASA Engineering and Safety Center<br/>Technical Assessment Report</b> | Document #:<br><b>NESC-RP-12-00822</b> | Version:<br><b>1.0</b> |
| Title:<br><b>Probing Aircraft Flight Test Hazard Mitigation<br/>for the ACCESS Research Team</b> |   | Page #:<br>48 of 118                   |                        |

The NESC team discussed that while ACCESS pilots could learn academic lessons from these DLR comments, they should not assume that flight hazards were mitigated through someone else's experience.


DLR pilots described a near-field sampling test as follows, paraphrased from team notes:

“Rendezvous with the lead aircraft between 27,000 and 35,000 ft. Traffic Alert and Collision Avoidance System (TCAS) is used initially by both aircraft to provide orientation and distance cues; once visual sighting is confirmed, TCAS is shut off. The Falcon crew sometimes ask the lead aircraft to adjust heading prior to or during rendezvous to optimize contrail visibility. The Falcon approaches from aft and below the lead aircraft centerline to the prescribed near-field distance, consistent with military inflight refueling techniques. Minimum aircraft fore-and-aft separation is established visually from previous pilot formation flight experience. No Falcon cockpit or science instrumentation is used to gauge near-field distance. Maximum separation for near-field work is 1 to 2 nm behind the lead aircraft. To begin sampling, the pilot slowly moves the Falcon outboard of the lead aircraft centerline until visually established inside an exhaust contrail. Loss of sight of the outside horizon is possible at this point and is considered normal for near-field sampling. Onboard scientists or technicians could confirm presence within the exhaust plume. As the Falcon moves farther aft of the lead aircraft in near field, perceived variations in the washboard turbulence pattern are used as a cue for when engine exhaust and wingtip vortices begin to intermix. This is reported to begin while moving aft to about 5 wingspans” behind a DC-8. Exit from near-field flight is accomplished by descending until well clear visually of the contrail (altitude separation not specified). The Falcon pilot moves laterally outboard of the lead aircraft path to maintain visual reference on the lead aircraft as during the approach. Once beneath and laterally clear, the Falcon pilot climbs outboard and above the contrail level to position for far-field sampling entry.”

### **Near-Field Geometry and Safe Operating Limits**


Because of insufficient information for heavy transport aircraft operating at high altitudes in a clean wing configuration, the NESC team could not rigorously determine forward and aft near-field safe operating limits, as had been a plan objective. To better characterize DC-8 near-field geometry, however, the NESC team developed best estimates for certain near-field aspects and events, including vortex migration and engine exhaust plume spreading and roll-up.

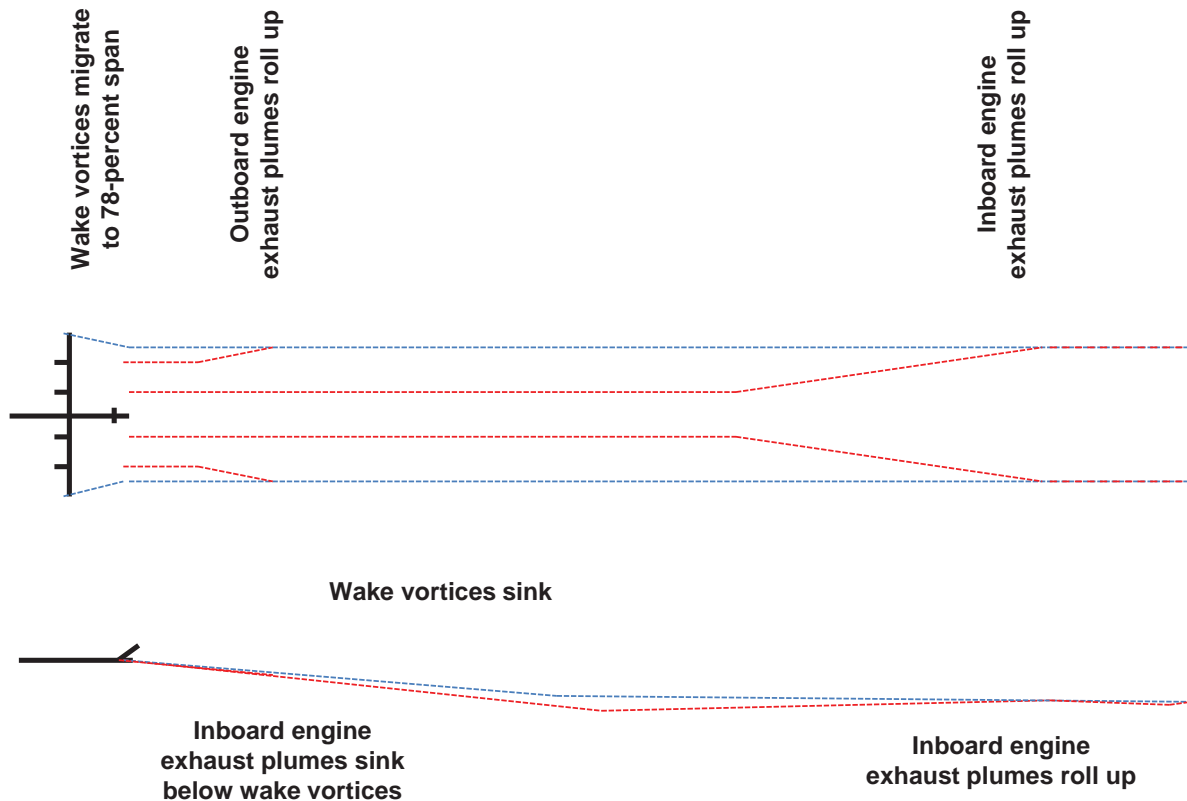
- Analyses support that the core radii of the DC-8 wingtip vortices can be assumed to be about 1.5 ft and virtually constant throughout the near field.
- Theory predicts that the DC-8 wingtip vortices would migrate inboard to a position about 115 ft apart from each other within about 150 ft aft of the aircraft and remain stable at that position throughout the near field.

|  |   |  |                        |
|--|---|--|------------------------|
|                 | <b>NASA Engineering and Safety Center<br/>Technical Assessment Report</b> | Document #:<br><b>NESC-RP-12-00822</b> | Version:<br><b>1.0</b> |
| Title:<br><b>Probing Aircraft Flight Test Hazard Mitigation<br/>for the ACCESS Research Team</b> |   | Page #:<br>49 of 118                   |                        |

- Pilot observations and research findings suggest that the DC-8 outboard engine exhaust plumes will migrate outboard and roll up around the wingtip vortices between 150 and 750 ft aft of the aircraft.
- Observations suggest the DC-8 inboard engine exhaust plumes will descend relative to the wingtip vortices and reach a maximum unknown descent distance at about 600 ft aft of the aircraft.
- Pilot experience suggests that the inboard engine exhaust plume would spread in the near field with about a 5-degree spread angle, adding about 9 ft to the radius of the plume for every 100 ft aft of the aircraft.
- Research data suggest that the inboard engine exhaust velocity would diminish to less than 10 percent of its original value by 750 ft aft of the aircraft.
- Observations and research findings suggest the DC-8 inboard engine exhaust plumes will simultaneously ascend and migrate outboard toward the wingtip vortices and roll up around the wingtip vortices beyond 1,350 ft aft of the aircraft.

Figure 7.1-10 depicts some key elements of the NESC team's ultimate understanding of near-field sample-area geometry.

|  |   |  |                        |
|--|---|--|------------------------|
|                 | <b>NASA Engineering and Safety Center<br/>Technical Assessment Report</b> | Document #:<br><b>NESC-RP-12-00822</b> | Version:<br><b>1.0</b> |
| Title:<br><b>Probing Aircraft Flight Test Hazard Mitigation<br/>for the ACCESS Research Team</b> |   |  | Page #:<br>50 of 118   |




*Figure 7.1-10. Notional Depiction of Three-Dimensional Near-Field Sample-Area Geometry*

### 7.1.3 Far-Field Behavior

The NESC team considered available data to understand the far-field behavior and geometry of wake vortices with exhaust plumes rolled up around them and to discuss implications for flight sampling techniques and test hazard mitigation. Far-field videos of previous NASA experiments were reviewed; experiential comments from DLR pilots who performed far-field flight experiments were reviewed; a paper describing a Canadian NRC flight experiment was reviewed; and far-field vortex research information was considered and discussed.

#### Far-Field Video Review

Prior to the September 2012 teleconference with the DLR Falcon pilots, it appeared that in order to obtain far-field exhaust data, the ACCESS pilots would have had to directly and intentionally penetrate wake vortices. Team discussions focused on wake vortex decay models and on characterizing Falcon loads versus vortex strength to identify a safe far-field distance. The team conducted independent loads analyses at three vortex strengths. Results of these loads analyses are described in Section 7.2.3.

|  |   |  |                        |
|--|---|--|------------------------|
|                 | <b>NASA Engineering and Safety Center<br/>Technical Assessment Report</b> | Document #:<br><b>NESC-RP-12-00822</b> | Version:<br><b>1.0</b> |
| Title:<br><b>Probing Aircraft Flight Test Hazard Mitigation<br/>for the ACCESS Research Team</b> |   | Page #:<br>51 of 118                   |                        |

The NESC team reviewed videos of NASA B-737 and OV-10 aircraft penetrating C-130 wingtip vortices that were made visible by smoke generated from C-130 smoker pods [ref. 25]. Figure 7.1-11 is a screen grab from this video with the B-737 trail aircraft approaching the C-130 vortex pair.



*Figure 7.1-11. B-737 Approaching C-130 Vortex Pair in Far Field*

The NESC team observed that the vortices in the video exhibited synchronized chaotic responses to atmospheric inputs at times and asynchronous responses at other times. The vortices interacted with and were independently perturbed when encountering the aircraft. The interaction included changes in direction, structure, and diffusion. The B-737 and OV-10 both responded to vortex penetration predominantly in roll. The OV-10 was seen to experience considerably larger roll perturbations, logically because of its smaller roll moment of inertia. The dominant effect of roll moment of inertia on wake vortex impact is discussed in reference 20.

### **DLR Far-Field Observations**

A revelation from the September 2012 DLR teleconference about far-field vortex decay behavior changed the project team's plans and the NESC team's focus. The DLR pilots described a consistently observed phenomenon that made far-field sampling possible without direct vortex penetration. They observed that between 2 and 20 miles behind the leader aircraft, some of the rolled-up exhaust contrail gases separated above the vortices and rose up away from them. Figures 7.1-12 through 7.1-14, provided by DLR, show examples of this phenomenon.





**NASA Engineering and Safety Center  
Technical Assessment Report**

Document #:  
**NESC-RP-  
12-00822**

Version:  
**1.0**

Title:

**Probing Aircraft Flight Test Hazard Mitigation  
for the ACCESS Research Team**


Page #:  
52 of 118



*Figure 7.1-12. DLR Video Screen Grab showing Far-Field Separation:  
Diffuse Exhaust Contrail above Wake Vortices*



*Figure 7.1-13. DLR Video Screen Grab showing Diffuse Exhaust Contrail  
above A-380 Wake Vortices*

|  |   |   |                        |
|--|---|---|------------------------|
|                 | <b>NASA Engineering and Safety Center<br/>Technical Assessment Report</b> | Document #:<br><b>NESC-RP-<br/>12-00822</b> | Version:<br><b>1.0</b> |
| Title:<br><b>Probing Aircraft Flight Test Hazard Mitigation<br/>for the ACCESS Research Team</b> |   | Page #:<br>53 of 118                        |                        |




*Figure 7.1-14. DLR Video Screen Grab showing Diffuse Exhaust Contrail above A-340 Wake Vortices*

The DLR pilots described these separated exhaust gases as forming a rising diffuse contrail above the vortices. At distances beyond 2 miles behind clean wing four-engine aircraft, they reported that they routinely observed exhaust/vortex separations rising greater than 300 ft vertically. They indicated that there was variability in this behavior—apparently uncharacterized—but that they had successfully sampled this diffuse exhaust material while generally avoiding the hazardous vortices below. They described feeling “light turbulence” when sampling the diffuse exhaust gas region, which provided feedback that they were on condition. They described a typical far-field sampling event as below (paraphrased):

“Align the aircraft above a contrail, behind the rolled-up, intermixed area of exhaust and vortex. The contrail is invaluable in identifying this area. Between 10 and 20 nm behind the lead aircraft, identify an exhaust plume visually separated above the vortices. Approach the contrails in the far field from above due to the progressive sinking behavior of the exhaust and the wingtip vortex paths. To exit the contrail, climb above it and move laterally away.”

The DLR pilots experienced an unspecified number of inadvertent far-field wake vortex encounters between an estimated 10 to 20 miles behind the leader aircraft. They described the events as occurring under conditions when visible contrails began to disappear. The NESC team observed that the distance where the separation phenomenon would begin, the rate at which the

|  |   |  |                        |
|--|---|--|------------------------|
|                 | <b>NASA Engineering and Safety Center<br/>Technical Assessment Report</b> | Document #:<br><b>NESC-RP-12-00822</b> | Version:<br><b>1.0</b> |
| Title:<br><b>Probing Aircraft Flight Test Hazard Mitigation<br/>for the ACCESS Research Team</b> |   | Page #:<br>54 of 118                   |                        |

separation would progress, and the distance at which it would dissipate would all be critically dependent on atmospheric conditions, and on the generator aircraft type, weight, speed, and altitude. The NESC team also noted that significant cruise upsets have been observed from vortex encounters beyond 20 miles aft of aircraft with an MTOW greater than 300,000 lb [ref. 26].

The DLR pilots reported that when these encounters occurred they did not resist the rapid onset of forces by using the flight controls, but rather allowed the vortex to “spit out” the Falcon. This was described as a technique rather than a mission rule. They reported that roll excursions never exceeded a 90-degree bank angle, roll rates never exceeded 60 degrees per second, and pitch excursions never exceeded  $\pm 5$  degrees.

Once clear of the vortex and referencing the visual horizon outside the windscreen, the pilot would perform a standard recovery maneuver depending on the attitude of the aircraft. Visual recovery was characterized as “very natural” for pilots trained in aerobatics. No departures from controlled flight (also known as upsets) were reported. They reported that structural damage was never discovered in post-encounter special inspections or in subsequent regularly scheduled maintenance inspections.

DLR pilots experienced only one single-engine flameout in 20 years of using the Falcon 20 as a follower aircraft. After this event, the engine was restarted prior to landing, and no damage was noted during the post-flight inspection. The NESC team noted that the DLR Falcon 20 uses different engines than the NASA Falcon 20.


### **NRC Far Field Observations**

As described in Section 6.2, the Canadian NRC conducted far-field experiments flying a Falcon 20 between 1 and 6 nm behind a three-engine B-727 medium-wake-category transport aircraft to collect wake vortex velocity data [ref. 6].

The NRC pilots always observed two conduct rules: (1) fly under conditions when visible contrails of the vortex are present and (2) do not enter or fly through the vortex to obtain experimental data.

Reference 6 included power spectral density plots with turbulence levels observed to be consistent with typical atmospheric clear-air turbulence measurements. This could suggest that the region near a wake vortex may contain turbulent flow, necessitating combining dynamic gust loads with static vortex encounter loads when computing total Falcon loads behind the DC-8. Also of note, the NRC measured wake vortex strengths to decay by 12 percent between about 2 to 3 nm behind the B-727.

Figure 7.1-15, reprinted from the NRC paper, shows exhaust gas separating from B-727 wake vortices 1.5 nm behind the aircraft at an altitude of 28,000 ft. This is apparently the same phenomenon reported by the DLR pilots.

|  |   |  |                        |
|--|---|--|------------------------|
|                 | <b>NASA Engineering and Safety Center<br/>Technical Assessment Report</b> | Document #:<br><b>NESC-RP-12-00822</b> | Version:<br><b>1.0</b> |
| Title:<br><b>Probing Aircraft Flight Test Hazard Mitigation<br/>for the ACCESS Research Team</b> |   | Page #:<br>55 of 118                   |                        |



*Figure 7.1-15. NRC Image of Diffuse Exhaust Contrail above B-727 Wake Vortices Far Field*

### **Far-Field Research Information**

The observed separation phenomenon is discussed in references 19, 22, and 23 and is thought to be caused by buoyancy effects from the heated jet gases, by deficiencies or enhancements of the lift carryover across the fuselage-shrouded wing, and by the onset of long-wave wake vortex instability [ref. 19]. Research suggests that when engine thrust is greater than idle, the separation distance between the upper diffuse exhaust plume and the vortex may be smaller behind clean wings with elliptical lift distributions than it would be behind wings with deployed surfaces [ref. 22].

The NESC team reviewed computational results by Rossow and Brown [ref. 19], which indicated that the onset of separation when robust engine thrust exhaust is used can be observed in as few as 10 wake vortex spans behind the aircraft. One wake vortex span is 78 percent of the geometric wingspan for assumed elliptically loaded wings, about 115 ft for the DC-8.

The team reviewed Rossow and Brown's computational model (Figure 7.1-16) and calculated theoretical separation distances for a DC-8 wake vortex. The results suggested that by 5,800 ft (50 wake vortex spans) aft of a DC-8, the exhaust contrail would be about 175 ft (1.5 wake vortex spans) above the wingtip vortex. At 11,600 ft aft, it would be about 350 ft above the wingtip vortices. A vertical separation of 300 ft would occur at about 10,000 ft (1.9 miles) aft of the DC-8. This result was consistent with the DLR pilot's reported experience of a 2-mile forward limit for their far-field experiments.

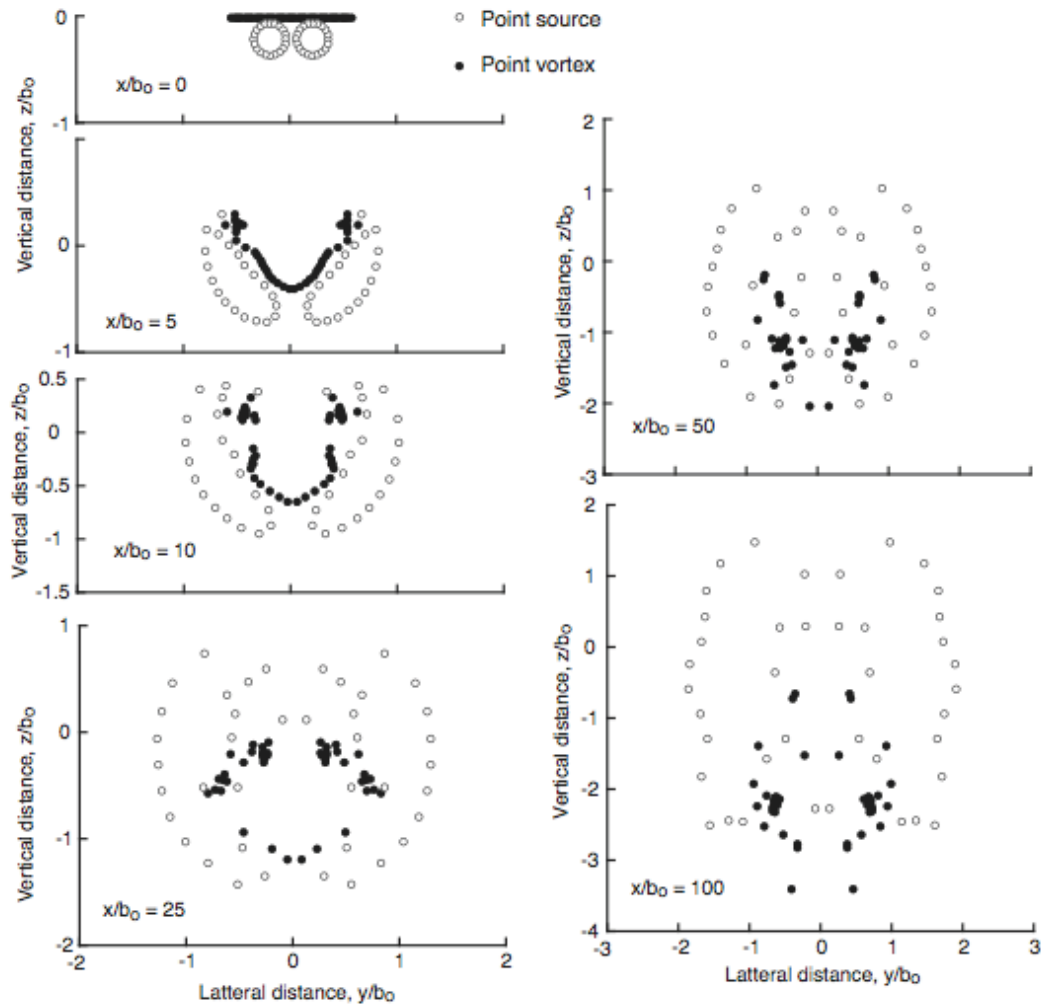


Title:

Probing Aircraft Flight Test Hazard Mitigation  
for the ACCESS Research Team

Page #:


56 of 118



**Figure 7.1-16. Qualitative Computation of Formation of Shield Composed of Engine-exhaust Products (open circles) around Vortex Wake (filled circles) when Engine Thrust is Robust [ref. 19]**

The NESC team speculated that thermal or species buoyancy differences may result in lighter gas constituents like CO being overrepresented in the rising exhaust, while heavier constituents like CO<sub>2</sub> might be underrepresented. This could be consequential to the ACCESS science experiment but not to safety.



|  |   |  |                        |
|--|---|--|------------------------|
|                 | <b>NASA Engineering and Safety Center<br/>Technical Assessment Report</b> | Document #:<br><b>NESC-RP-12-00822</b> | Version:<br><b>1.0</b> |
| Title:<br><b>Probing Aircraft Flight Test Hazard Mitigation<br/>for the ACCESS Research Team</b> |   | Page #:<br>57 of 118                   |                        |

## Far-Field Geometry and Safe Operating Limits

Because of insufficient information for heavy transport aircraft operating at high altitude in clean wing configuration, the NESC team could not rigorously determine a forward far-field safe operating limit, as had been a plan objective. The team examined certain far-field aspects and events, including vortex/plume evolution, separation, and decay, but could make no predictions.

The primary element of far-field geometry noted was that at a distance of about 2 miles behind the DC-8 a 300-ft separation of gases above the vortices could occur if conditions were advantageous.

The project team discussed the possibility that during the planned flight testing timeframe, mid-February through mid-April 2013, they may have difficulty locating atmospheric conditions over the R-2508 Complex that cause visualization of the far-field separation phenomenon described by the DLR pilots. They considered transiting to “whiskey areas”<sup>1</sup> if conditions were insufficient. The NESC team considered this prudent planning.

The NESC team discussed the risk that the Falcon pilot may inadvertently and without awareness drift closer than 300 ft to the vortex in the far field. This could occur if the vertical separation distance insidiously shrinks at a given sampling distance. Given the uncharacterized and probably chaotic nature of the separation phenomenon, the distance could even close unpredictably to zero. The NESC team discussed that if the Falcon should descend into a vortex at a shallow grazing angle (interpreted as less than 5 degrees) the aircraft may deflect off the vortex as per theory [ref. 27]. The DLR reports that on the occasions when pilots inadvertently encountered a vortex they found it difficult to stay inside the vortex was consistent with this research finding.


### 7.1.4 Mid-Field Behavior

Between the near and far field of the DC-8 exhaust wake and vortex flows, there is a less clearly researched “mid field” transition region that will be specifically avoided during the ACCESS research flight experiments. The project team planned to visually identify the aft boundary of their near-field sample region by noting where the inboard engine exhaust plumes visibly roll up with the wingtip vortices. After the September 2012 teleconference with DLR, the project plan was to visually identify the forward boundary of the far-field region by identifying where the exhaust gas separation visibly reached 300 ft vertical distance above the vortices.

The NESC team found few studies that describe the aerodynamics, mixing, and strength of vortical flow in the mid-field region but noted that aircraft operating in the National Airspace System avoid this region because aircraft upset risks are recognized to be significant.

---

<sup>1</sup> Whiskey areas are aviation warning areas often used for military flying, wherein participating aircraft agree between themselves what they will do, and wherein they tend to operate under “see and avoid” visual flight rules (VFR). In these areas, pilots may or may not need to advise controllers of their intentions with respect to speeds or maneuvers, as long as they stay in the area. Air traffic control tries to keep instrument flight rule traffic clear of VFR traffic in warning areas.

|  |   |  |                        |
|--|---|--|------------------------|
|                 | <b>NASA Engineering and Safety Center<br/>Technical Assessment Report</b> | Document #:<br><b>NESC-RP-12-00822</b> | Version:<br><b>1.0</b> |
| Title:<br><b>Probing Aircraft Flight Test Hazard Mitigation<br/>for the ACCESS Research Team</b> |   | Page #:<br>58 of 118                   |                        |

## 7.2 Vortex Encounter Loads

### 7.2.1 Assessment of Project Loads Analyses


The NESC team assessed the results, methods, and assumptions in the ACCESS August 2012 wake model, aerodynamic, and structural analyses. Project presentation charts describing these analyses can be found in Appendix D.

The NESC team discussed the project's DC-8 trailing vortex model (i.e., the Proctor model, described in Section 6.4.1). This lifting line model assumed a conservative elliptic wing loading and vortex core assumptions. It did not include the influence of horizontal tail vortices. The resulting vortex strength would be conservative. The project's three-phase vortex decay model was valid and conservative. For the near-field distances planned by the ACCESS tests, vortex decay could be assumed to be zero. For the far field, vortex decay could be highly variable. The NESC team concluded that the project's decay model was valid, while noting that a wide variety of vortex decay models are employed among discipline analysts.

The NESC team discussed the project's static aerodynamic loads analyses (i.e., the Vicroy analyses, described in Section 6.4.2). This analysis used strip theory aerodynamic models, which would be expected to lead to higher loads than distributed panel models. Worst-case Falcon 20 tail loads were obtained by placing the cruciform juncture of the model's horizontal and vertical tail conservatively at the center of the Proctor vortex model. The project team acknowledged that in this static analysis no inertial relief was included. This is significant because an aircraft in physical flight would be dynamically rolled in response to encountering a wake vortex, and this response would logically relieve the airplane's tail loads. In addition, if the aircraft's dynamic response was included, then the maximum bending moment on its vertical tail may not occur with the vortex precisely centered on the tail juncture. The assessment team considered the project team's spreadsheet analysis a valid method for a rapid conservative assessment of tail loads.

The NESC team discussed the project's structural loads analyses (i.e., the Pagnatta analyses, described in Section 6.4.3). These analyses used the Vicroy aerodynamic loads computed for the Falcon horizontal and vertical tail in a wake vortex encounter and superimposed gust encounter loads.

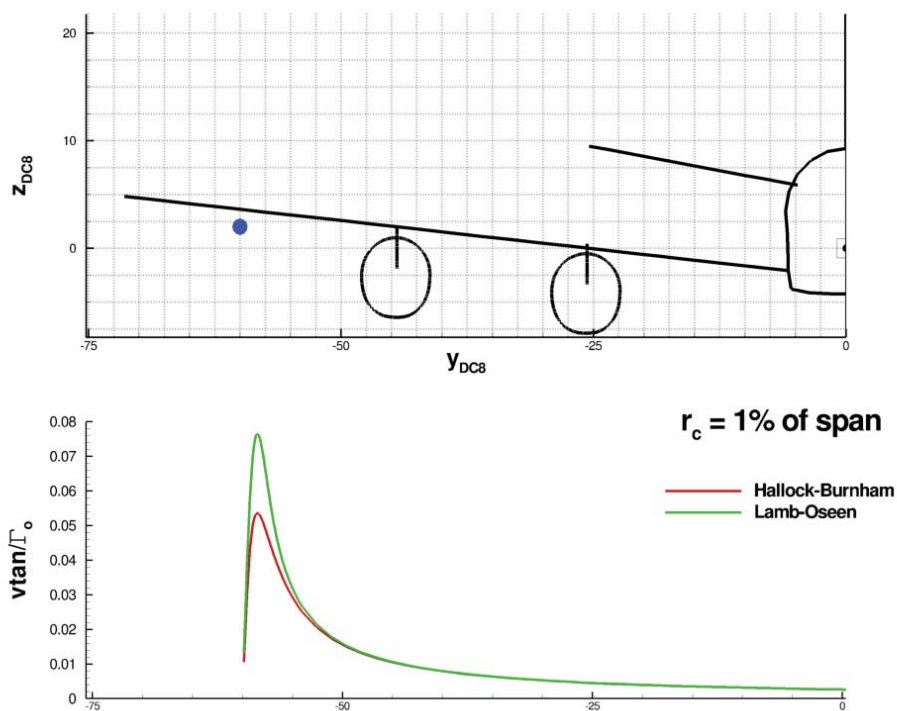
The project's superposition of worst-case vortex-induced loads and worst-case gust loads showed loads and moments that significantly exceeded nominal expected flight loads. The NESC team considered this superposition unnecessarily conservative. However, without detailed knowledge of Falcon aircraft design load conditions, this could not be definitively determined.

|  |   |  |                        |
|--|---|--|------------------------|
|              | <b>NASA Engineering and Safety Center<br/>Technical Assessment Report</b> | Document #:<br><b>NESC-RP-12-00822</b> | Version:<br><b>1.0</b> |
| Title:<br><b>Probing Aircraft Flight Test Hazard Mitigation for the ACCESS Research Team</b> |   | Page #:<br>59 of 118                   |                        |

## 7.2.2 Independent Loads Analyses

### Vortex Model

The NESC team conducted independent aerodynamic loads analyses. The NESC team's model used the Lamb-Oseen velocity characterization. A comparison between this model and the Burnham-Hallock model used by Proctor is shown for the DC-8 and depicted in Figure 7.2-1.




**Figure 7.2-1. Comparison of Lamb-Oseen and Burnham-Hallock Tangential Velocity Distributions**

The blue dot represents the location of the center of a 1-percent primary wingtip vortex, and the distribution shows the inboard tangential velocities ( $v_{tan}$ ) induced by the vortex, normalized by vortex strength ( $\Gamma_0$ ). Both distributions represent a 1-percent vortex core radius. The Lamb-Oseen model core peak velocity is notably higher than that of the Burnham-Hallock model used by the project team. The vortex-induced velocities 10 ft inboard from the core (or outboard) are about the same for both models.

### Aircraft Models

The NESC team obtained DC-8 and Falcon 20 aircraft geometry data sufficient to construct aerodynamic models of both aircraft. The NESC team created a computer-aided design model for the DC-8 using information found in 1967 and 1981 proprietary manufacturer documents already available to team members at DFRC. This information is not described herein to protect

|  |   |                         |            |
|--|---|-------------------------|------------|
|       | <b>NASA Engineering and Safety Center<br/>Technical Assessment Report</b> | Document #:             | Version:   |
|  |   | <b>NESC-RP-12-00822</b> | <b>1.0</b> |
| Title:   |   | Page #:                 |            |
| <b>Probing Aircraft Flight Test Hazard Mitigation<br/>for the ACCESS Research Team</b> |   | 60 of 118               |            |

its proprietary status. The NESC team derived a simplified aerodynamic Falcon geometric model by digitizing figures found in reference 4. Digitized Falcon fuselage, wing, horizontal and vertical tails are shown in Appendix E. Table 7.2-1 shows key aircraft model parameters that were used in the team's aerodynamic analyses.

*Table 7.2-1. Key Aircraft Model Parameters Used in the NESC Aerodynamic Analyses*

|  | <b>DC-8</b> | <b>Falcon 20 (heavy)</b> | <b>Falcon 20 (light)</b> |
|--|-------------|--------------------------|--------------------------|
| Weight (lb)                                    | 280,000     | 31,900                   | 24,150                   |
| Wingspan ( $b$ , ft)                           | 149         | 53.5                     | 53.5                     |
| Reference area ( $S_{ref}$ , ft <sup>2</sup> ) |             | 449.9                    | 449.9                    |
| Reference length ( $L_{ref}$ , ft)             |             | 9.33                     | 9.33                     |

### Flight Conditions

Static aerodynamic loads were obtained at nominal flight conditions at an altitude of 25,000 ft, a velocity of 711.27 ft/sec (Mach 0.7), and a dynamic pressure of 269.7 lb/ft<sup>2</sup>. These conditions were chosen to represent conservative flight conditions at which vortex-induced loads may occur.


### Analysis Tools

The NESC team performed aerodynamic loads and flight dynamics studies using Nielsen Engineering and Research (NEAR) aerodynamic prediction codes: the STRLNCH store separation analysis tools [refs. 33-36] and the Missile Distributed Loads (MISDL) and Missile Loads 3 (MISL3) codes [refs. 37-40]. These were developed by NEAR and have been validated with flight data for some previous applications, including the release of stores, experimental aircraft, rockets, and missiles from carrier aircraft.

### MISDL Analysis Code

The MISDL code was used to model the DC-8 and Falcon aircraft. The DC-8 was modeled to determine its trailing vortex wake at trimmed flight conditions. The Falcon was modeled to predict the aerodynamic loads acting on it in the free stream and when immersed in the trailing wake of the DC-8 aircraft. Both aircraft were trimmed under free-stream flight conditions by iterating on angle of attack and horizontal tail deflection until zero pitching moment was achieved at lift equal to weight. Thrust was presumed to be equal to drag under trimmed conditions, and the center-of-gravity location was assumed to be at the quarter-chord of the mean aerodynamic center. The trim angle of attack of the DC-8 was 1.35 degrees, and the trim angle of attack of the Falcon at a weight of 32,000 lb was 1.0 degrees.

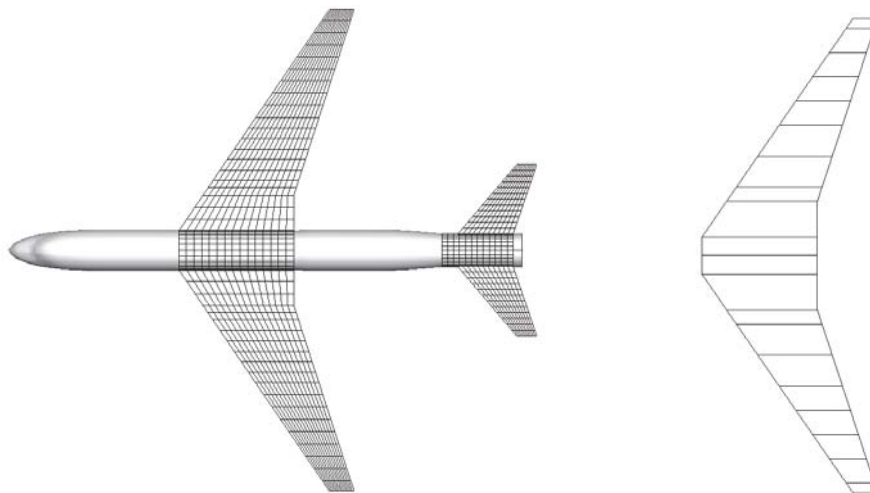
MISDL is a singularity and panel-method-based engineering aerodynamic prediction method, which includes high-angle-of-attack body and fins vortex models, rotational rates, and nonuniform flow effects. MISDL is capable of modeling noncircular bodies and fins with arbitrary planforms, orientations, and dihedral angles. Rotational rates and nonuniform flow effects are included in the modeling so that store separation and flight dynamic analyses can be performed. MISDL uses classical aerodynamic flow models based on solving potential flow

|  |   |   |                        |
|--|---|---|------------------------|
|                 | <b>NASA Engineering and Safety Center<br/>Technical Assessment Report</b> | Document #:<br><b>NESC-RP-<br/>12-00822</b> | Version:<br><b>1.0</b> |
| Title:<br><b>Probing Aircraft Flight Test Hazard Mitigation<br/>for the ACCESS Research Team</b> |   | Page #:<br>61 of 118                        |                        |

equations, Laplace's equation with compressibility corrections, classical singularity methods augmented with body and fin vortex modeling, and wing stall models based on empirical data.

The flow models in the MISDL program are valid for subsonic Mach numbers up to the critical speed or onset of transonic flow. The Göthert compressibility correction is included. The flow models include fuselage high-angle-of-attack vortex shedding and a vortex-lattice panel method for modeling the lifting surfaces (e.g., wing, tails). An interference shell is used in wing/tail sections to model wing/tail-on-fuselage aerodynamic interference. For subsonic flow, the fuselage is modeled with three-dimensional sources/sinks and doublets to model volume and angle-of-attack effects, respectively. Conformal mapping techniques are used to model the noncircular fuselage cross sections. The lifting surface models represent effects of lift, including camber and thickness (source panels). Further details of the vortex lattice panel method and other singularity-based flow models are described in reference 37. MISDL includes first-order corrections to the wing horseshoe vortex panel method to account for high-angle-of-attack effects. This includes a semi-empirical stall model to modify wing loading at high angles of attack. A vortex core model is included to model the viscous core of the wake vortices.

A typical panel layout for a DC-8 wing and horizontal tail is shown on the left side of Figure 7.2-2. A less complex strip theory model of a DC-8 wing is shown on the right side for comparison.



*Figure 7.2-2. Panel Layout for DC-8 Wing and Horizontal Tail (left) and Strip Theory Model of DC-8 Wing (right)*





Title:

Probing Aircraft Flight Test Hazard Mitigation  
for the ACCESS Research Team

Page #:

62 of 118

Predicted span-load distributions for a DC-8 wing and horizontal tail are shown in Figure 7.2-3 below for an assumed nominal DC-8 weight in cruise at Mach 0.66 at an altitude of 30,480 ft. Notice that the fuselage influence and the break in wing trailing-edge sweep cause the span loading to be slightly different from an elliptic loading distribution.

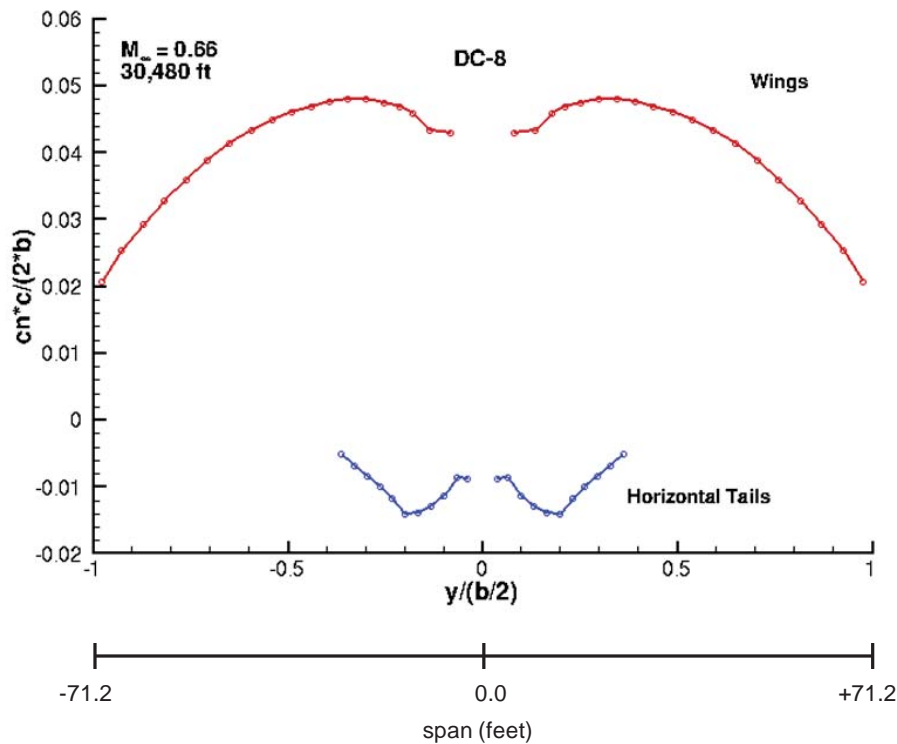


Figure 7.2-3. Predicted Span-Load Distributions for DC-8 Wing and Horizontal Tail


|  |   |                         |            |
|--|---|-------------------------|------------|
|       | <b>NASA Engineering and Safety Center<br/>Technical Assessment Report</b> | Document #:             | Version:   |
|  |   | <b>NESC-RP-12-00822</b> | <b>1.0</b> |
| Title:   |   | Page #:                 |            |
| <b>Probing Aircraft Flight Test Hazard Mitigation<br/>for the ACCESS Research Team</b> |   | 63 of 118               |            |

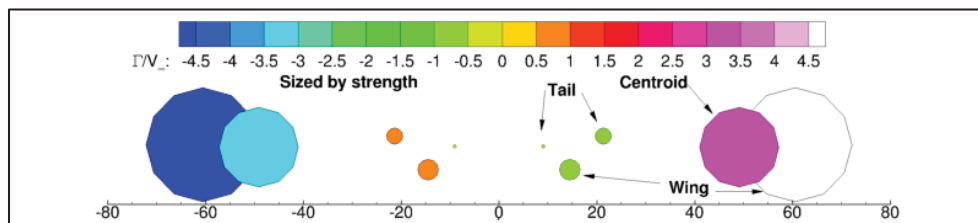
Table 7.2-2 shows the key modeling assumptions made by the NESC team as compared with the project team’s assumptions. Where possible, the NESC team tried to match the project team’s assumptions.

*Table 7.2-2. Key Assumptions Used for NESC and Project Models*


| NESC Model  | Project’s Model   |
|---|---|
| DC-8 weight = 280,000 lb  | DC-8 weight = 280,000 lb  |
| Falcon weight = 31,900 lb   | Falcon weight = N/A (not specified because no inertial loading was calculated)                              |
| Altitude = 25,000 ft  | Altitude = 27,000 ft  |
| 1- to 3.5-percent core radii models   | 1-percent core radius model   |
| No vortex decay   | Linear rate of decay model  |
| Wake modeled by multiple vortices from wing and tail                              | Wake represented by vortex pair from wing   |
| Panel Method  | Aerodynamic Strip Theory  |
| Calculated wing distribution  | Assumed elliptically loaded wing  |
| Some computations with estimated aircraft inertia                                 | All computations without inertial loads   |
| Digitized Falcon geometry   | Digitized Falcon geometry   |
| Vortex loads in combination with level flight loads                               | Vortex loads in combination with level flight loads and possibly gust loads                                 |
| Calculated tail load with the nose of the Falcon anywhere in the wake of the DC-8 | Assumed worst case tail load was with vortex centered at the cruciform of the vertical and horizontal tails |
| Compared vortex loads to fin gust load and rudder load, but not in combination    | Compared vortex loads to fin gust load and fin gust + rudder load   |

### DC-8 Vorticity Model Results

DC-8 wake vortices from the MISDL model are shown in Figure 7.2-4.



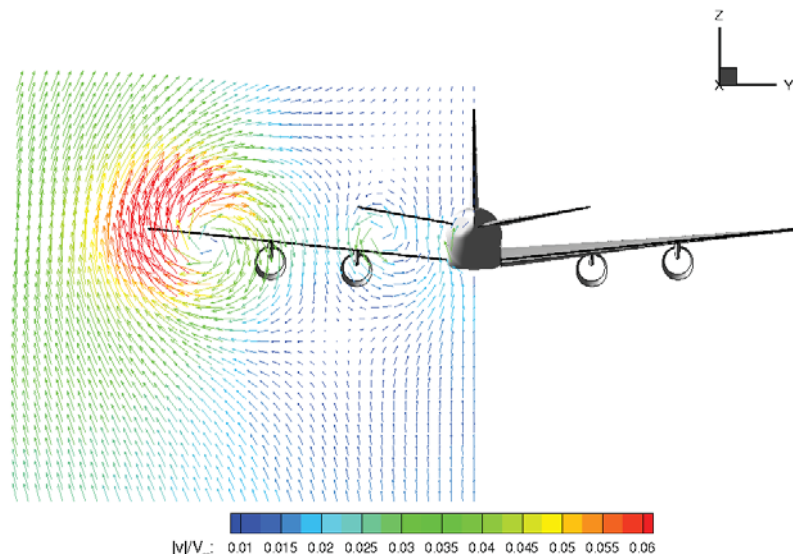
*Figure 7.2-4. DC-8 Model Wake Vortices*

|  |   |  |                        |
|--|---|--|------------------------|
|             | <b>NASA Engineering and Safety Center<br/>Technical Assessment Report</b> | Document #:<br><b>NESC-RP-12-00822</b> | Version:<br><b>1.0</b> |
| Title:<br><b>Probing Aircraft Flight Test Hazard Mitigation for the ACCESS Research Team</b> |   | Page #:<br>64 of 118                   |                        |

Shown on each side for a full DC-8 148-ft wingspan is one primary wingtip vortex, one secondary vortex associated with an inner wing feature, and two horizontal tail vortices. Engines and pylons were not modeled for this analysis. The size of each symbol represents the relative strength of each vortex. The color represents strength and rotational direction; positive is counterclockwise when viewed looking forward. It can be seen that on a given side of the aircraft, the horizontal tail vortices are opposite in direction to the wing vortices. This is because the wings are generating lift and the horizontal tails are generating aerodynamic down forces to balance the aircraft in pitch. Two “centroid” vortices are also shown. These are the weighted averages of all of the vortices on each side of the aircraft.

The NESC team used all of the individual vortices in their noted positions for Falcon vortex-induced aerodynamic load estimates. In the physical near field before the vortices have rolled up together, this would be close to the true situation; in the far field, this would be a conservative assumption.


Figure 7.2-5 shows the DC-8 velocity flow field used in the NESC analyses. Vectors represent velocity components in the Y-Z plane at the DC-8 tail location. Colors represent these vector component values relative to the free-stream velocity. No decay of the vortex strength has been included.



*Figure 7.2-5. Velocity Flow Field Depiction behind Model DC-8*

### **Aerodynamic Loads Contour Maps**

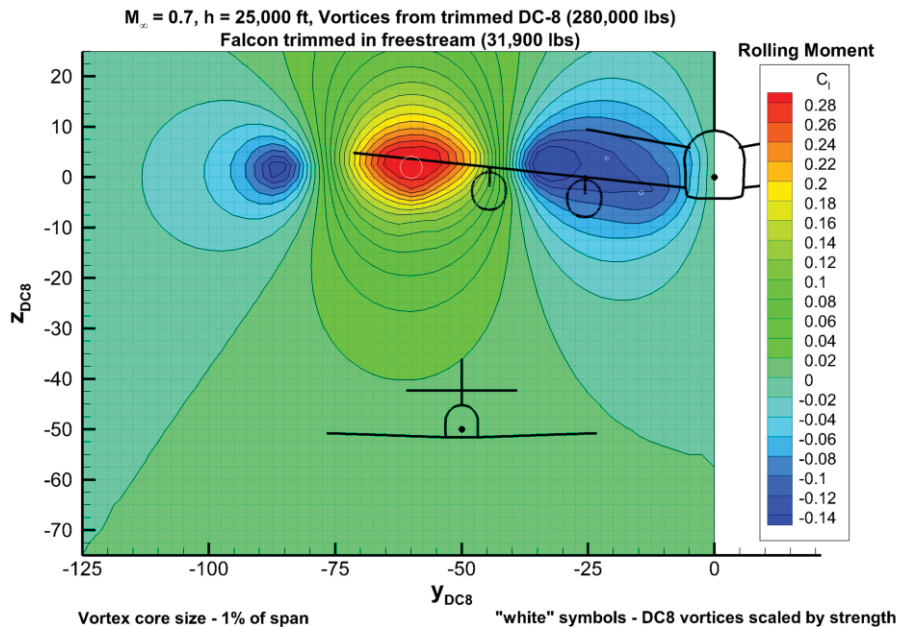
More than two thousand production runs of MISDL were conducted with the Falcon 20 in various locations on a grid behind the DC-8 multi-vortex field, first with a 1-percent vortex core size. The Falcon in a cruise trim attitude was placed in the vortex field, and the aerodynamic characteristics in the nonuniform velocity field were calculated.

|  |   |  |                        |
|--|---|--|------------------------|
|             | <b>NASA Engineering and Safety Center<br/>Technical Assessment Report</b> | Document #:<br><b>NESC-RP-12-00822</b> | Version:<br><b>1.0</b> |
| Title:<br><b>Probing Aircraft Flight Test Hazard Mitigation for the ACCESS Research Team</b> |   | Page #:<br>65 of 118                   |                        |

Contour maps were created in a  $Y$ - $Z$  plane that intersects the DC-8 airplane at its tail cone. These show the computed induced rolling moment ( $C_l$ ), the induced normal force ( $\Delta C_N$ ), the induced pitching moment ( $C_m$ ), the induced yawing moment ( $C_n$ ), and induced side force ( $C_Y$ ) acting on the Falcon at its center of gravity.

Figure 7.2-6 shows the resulting contour map for the Falcon rolling moment coefficient for near-field locations behind the left side of the DC-8, looking forward. The primary wingtip vortex is located at approximately  $-60$  ft (outboard) and  $+2$  ft (up) from the DC-8 model reference  $Y$ - $Z$  origin. To interpret this data, the reader should place the Falcon  $Y$ - $Z$  origin at any place on the grid and read the resulting parameter value. The Falcon is shown for scale purposes at location ( $Y = -50$ ,  $Z = -50$ ). At this location, the flow field is relatively benign and the Falcon rolling moment coefficient is about  $+0.01$ . At the vortex core center ( $Y = -60$ ,  $Z = +2$ ), the rolling moment coefficient on the aircraft is approximately  $+0.28$ . Positive  $C_l$  is defined as right wing down.

Figures 7.2-7 and 7.2-8 show similar maps for the Falcon normal force (“lift”) coefficient and pitching moment coefficient, respectively.



**Figure 7.2-6. Induced Rolling Moment Coefficient ( $C_l$ )**



Title:

Probing Aircraft Flight Test Hazard Mitigation  
for the ACCESS Research Team

Page #:

66 of 118

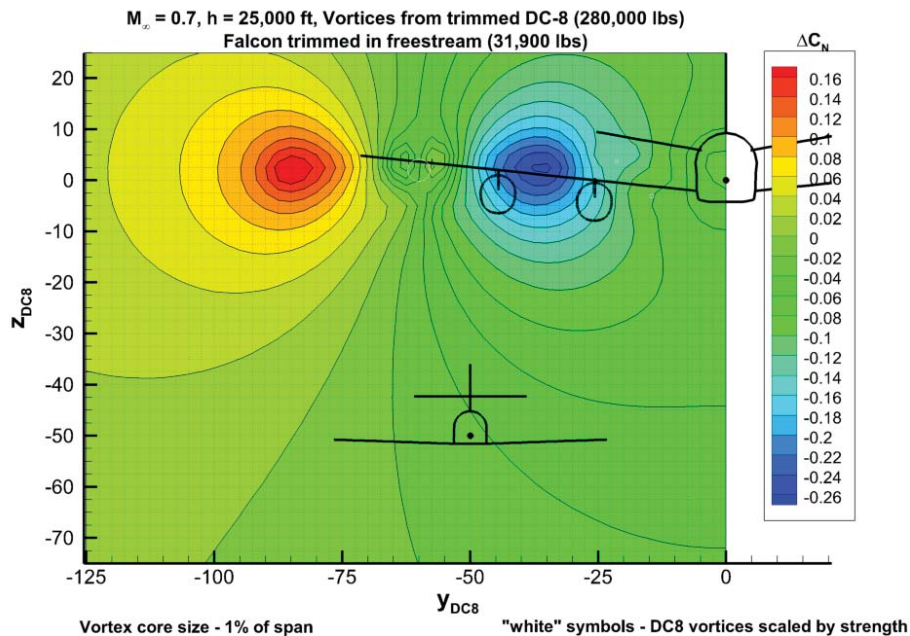


Figure 7.2-7. Induced Normal Force Coefficient ( $\Delta C_N$ )

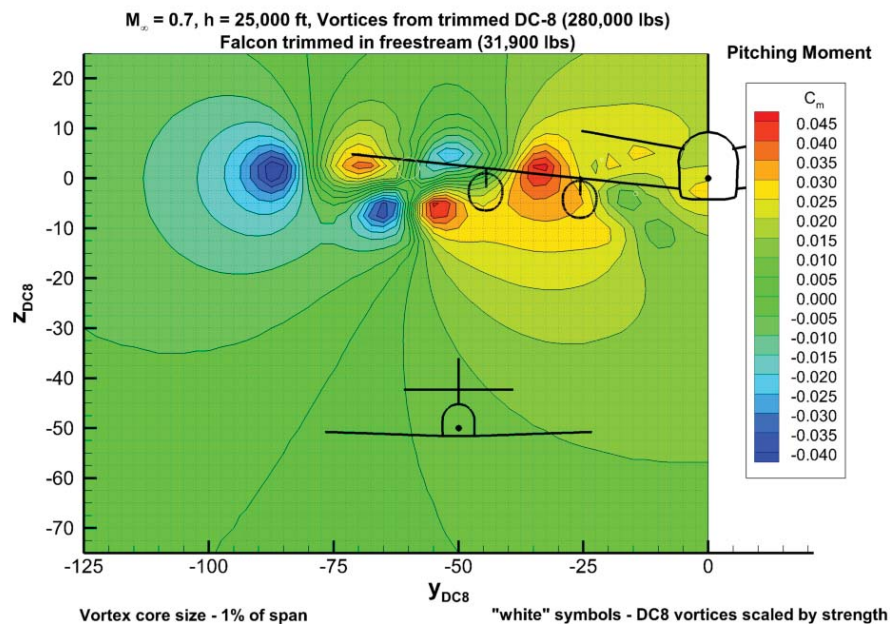


Figure 7.2-8. Induced Pitching Moment Coefficient ( $C_m$ )

Similar contour maps were generated for the induced normal forces and bending moments on the Falcon's aerodynamic surfaces. Figures 7.2-9 and 7.2-10 show the induced normal force and





Title:

Probing Aircraft Flight Test Hazard Mitigation  
for the ACCESS Research Team

Page #:

67 of 118

bending moment on the Falcon's right horizontal tail. Figures 7.2-11 and 7.2-12 show the induced normal force and bending moment on the Falcon's left horizontal tail.

Figures 7.2-13 and 7.2-14 show the induced normal force and bending moment on the Falcon's vertical tail. It's important to note that the mapped vertical tail loads do not include horizontal tail loads. Because of the Falcon's cruciform tail configuration, the computation of a total vertical tail bending moment would necessarily need to include the addition of the horizontal tail bending moments.

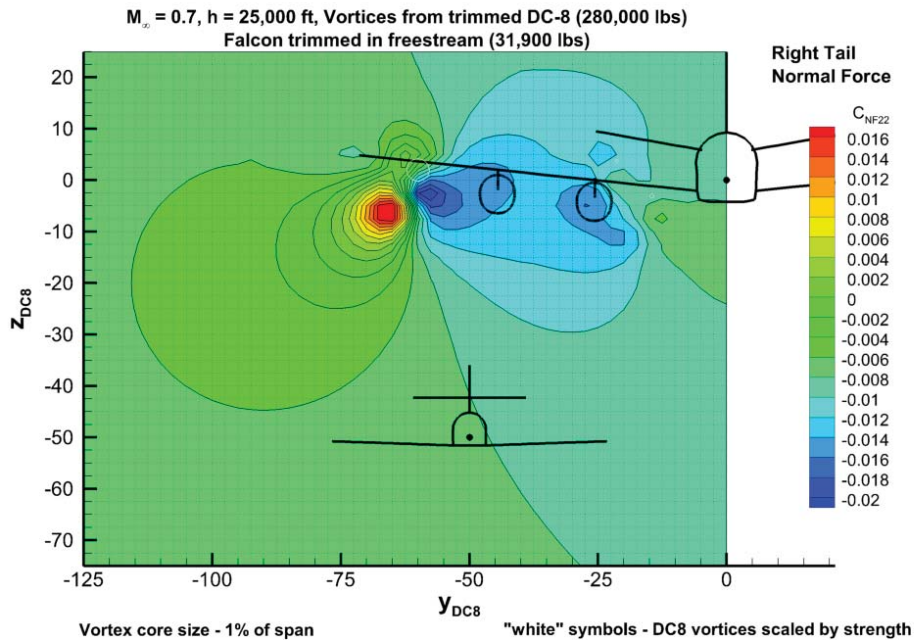


Figure 7.2-9. Near-Field Map of Falcon Right Horizontal Tail Normal Force Coefficient ( $C_{NF22}$ )



Title:

Probing Aircraft Flight Test Hazard Mitigation  
for the ACCESS Research Team

Page #:

68 of 118

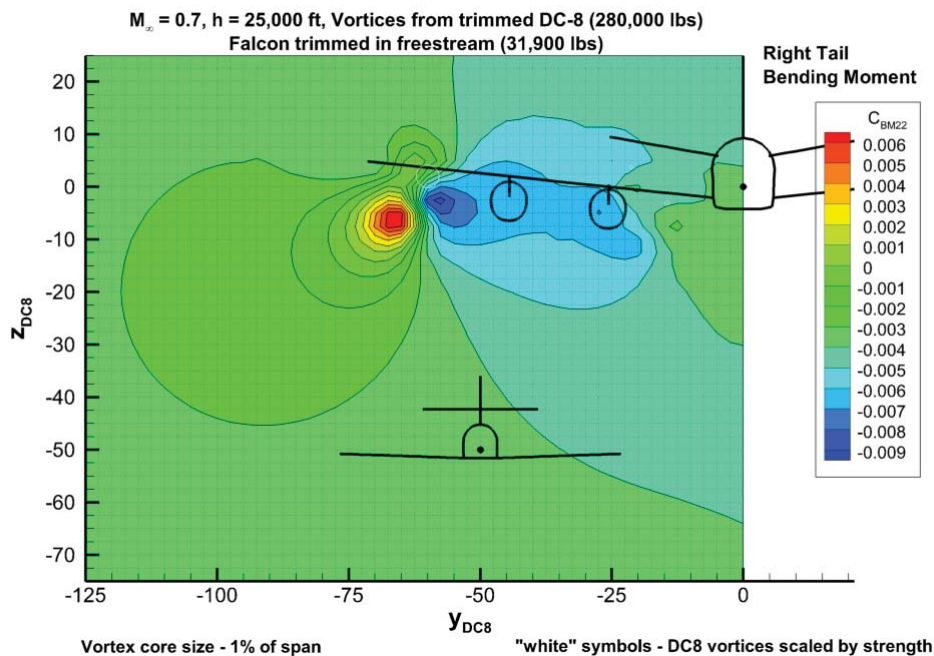


Figure 7.2-10. Near-Field Map of Falcon Right Horizontal Tail Bending Moment Coefficient ( $C_{BM22}$ )

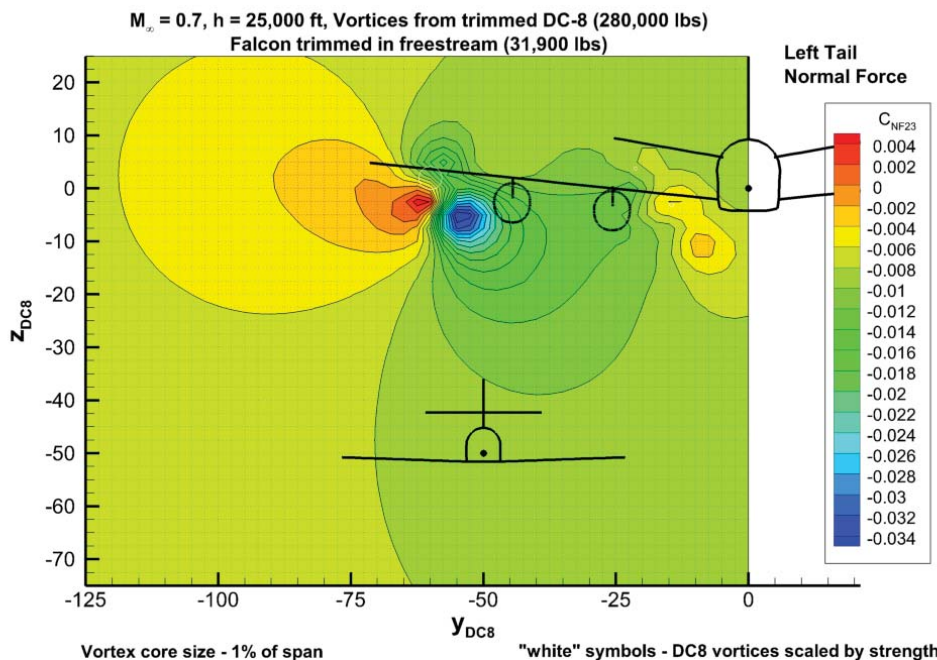


Figure 7.2-11. Near-Field Map of Falcon Left Horizontal Tail Normal Force Coefficient ( $C_{NF23}$ )



Title:

Probing Aircraft Flight Test Hazard Mitigation  
for the ACCESS Research Team

Page #:

69 of 118

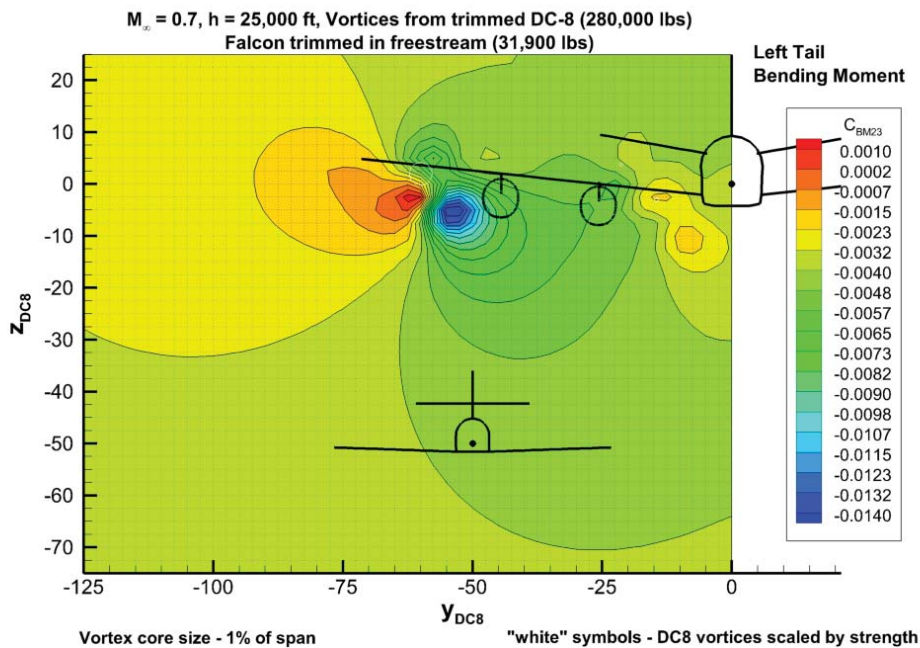


Figure 7.2-12. Near-Field Map of Falcon Left Horizontal Tail Bending Moment Coefficient ( $C_{BM23}$ )

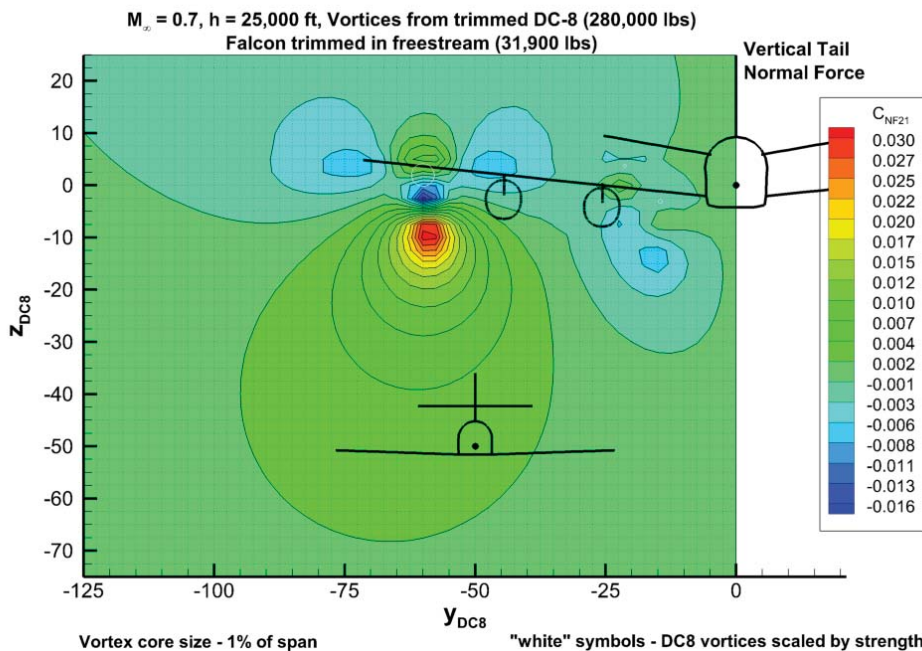


Figure 7.2-13. Near-Field Map of Falcon Vertical Tail Alone Normal Force Coefficient ( $C_{NF21}$ )



Title:

Probing Aircraft Flight Test Hazard Mitigation  
for the ACCESS Research Team

Page #:

70 of 118

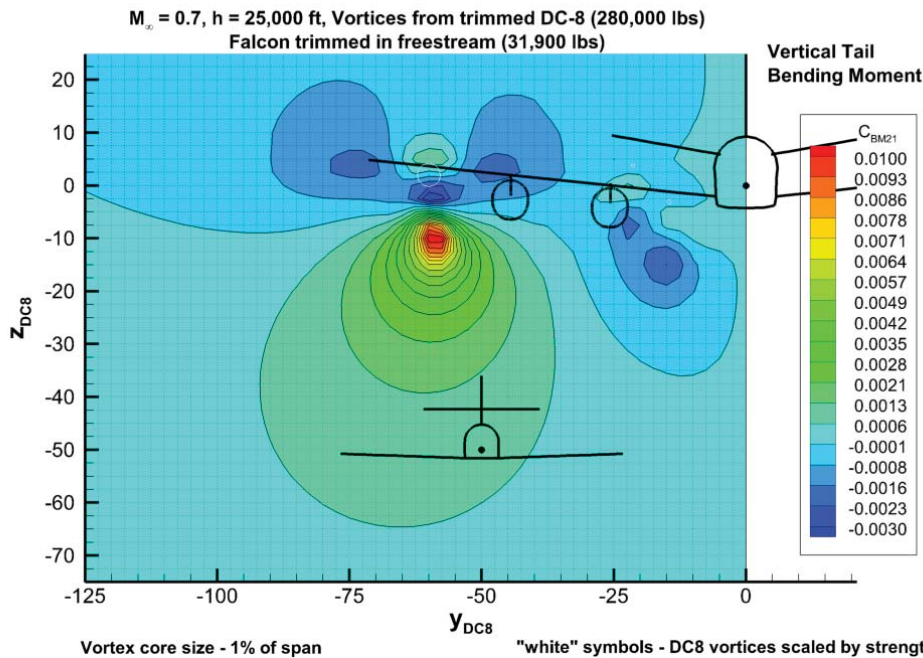


Figure 7.2-14. Near-Field Map of Falcon Vertical Tail (Alone) Bending Moment Coefficient ( $C_{BM21}$ )


Contour maps generated for the left- and right-wing normal forces and bending moments for the Falcon are not shown here. Summarized coefficient data for all mapped parameters can be found in Appendix E. All data were provided to the stakeholder as a deliverable.

### Structural Loads Assessment

Falcon 20 strength-capability information was not available from the manufacturer at a cost or on a schedule that was practicable for the project, but Falcon 20 loads values for gust response conditions that often envelop design conditions were found documented in a publically available 1966 Dassault document [ref. 40].

Table 7.2-3 shows for these load conditions the maximum shear and bending moment for each Falcon component. The NESC team treated these loads as if they were design limit load (DLL) conditions that defined the airplane's limit load envelope. This assumption was conservative because the envelope could only be larger, if, for example, design conditions with larger values were missing from this list.




|   |   |  |                        |
|---|---|--|------------------------|
|  | <b>NASA Engineering and Safety Center<br/>Technical Assessment Report</b> | Document #:<br><b>NESC-RP-<br/>12-00822</b>  | Version:<br><b>1.0</b> |
|   |   | <b>Probing Aircraft Flight Test Hazard Mitigation<br/>for the ACCESS Research Team</b> |                        |

*Table 7.2-3. Falcon 20 Presumed DLL Conditions*

|                              | Documented<br>Maximum<br>Design<br>Condition | Documented<br>Maximum Design<br>Shear, lb | Documented<br>Maximum Design<br>Bending Moment,<br>ft-lb |
|------------------------------|--|---|--|
| Right Wing                   | Vertical Gust                                | 46,247                                    | 485,441  |
| Left Wing                    | Vertical Gust                                | 46,247                                    | 485,441  |
| Vertical Tail                | Lateral Gust                                 | 4,737                                     | 14,331   |
| Right Horizontal             | Vertical Gust                                | -10,043                                   | -50,213  |
| Left Horizontal              | Vertical Gust                                | -10,043                                   | 50,213   |
| Differential Horizontal Load | Unsymmetric<br>Vertical Gust                 | -2,008                                    | -10,040  |

The data associated with each generated contour map was searched to find the largest aerodynamic load and bending moment for each Falcon component, and these were compared with the design limit load conditions. Table 7.2-4 shows the NESC team's peak computed loads and the project team's peak computed loads. All loads are also shown as a percent of DLL, where a value of 100-percent would indicate a zero margin with the inferred design limit load envelope. Note that in the table the bold red font denotes that the inferred DLLs were exceeded.



|  |   |                         |            |
|--|---|-------------------------|------------|
|       | <b>NASA Engineering and Safety Center<br/>Technical Assessment Report</b> | Document #:             | Version:   |
|  |   | <b>NESC-RP-12-00822</b> | <b>1.0</b> |
| Title:   |   |                         | Page #:    |
| <b>Probing Aircraft Flight Test Hazard Mitigation<br/>for the ACCESS Research Team</b> |   |                         | 72 of 118  |

*Table 7.2-4. Computed Vortex-induced Loads for a 1-percent Vortex Core*

|                              | Documented Maximum Design Condition | NESC TEAM Computed Vortex Induced Shear (1% Core Radius) |             | ACCESS TEAM Computed Shear | NESC TEAM Computed Vortex Induced Bending Moment (1% Core Radius) |             | ACCESS TEAM Computed Bending Moment |
|------------------------------|-------------------------------------|--|-------------|----------------------------|---|-------------|-------------------------------------|
|                              |                                     | lb   | % DLL       | % DLL                      | ft-lb   | % DLL       | % DLL                               |
| Right Wing                   | Vertical Gust                       | 30,321   | 65.6        | N/A                        | 335,771   | 69.2        | N/A                                 |
| Left Wing                    | Vertical Gust                       | 29,943   | 64.7        | N/A                        | 286,988   | 59.1        | N/A                                 |
| Vertical Tail                | Lateral Gust                        | 3,769  | 79.6        | 18                         | 13,278  | 92.7        | <b>327</b>                          |
| Right Horizontal             | Vertical Gust                       | -2,678   | 26.7        | <b>184</b>                 | -10,702   | 21.3        | <b>180</b>                          |
| Left Horizontal              | Vertical Gust                       | -4,413   | 43.9        | <b>184</b>                 | 16,817  | 33.5        | <b>180</b>                          |
| Differential Horizontal Load | Unsymmetric Vertical Gust           | -2,887   | <b>144.</b> | N/A                        | -10,969   | <b>109.</b> | N/A                                 |

The NESC team noted that the location used by the project team to sum the vertical tail bending moment may have been different from the point used by NESC team. The tabulated total vertical tail bending moment computed by the NESC team includes added differential horizontal tail load bending moments.

### 7.2.3 Core Size Sensitivity Analysis

The NESC team did not assess vortex decay models but observed that vortex-induced aerodynamic predictions in the far field are largely dependent on the selected vortex decay model. The more quickly a DC-8 primary wingtip vortex decays into the far field, the larger its core size will be, the smaller the induce velocities will be, and the smaller induced influence the vortex will have on the Falcon if inadvertently encountered.

The results given in the previous section were obtained for a 1-percent DC-8 primary vortex core size to represent the most conservative vortex interference effects on the Falcon. The NESC team repeated the contour mapping process for core sizes of 2.0- and 3.5-percent of the DC-8 wingspan. The team conducted 2000 additional computational runs for each. These resulting data may be useful for the project team for use with their chosen vortex decay assumptions.

Figure 7.2-15 shows computed tangential velocity, normalized by the vortex strength (which is proportional to the weight of the DC-8), through the center of the primary tip vortex for the three



Title:

Probing Aircraft Flight Test Hazard Mitigation  
for the ACCESS Research Team

Page #:

73 of 118

core radii ( $r_c$ ). It can be seen that the core size has a large effect on the peak velocity induced by the vortex but that a short distance outside the core the induced velocity is the same for all core radii.

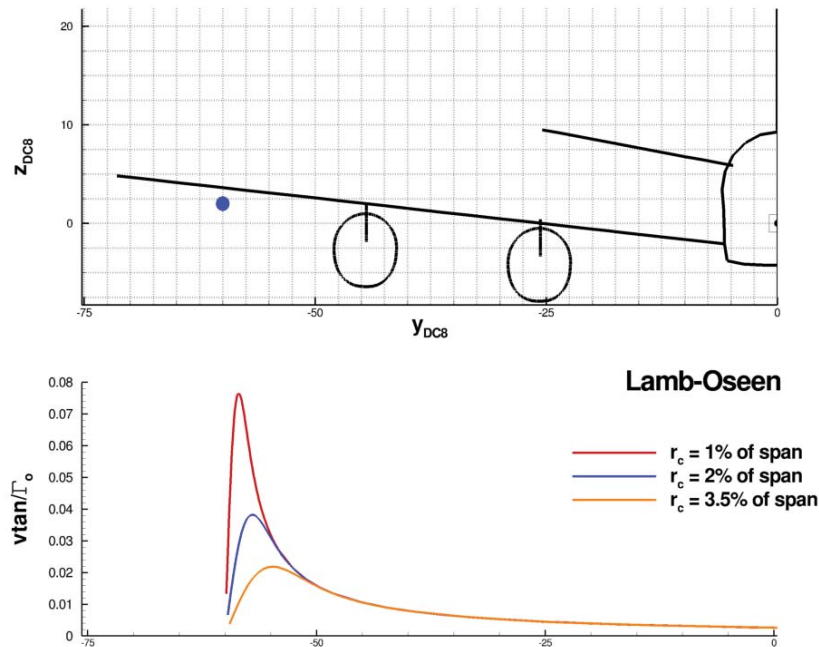



Figure 7.2-15. Core Radius Effect on Vortex-Induced Tangential Velocity

The results of the maximum forces and bending moments on the Falcon components are shown in Table 7.2-5. Contour maps are shown in Appendix E. The flight conditions for all results were at Mach 0.7 at an altitude of 25,000 ft to illustrate the potential problems associated with trailing vortex interference. These contours will change with DC-8 weight, Mach number, and altitude. Coefficient data files for these sample flight conditions were provided to the stakeholder as a deliverable.

|  |   |                         |            |
|--|---|-------------------------|------------|
|       | <b>NASA Engineering and Safety Center<br/>Technical Assessment Report</b> | Document #:             | Version:   |
|  |   | <b>NESC-RP-12-00822</b> | <b>1.0</b> |
| Title:   |   |                         | Page #:    |
| <b>Probing Aircraft Flight Test Hazard Mitigation<br/>for the ACCESS Research Team</b> |   |                         | 74 of 118  |

*Table 7.2-5. Falcon Maximum Forces and Bending Moments for Three Vortex Core Sizes*


| Falcon Component      | Maximum                      | Falcon<br>Baseline | DC-8 Vortex Core Radius (percent of wingspan) |         |         |
|-----------------------|------------------------------|--------------------|---|---------|---------|
|                       |                              |                    | 1%  | 2%      | 3.5%    |
| Right Wing            | Normal Force, lb             | 14,999             | 30,321  | 26,762  | 23,425  |
|                       | Bending Moment, ft-lb        | 151,921            | 335,771                                       | 287,860 | 243,776 |
| Left Wing             | Normal Force, lb             | 14,999             | 29,943  | 25,145  | 21,914  |
|                       | Bending Moment, ft-lb        | 151,921            | 286,988                                       | 253,704 | 223,424 |
| Vertical Tail         | Normal Force, lb             | 0                  | 3,769   | 2,486   | 1,559   |
|                       | Bending Moment, ft-lb        | 0                  | 12,005  | 7,332   | 4,379   |
|                       | Total* Bending Moment, ft-lb | 0                  | 13,278  | 9,120   | 6,180   |
| Right Horizontal Tail | Normal Force, lb             | -864               | -2,678  | -1,948  | -1,862  |
|                       | Bending Moment, ft-lb        | -3,891             | -10,702                                       | -7,970  | -7,641  |
| Left Horizontal Tail  | Normal Force, lb             | -864               | -4,413  | -3,067  | -2,191  |
|                       | Bending Moment, ft-lb        | -3,891             | -16,817                                       | -12,153 | -8,876  |

#### 7.2.4 Dynamic Simulations

The NESC team ran six-degree-of-freedom (6-DOF) simulations using the NEAR STRLNCH code to investigate Falcon trajectories beginning at various locations in the DC-8 wake. All assumed a 1-percent DC-8 wingtip vortex core size. A brief description of the STRLNCH method is presented below. This section will describe the tools, assumptions, and procedure used to obtain these simulations results. Results are included for six simulations of Falcon response in the DC-8 vortex wake, representing three key initial positions and two Falcon weights. Aerodynamic characteristics of the Falcon and loads and moments on each component of its wing and tail were provided as a deliverable to the stakeholder. Summaries are included in Appendix F.

#### STRLNCH Aircraft Store Separation Code

The NEAR STRLNCH aircraft store separation simulation code [refs. 33–36] was used to model and predict 6-DOF uncontrolled trajectory characteristics of a Falcon aircraft starting at selected positions following directly behind a leader DC-8 “parent” aircraft. STRLNCH had previously been validated by the company with wind-tunnel and flight-test data for many 6-DOF trajectory simulations and flow-field studies for a variety of configurations. Separation studies had been

|  |   |   |                        |
|--|---|---|------------------------|
|                 | <b>NASA Engineering and Safety Center<br/>Technical Assessment Report</b> | Document #:<br><b>NESC-RP-<br/>12-00822</b> | Version:<br><b>1.0</b> |
| Title:<br><b>Probing Aircraft Flight Test Hazard Mitigation<br/>for the ACCESS Research Team</b> |   | Page #:<br>75 of 118                        |                        |

performed on external tanks, pods, bombs, missiles, rockets, launch vehicles, and aircraft, as documented in references 35, 36, and 42–57.

The STRLNCH code used classical aerodynamic flow models to predict the flow in the vicinity of an aircraft. It used parent aircraft perturbation velocities, including effects of the trailing wing and tail vortex wakes. Its flow models were based on solving potential flow equations and Laplace’s equation with compressibility corrections. It used classical singularity methods augmented with body and fin vortex modeling and wing stall models based on empirical data.

STRLNCH can model flow effects due to combined angle of pitch and sideslip, as well as rotational rates of the parent aircraft. The NEAR MISDL [refs. 37–40] and MISL3 [refs. 39, 40, 58, 59] programs were used to model Falcon 20 aerodynamic forces and moments for the simulation. The maximum parent-aircraft angle of attack at launch was set by the validity of the fuselage vortex shedding and wing stall models. This angle was about 30 degrees. The store incident angle of attack was approximately 30 degrees using the MISDL module and may range up to 90 degrees using the MISL3 module.


STRLNCH flow models were valid for subsonic Mach numbers up to the critical speed or onset of transonic flow. The Göthert compressibility correction was included. The aircraft flow models included high-angle-of-attack fuselage vortex shedding, a vortex-lattice panel method for modeling the wing/pylon, and an interference shell for wing-on-fuselage aerodynamic interference.

The fuselage was modeled with three-dimensional sources/sinks to model volume and doublets to model angle-of-attack effects. Conformal mapping techniques were used to model noncircular fuselage cross sections. The wing and pylon flow models represented effects of lift and thickness (source panels). Further details of the vortex lattice panel method and other singularity-based flow models are described in reference 36.

STRLNCH included first-order corrections to the wing horseshoe vortex panel method to account for high-angle-of-attack effects. This included a semi-empirical stall model to modify wing loading at high angles of attack.

### **Mass property estimation**

Falcon mass property data were not available from Dassault but were required for the dynamic simulations. The team estimated Falcon moments of inertia using known values for a similar aircraft and a method described in Roskam’s *Airplane Design Part V: Component Weight Estimation* [ref. 60]. The NESC team learned that a Federal Aviation Administration (FAA) safety oversight group had routinely used this same method to estimate roll moments of inertia when conducting safety assessments of wake vortex core encounters where manufacturer data were not available. The FAA group was reported to have found the method to be accurate to within 20 percent. The method requires reference aircraft to be of similar configuration but does not require it to be of similar weight.

|  |   |                         |            |
|--|---|-------------------------|------------|
|       | <b>NASA Engineering and Safety Center<br/>Technical Assessment Report</b> | Document #:             | Version:   |
|  |   | <b>NESC-RP-12-00822</b> | <b>1.0</b> |
| Title:   |   | Page #:                 |            |
| <b>Probing Aircraft Flight Test Hazard Mitigation<br/>for the ACCESS Research Team</b> |   | 76 of 118               |            |

The NESC team reviewed several sources, including *Jane's All the Worlds Aircraft* [ref. 61], to consider aircraft types similar in their configuration to the Falcon 20 for which dimensional and mass property information was available. The NESC team chose the Cessna Citation II Model 550, shown in Figure 7.2-16. The Cessna 550 has two fuselage-mounted turbofan engines and a cruciform configuration tail structure. It was used by the U.S. Customs and Boarder Protection Agency and by the U.S. Navy (designated the T-47A).



*Figure 7.2-16. Cessna 550*


Cessna 550 mass property data were available to the team but are not shown here to protect proprietary information. A basic comparison of the Falcon 20 and the Cessna 550 is shown in Table 7.2-6.

*Table 7.2-6. Basic Comparison Between Cessna 550 and Falcon 20*

|            | MTOW<br>(lb) | Span<br>(ft, in) | Length<br>(ft, in) | Height<br>(ft, in) | Wing Area<br>(ft <sup>2</sup> ) |
|------------|--------------|------------------|--------------------|--------------------|---------------------------------|
| Falcon 20  | 32,000       | 53, 6            | 56, 3              | 17, 7              | 450                             |
| Cessna 550 | 13,500       | 51, 8            | 47, 3              | 15, 0              | 323                             |

The NESC team recognized roll moment of inertia as a key factor in vortex encounter response. An aircraft's roll moment of inertia would largely depend on its fuel state, so Falcon operating



|  |   |                         |            |
|--|---|-------------------------|------------|
|       | <b>NASA Engineering and Safety Center<br/>Technical Assessment Report</b> | Document #:             | Version:   |
|  |   | <b>NESC-RP-12-00822</b> | <b>1.0</b> |
| Title:   |   |                         | Page #:    |
| <b>Probing Aircraft Flight Test Hazard Mitigation<br/>for the ACCESS Research Team</b> |   |                         | 77 of 118  |

empty weight (OEW) and MTOW were chosen for the simulations. The NESC team referred to these as the “light” and “heavy” conditions. Table 7.2-7 shows the Falcon inertial characteristics derived per the methods of Roskam [ref. 60]. The estimated Falcon roll moment of inertia ( $I_{xx}$ ) can be seen to vary by a roughly a factor of 2.

*Table 7.2-7. Falcon 20 Inertial Properties, Empty and at MTOW*

|                     | Weight (lb) | $I_{xx}$<br>(slug-ft <sup>2</sup> ) | $I_{yy}$<br>(slug-ft <sup>2</sup> ) | $I_{zz}$<br>(slug-ft <sup>2</sup> ) |
|---------------------|-------------|-------------------------------------|-------------------------------------|-------------------------------------|
| Falcon Light (OEW)  | 24,150      | 31,690                              | 94,922                              | 112,815                             |
| Falcon Heavy (MTOW) | 32,000      | 61,049                              | 76,522                              | 131,972                             |

### Simulations Conducted

The NESC team computed trajectories for the light and the heavy Falcon at three starting points in the DC-8 flow field, for a total of six simulations. The three starting points for the simulations are described below and are noted in Table 7.2-8.


*Table 7.2-8. Falcon 6-DOF Simulations*

| Simulation | Falcon Starting Point  | Comments   |
|------------|--|--|
| 1-Light    | Nose beginning at the location of maximum rolling moment (is not same as cruciform tail centered in vortex or aircraft nose centered in vortex). | This simulation assumes the Falcon has fully penetrated into a DC-8 primary wingtip vortex. This could represent a near-field inadvertent lateral drift into a vortex or a far-field inadvertent descent into a vortex that has not decayed (1-percent core size). |
| 1-Heavy    |  |  |
| 2-Light    | Nose beginning aligned with the centerline of the inboard engine.  | This simulation of a nominal near-field sampling mission includes no pilot inputs to maintain sampling position.   |
| 2-Heavy    |  |  |
| 3-Light    | Left wingtip beginning near the center of the DC-8 left wingtip vortex.  | This simulation assumes the Falcon has slowly drifted laterally in near field and has closed the clearance distance to zero between its wingtip and the DC-8 primary wingtip vortex.   |
| 3-Heavy    |  |  |

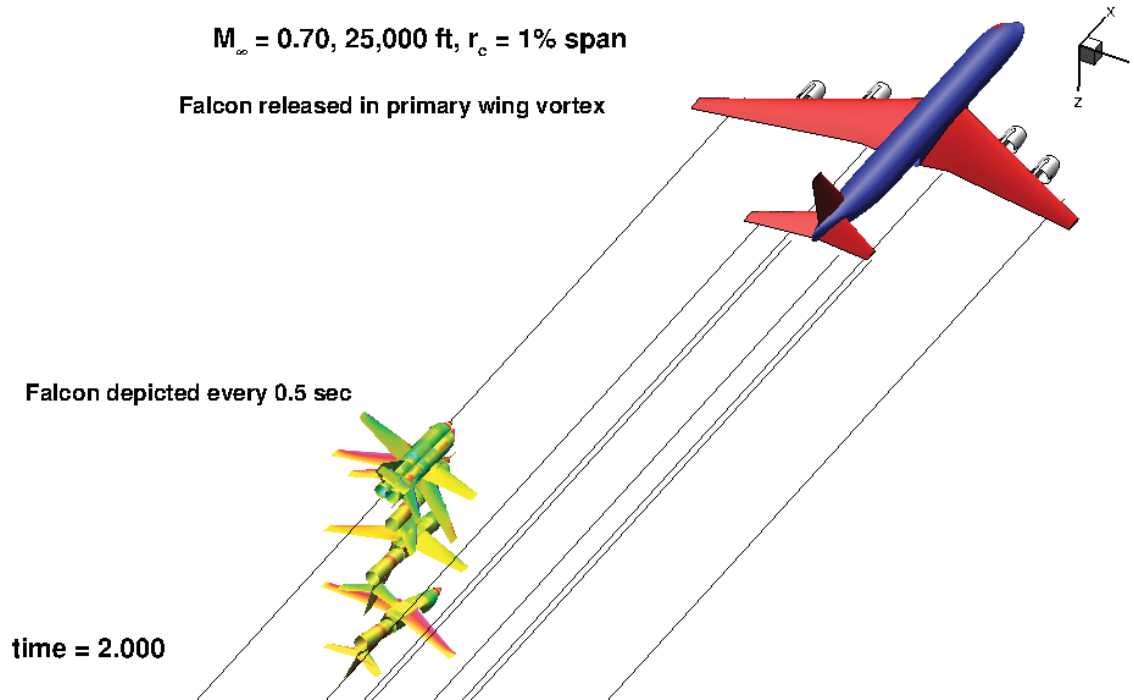
The six simulation results are described in the following subsections. Animation files for all six simulations were provided to the stakeholder as deliverables.

### Light Falcon Beginning in the Vortex

Simulation 1L (“light”) was conducted beginning with a light Falcon’s nose near the center of the primary vortex of the DC-8. The aircraft was positioned at the location of maximum induced rolling moment, as previously determined in Section 7.2. This case could represent a near-field inadvertent lateral drift into a vortex or a far-field inadvertent descent into a vortex that has not decayed (i.e., it is still a 1-percent core size). To begin the simulations, the Falcon was trimmed for cruise flight conditions without vortex interference and placed at the point of maximum

|  |   |  |                        |
|--|---|--|------------------------|
|                 | <b>NASA Engineering and Safety Center<br/>Technical Assessment Report</b> | Document #:<br><b>NESC-RP-12-00822</b> | Version:<br><b>1.0</b> |
| Title:<br><b>Probing Aircraft Flight Test Hazard Mitigation<br/>for the ACCESS Research Team</b> |   | Page #:<br>78 of 118                   |                        |

induced rolling moment. The aircraft was released and allowed to move in a 6-DOF trajectory with all controls fixed (i.e., a stick-fixed trajectory with no pilot input to the aircraft controls). Orthogonal view snapshots of Falcon position relative to the DC-8 are shown at half-second intervals in Figure 7.2-17.



*Figure 7.2-17. Simulation Depiction for Light Falcon Beginning in the Vortex*

In this trajectory simulation, the light Falcon was seen to roll with the right wing down at a roll rate that increased to more than 170 deg/sec at approximately 0.8 seconds after release. At that time, the Falcon had rolled to nearly 100 degrees. By approximately 1.8 seconds, the Falcon had rolled to nearly 190 degrees. When the simulation stopped at 2 seconds, the Falcon had nearly stabilized in an inverted attitude. The flight conditions of the Falcon in the simulated trajectory are shown in Figure 7.2-18 to illustrate the history of angle of attack ( $\alpha$ ); angle of sideslip ( $\beta$ ); roll ( $\Phi$ ), pitch ( $\Theta$ ), and yaw ( $\Psi$ ) angles; and angular rates ( $p$ ,  $q$ ,  $r$ ). Time histories of the Falcon aerodynamic force and moment coefficients are shown in Figure 7.2-19.



Title:

Probing Aircraft Flight Test Hazard Mitigation  
for the ACCESS Research Team

Page #:

79 of 118

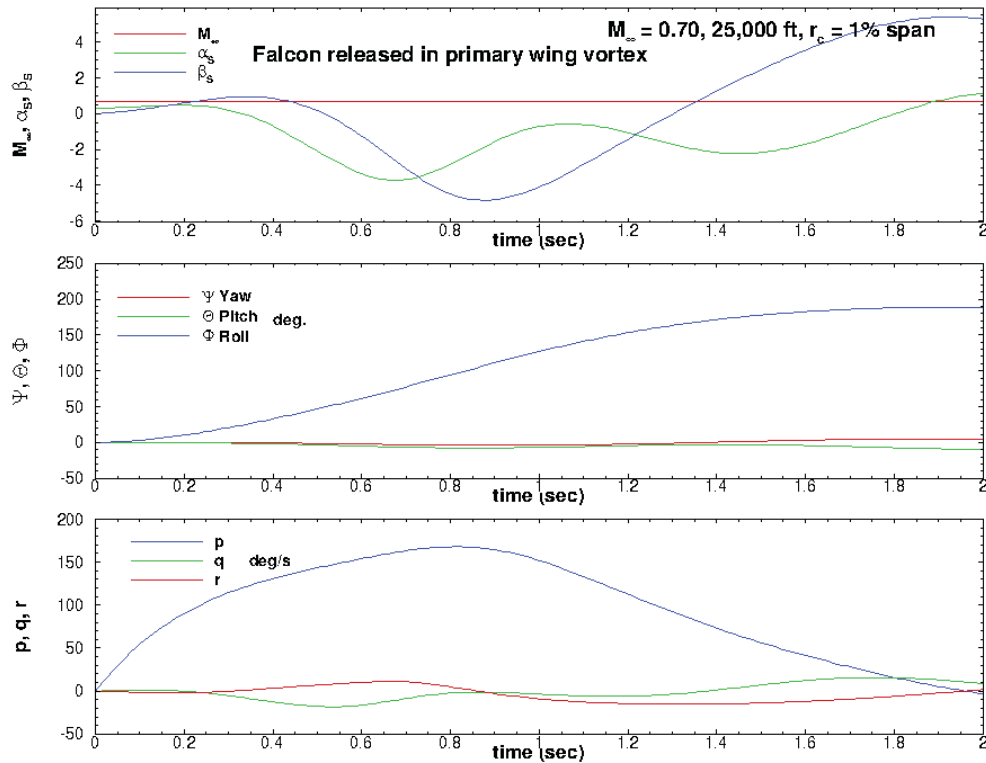


Figure 7.2-18. Response Data for Light Falcon Beginning in the Vortex

Computed wing and vertical and horizontal tail shears and bending moments for this simulation can be found in Appendix F. Because of the method employed to initialize the simulation, the team was unable to determine physically realistic peak differential horizontal tail shears or bending moments from the simulation for comparison with the static predictions. This could have provided an estimate of theorized inertial relief for those loads that were computed to exceed limit load in the static analysis (see Table 7.2-4).



Title:

Probing Aircraft Flight Test Hazard Mitigation  
 for the ACCESS Research Team

Page #:

80 of 118

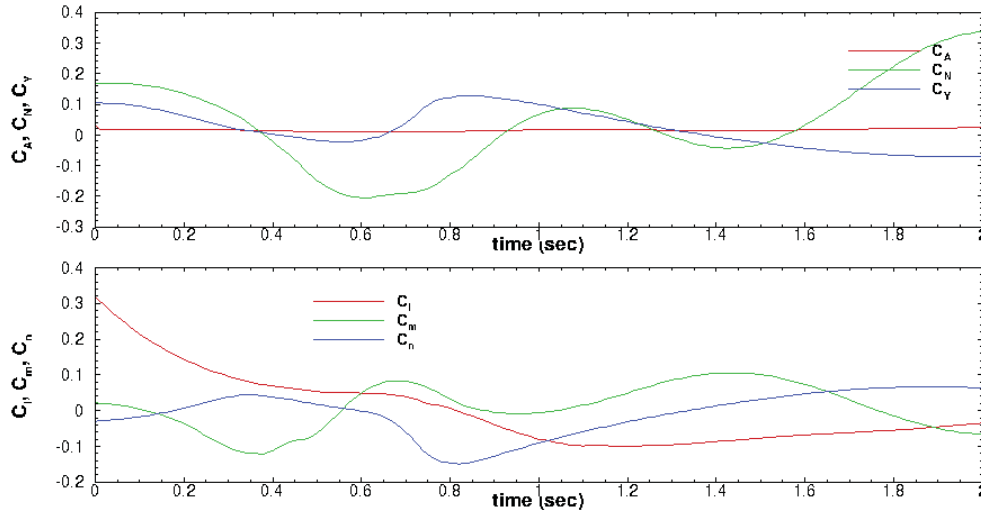


Figure 7.2-19. Force Data for Light Falcon Beginning in the Vortex

Heavy Falcon Beginning in the Vortex

Simulation 1H (“heavy”) was identical to 1L, except the Falcon inertial properties estimated for MTOW were used. Orthogonal view snapshots of the heavy Falcon position relative to the DC-8 are shown at half-second intervals in Figure 7.2-20.

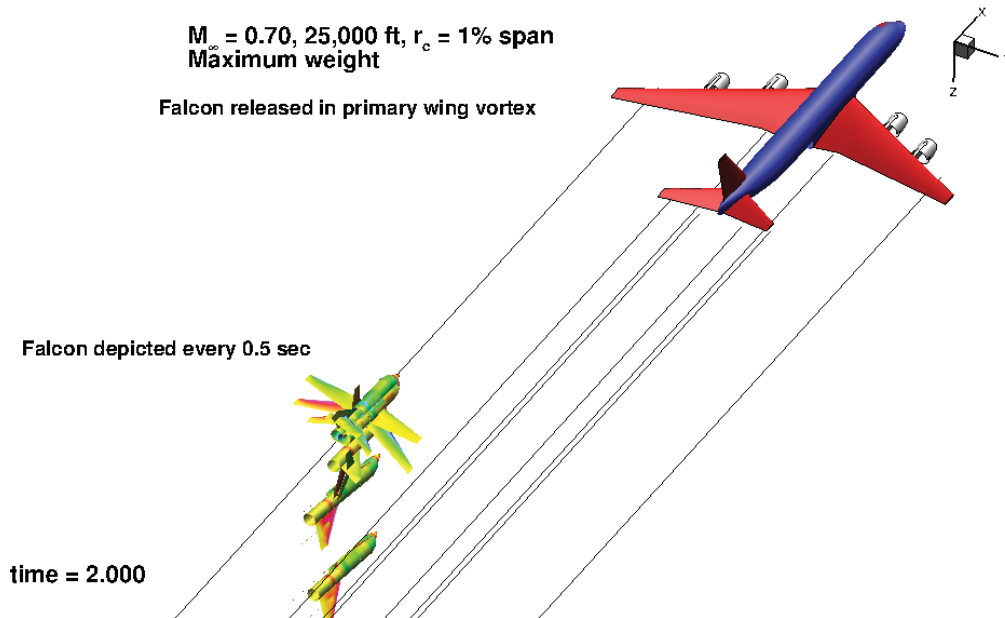


Figure 7.2-20. Simulation Depiction for Heavy Falcon Released in the Wingtip Vortex

In this trajectory simulation, the Falcon was seen to roll away naturally, with a maximum roll angle about of 130 degrees and 130 deg/sec maximum rate. Simulation flight condition and



Title:

Probing Aircraft Flight Test Hazard Mitigation  
for the ACCESS Research Team

Page #:

81 of 118

force coefficient results are shown in Figures 7.2-21 and 7.2-22, respectively. Computed wing, vertical tail, and horizontal tail shears and bending moments for this simulation can be found in Appendix F. This simulation differs slightly from the one described in the interim briefing to the project team. The earlier simulation began with the Falcon's nose aligned not at the location of maximum rolling moment but rather with the vortex; it reached a maximum roll attitude of only about 90 degrees.

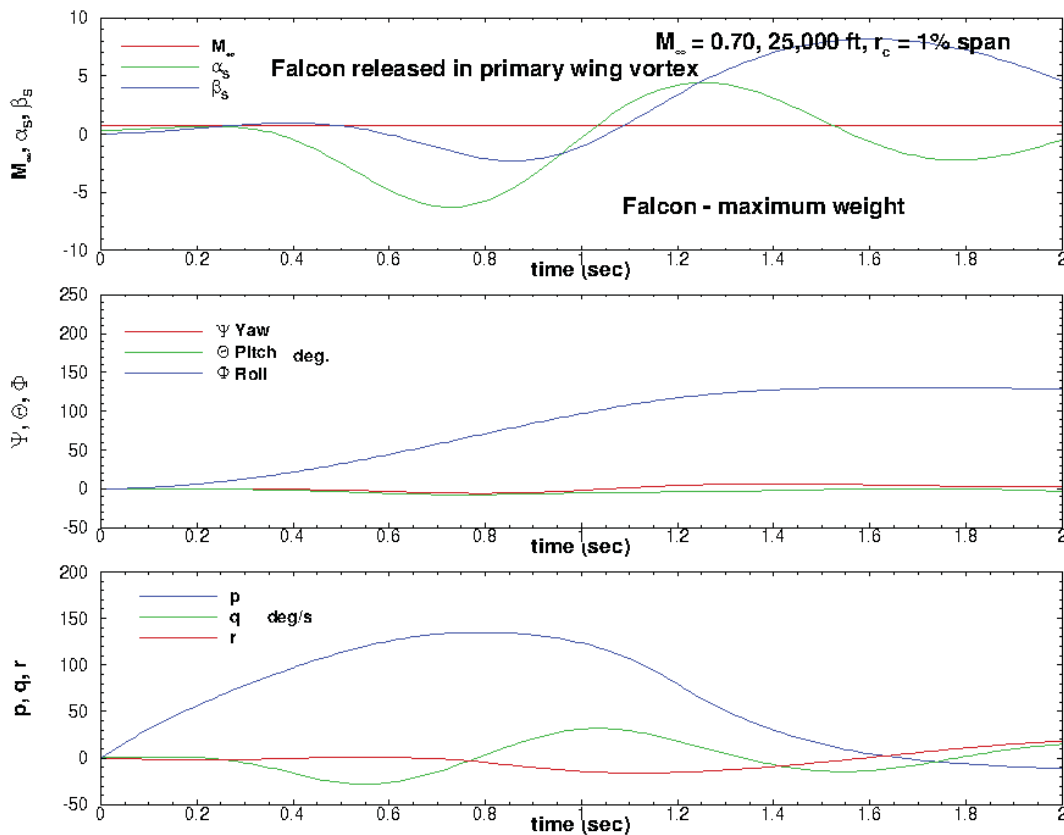


Figure 7.2-21. Response Data for Heavy Falcon Beginning in the Vortex





Title:

Probing Aircraft Flight Test Hazard Mitigation  
for the ACCESS Research Team

Page #:

82 of 118

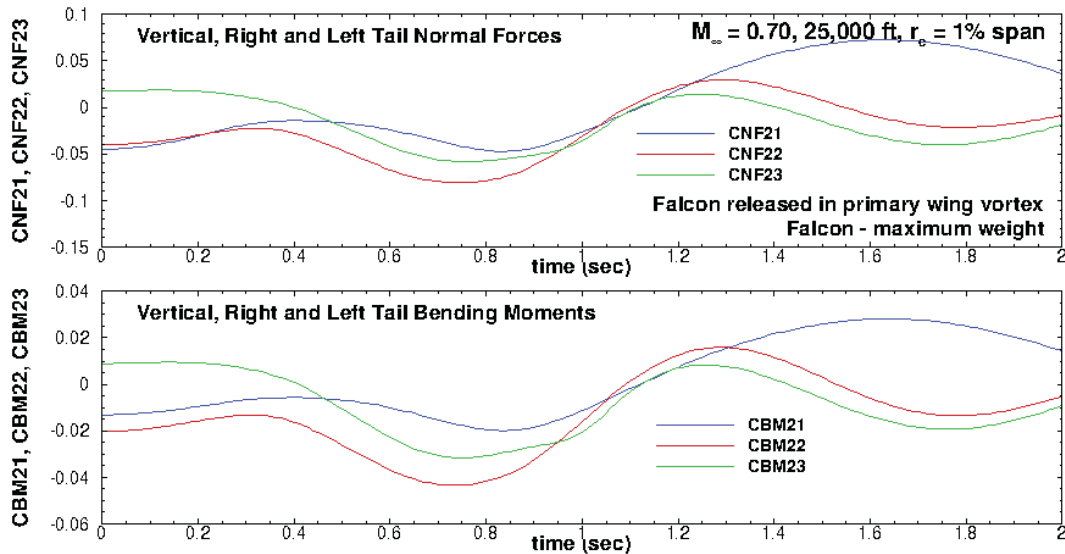

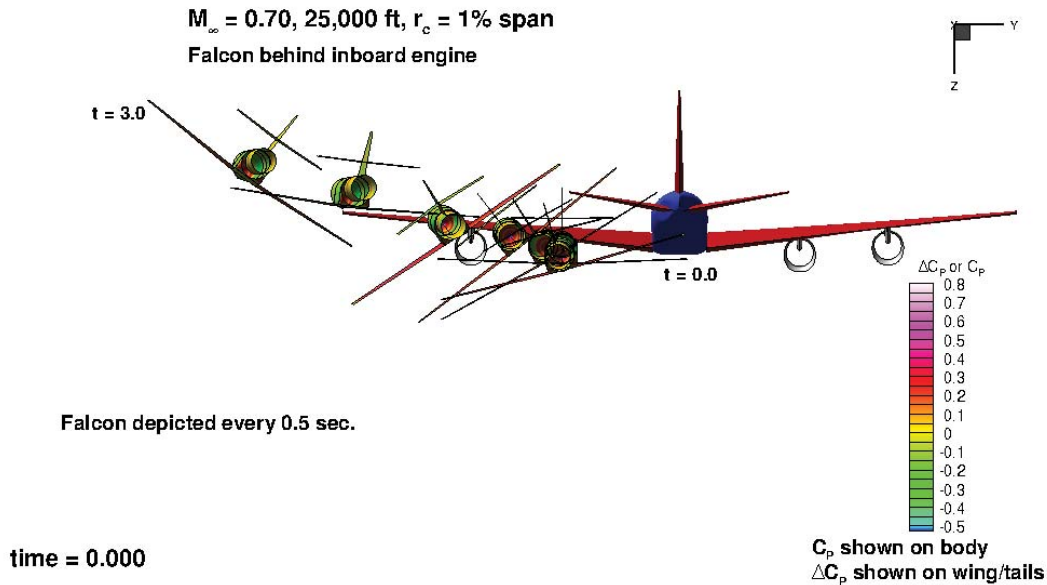


Figure 7.2-22. Force Data for Heavy Falcon Beginning in the Vortex

### Light Falcon Beginning behind the Inboard Engine

Simulation 2L was conducted beginning with a light Falcon's nose aligned on the centerline of the inboard DC-8 engine of the DC-8. This case could represent a nominal near-field sampling mission, but without pilot inputs to maintain sampling position. The initial flight conditions were the same as for simulation 1. Only the initial position of the Falcon was changed; the Falcon was trimmed for cruise flight in an undisturbed free stream and then released, stick fixed. This simulation was run for 3 seconds. Rear-view snapshots of Falcon position relative to the DC-8 are shown at half-second intervals in Figure 7.2-23.

|  |   |  |                        |
|--|---|--|------------------------|
|                 | <b>NASA Engineering and Safety Center<br/>Technical Assessment Report</b> | Document #:<br><b>NESC-RP-12-00822</b> | Version:<br><b>1.0</b> |
| Title:<br><b>Probing Aircraft Flight Test Hazard Mitigation<br/>for the ACCESS Research Team</b> |   | Page #:<br>83 of 118                   |                        |



**Figure 7.2-23. Simulation Depiction for Light Falcon Released Behind Inboard Engine**

In this trajectory simulation, the light Falcon was seen to drop its left wing, climb, and pass close to but directly above the vortex core. The aircraft is seen to reverse roll direction from about 40 degrees left wing down to 40 degrees right wing down in about 1 second as it traverses just above the vortex core. Peak roll rate during this time was about 120 deg/sec. Simulation flight condition and force coefficient results are shown in Figures 7.2-24 and 7.2-25, respectively. This simulation illustrated the possible consequences of an inadvertent lateral encounter with the vortex. It is important to reiterate, however, that this was a stick-free simulation with no pilot inputs.



Title:

Probing Aircraft Flight Test Hazard Mitigation  
for the ACCESS Research Team

Page #:

84 of 118

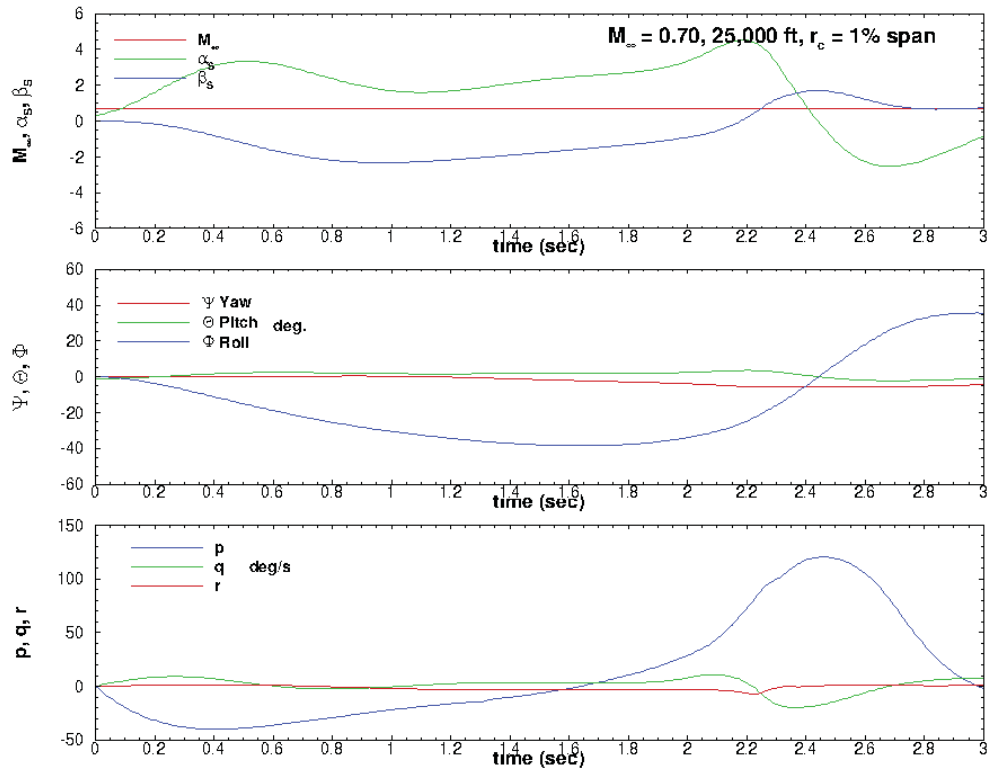


Figure 7.2-24. Response Data for Light Falcon Released Behind Inboard Engine

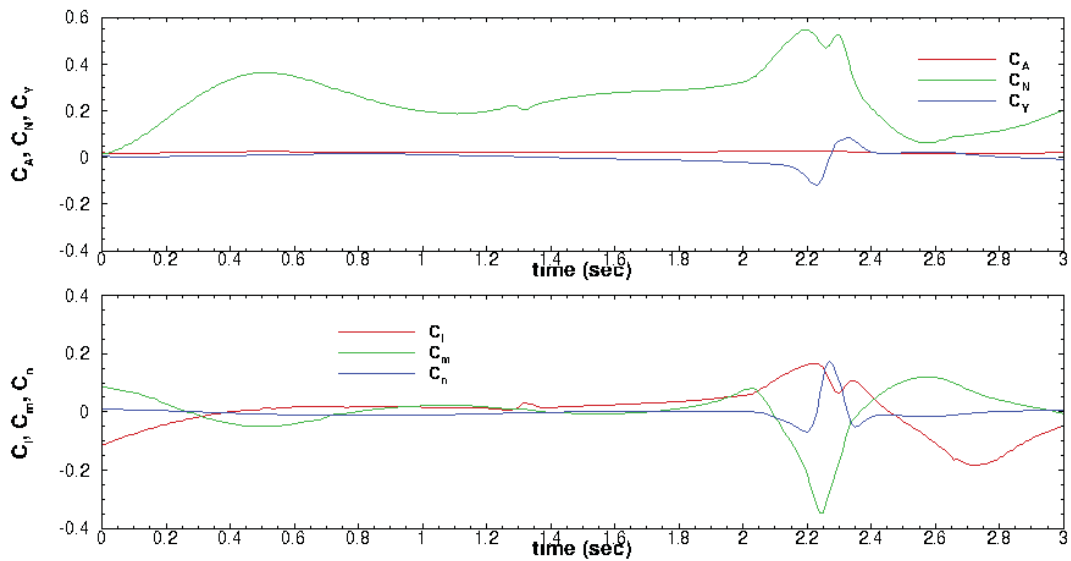

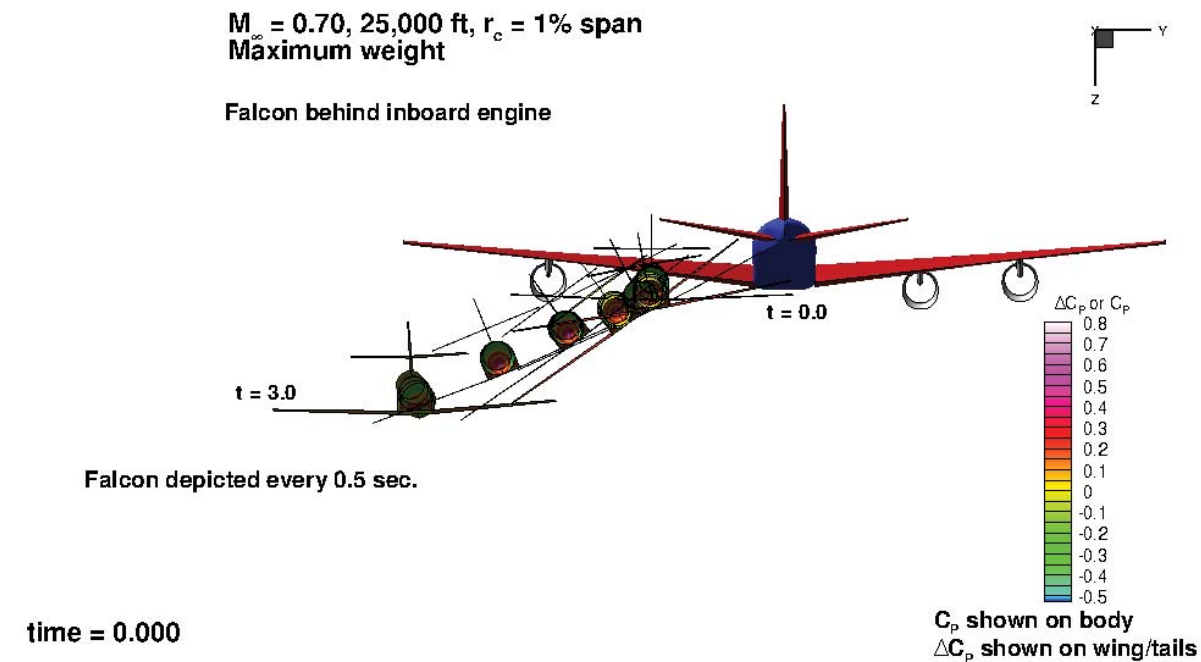


Figure 7.2-25. Force Data for Light Falcon Released Behind Inboard Engine

|  |   |                         |            |
|--|---|-------------------------|------------|
|       | <b>NASA Engineering and Safety Center<br/>Technical Assessment Report</b> | Document #:             | Version:   |
|  |   | <b>NESC-RP-12-00822</b> | <b>1.0</b> |
| Title:   |   | Page #:                 |            |
| <b>Probing Aircraft Flight Test Hazard Mitigation<br/>for the ACCESS Research Team</b> |   | 85 of 118               |            |

### Heavy Falcon Beginning behind the Inboard Engine

Simulation 2H (heavy) was identical to 2L, except that the Falcon inertial properties that were estimated for MTOW were used. This simulation was run for 3 seconds. Rear-view snapshots of the Falcon position relative to the DC-8 are shown at half-second intervals in Figure 7.2-26.



*Figure 7.2-26. Simulation Depiction for Heavy Falcon Released Behind Inboard Engine*

In this trajectory simulation, the heavy Falcon was seen to drop its left wing, descend, and pass benignly beneath the vortex. Simulation flight condition and force coefficient results are shown in Figures 7.2-27 and 7.2-28, respectively. Comparison of this heavy Falcon simulation result with that of the previous light Falcon simulation result could suggest an intermediate weight (and intermediate roll moment of inertia) where the Falcon could respond in a manner in which its empennage passes directly through the vortex core and experiences larger induced tail loads. Note that these simulations did not have pilot inputs to maintain the aircraft in its initial starting position.



Title:

Probing Aircraft Flight Test Hazard Mitigation  
for the ACCESS Research Team

Page #:

86 of 118

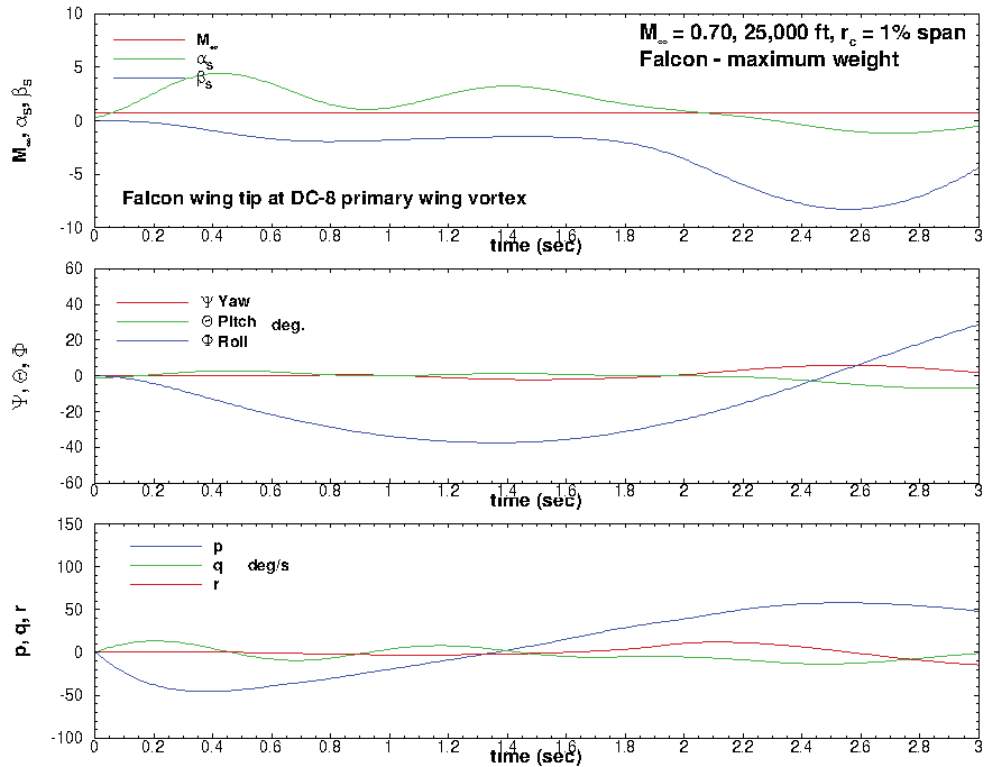


Figure 7.2-27. Response Data for Heavy Falcon Released Behind Inboard Engine

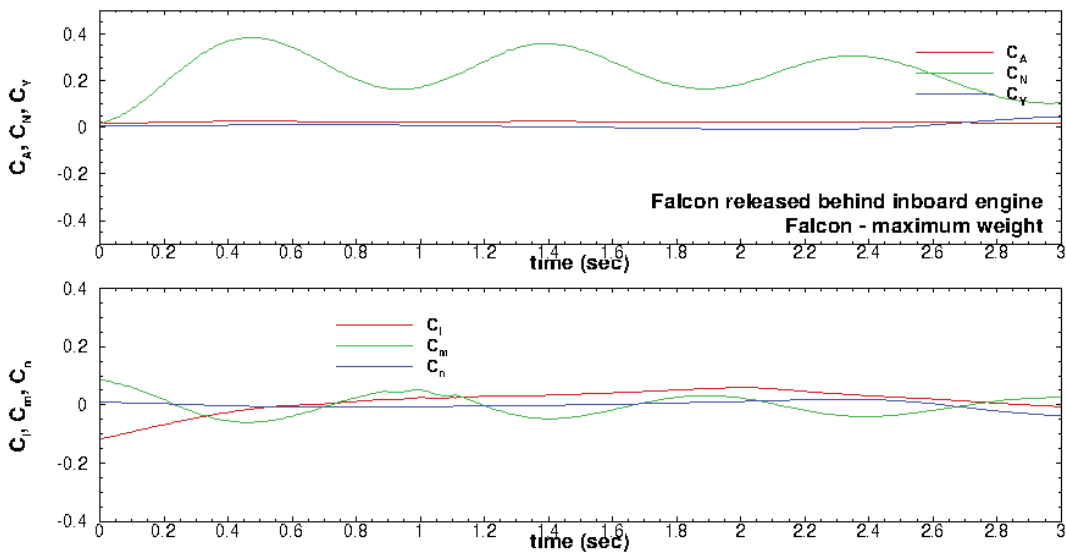



Figure 7.2-28. Force Data for Heavy Falcon Released Behind Inboard Engine

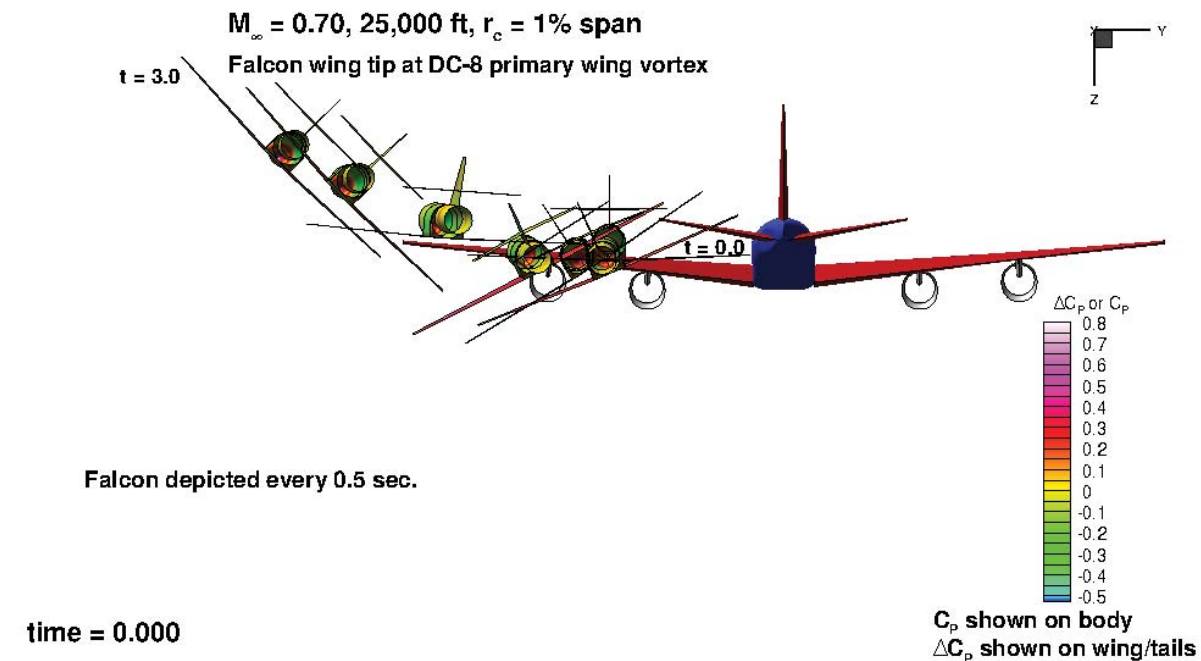


|  |   |                         |            |
|--|---|-------------------------|------------|
|       | <b>NASA Engineering and Safety Center<br/>Technical Assessment Report</b> | Document #:             | Version:   |
|  |   | <b>NESC-RP-12-00822</b> | <b>1.0</b> |
| Title:   |   | Page #:                 |            |
| <b>Probing Aircraft Flight Test Hazard Mitigation<br/>for the ACCESS Research Team</b> |   | 87 of 118               |            |

### Light Falcon Beginning with Wingtip near the Vortex

Simulation 3L was conducted beginning with a light Falcon positioned outboard from the inboard engine sampling position until its left wingtip was nearly in the center of the DC-8 primary vortex. This case could represent a condition where the Falcon has inadvertently drifted laterally in the near field and closed the clearance distance to zero between its wingtip and the DC-8 primary wingtip vortex. The flight conditions were the same as for the other simulations; only the initial position of the Falcon was changed. As before, the Falcon was trimmed for cruise flight in an undisturbed free stream and then released, stick fixed.

This simulation was run for 3 seconds. A snapshot of the Falcon at half-second intervals is shown in Figure 7.2-29. In this case, a rear view is shown for better clarity of the Falcon motion. At each instance in the simulation, all of the aerodynamic characteristics of the Falcon are available, as are the loads and moments on each component of the wing and tail.



*Figure 7.2-29. Simulation Depiction for Light Falcon Released with Wingtip in Vortex*

In this trajectory simulation, the light Falcon was seen to respond in a manner similar to that in simulation 2L. The aircraft is seen to drop its left wing, climb, and pass close to but directly above the vortex core. The aircraft reverses roll direction from about 35 degrees left wing down to 45 degrees right wing down in approximately 1.5 seconds as it traverses the vortex core. Peak roll rate at this time was about 110 deg/sec. The aircraft was still rolling left when it traversed the clockwise vorticity. The simulation flight conditions and force coefficient results are shown in Figures 7.2-30 and 7.2-31, respectively.



Title:

Probing Aircraft Flight Test Hazard Mitigation  
for the ACCESS Research Team

Page #:

88 of 118

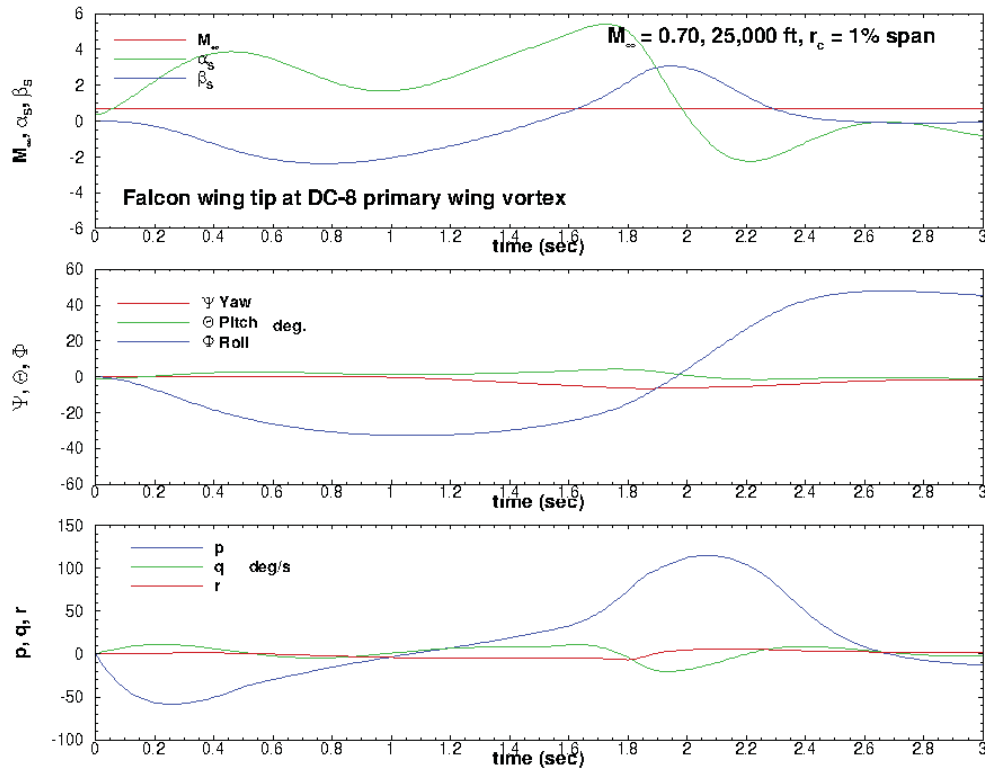


Figure 7.2-30. Response Data for Light Falcon Released with Wingtip in Vortex

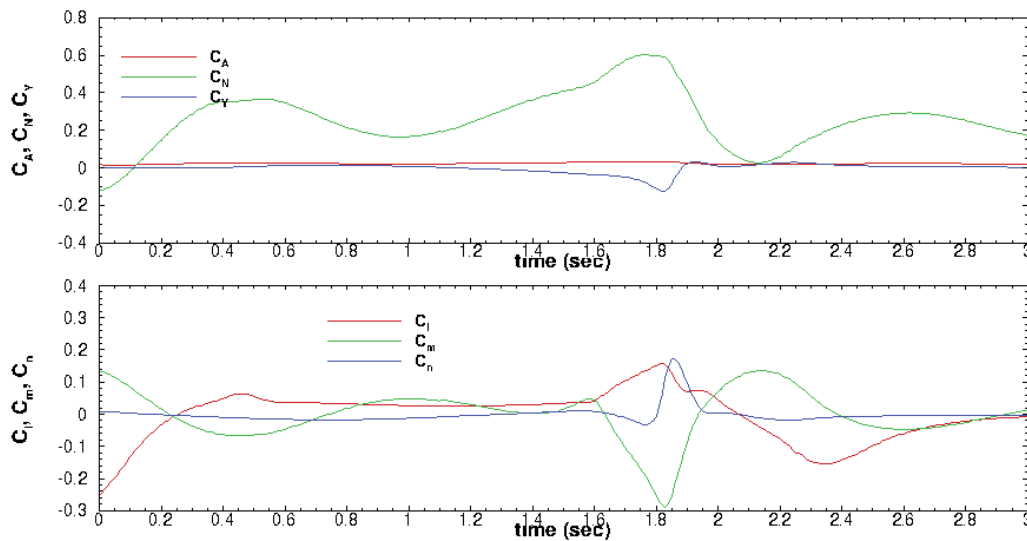



Figure 7.2-31. Force Data for Light Falcon Released with Wingtip in Vortex

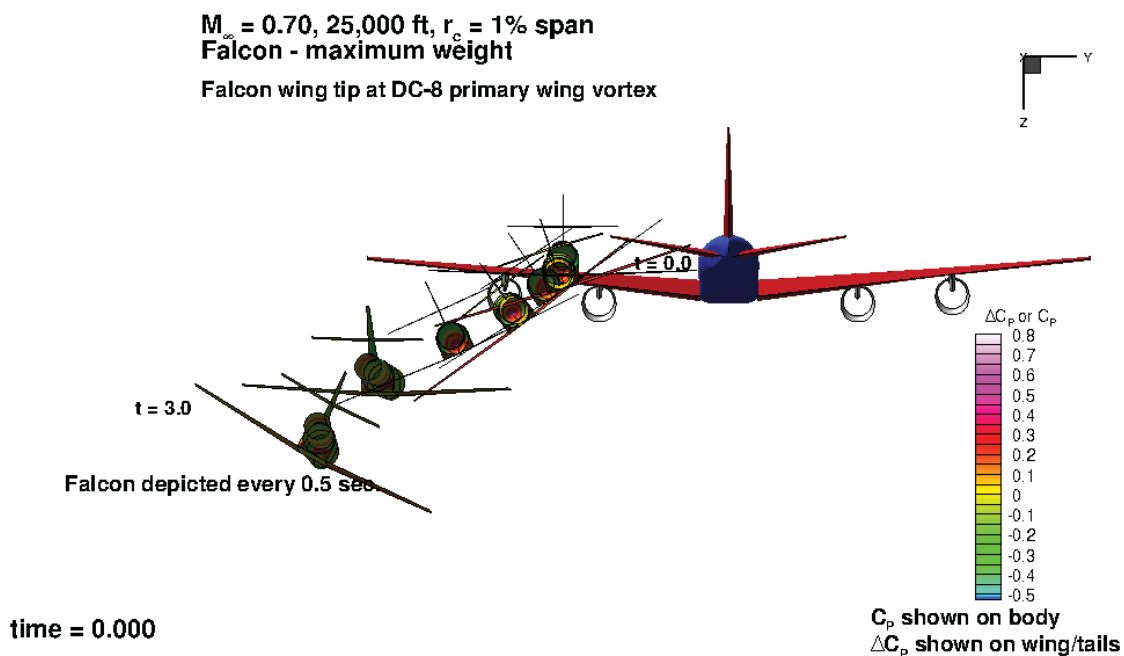
The NESC team attempted to query the simulation results to obtain peak horizontal tail differential shear and bending moment values to compare with the computed static load results.

|  |   |  |                        |
|--|---|--|------------------------|
|                 | <b>NASA Engineering and Safety Center<br/>Technical Assessment Report</b> | Document #:<br><b>NESC-RP-12-00822</b> | Version:<br><b>1.0</b> |
| Title:<br><b>Probing Aircraft Flight Test Hazard Mitigation<br/>for the ACCESS Research Team</b> |   | Page #:<br>89 of 118                   |                        |

An NESC team presumption was that inertial effects would generally relieve loads compared with static analyses. These simulation loads rose to a large peak well in excess of the limit load and then fall back down within just a few simulation integration steps. The values are not cited here because this stick-free simulation was not a credible real-world condition. However, the results illustrate that adverse phasing of flight rates could cause inertial effects to increase loads rather than just decrease them.

### Heavy Falcon Beginning with Wingtip near the Vortex

Simulation 3H (“heavy”) was identical to simulation 3L, except that the Falcon inertial properties estimated for MTOW were used. This simulation was run for 3 seconds. Rear-view snapshots of the Falcon position relative to the DC-8 are shown at half-second intervals in Figure 7.2-32.



*Figure 7.2-32. Simulation Depiction for Heavy Falcon Released with Wingtip in Vortex*

In this trajectory simulation, the heavy Falcon was seen to experience an initial roll to its left and then sideslip down and pass beneath the primary vortex. Simulation flight condition and force coefficient results are shown in Figures 7.2-33 and 7.2-34, respectively.



Title:

Probing Aircraft Flight Test Hazard Mitigation  
for the ACCESS Research Team

Page #:

90 of 118

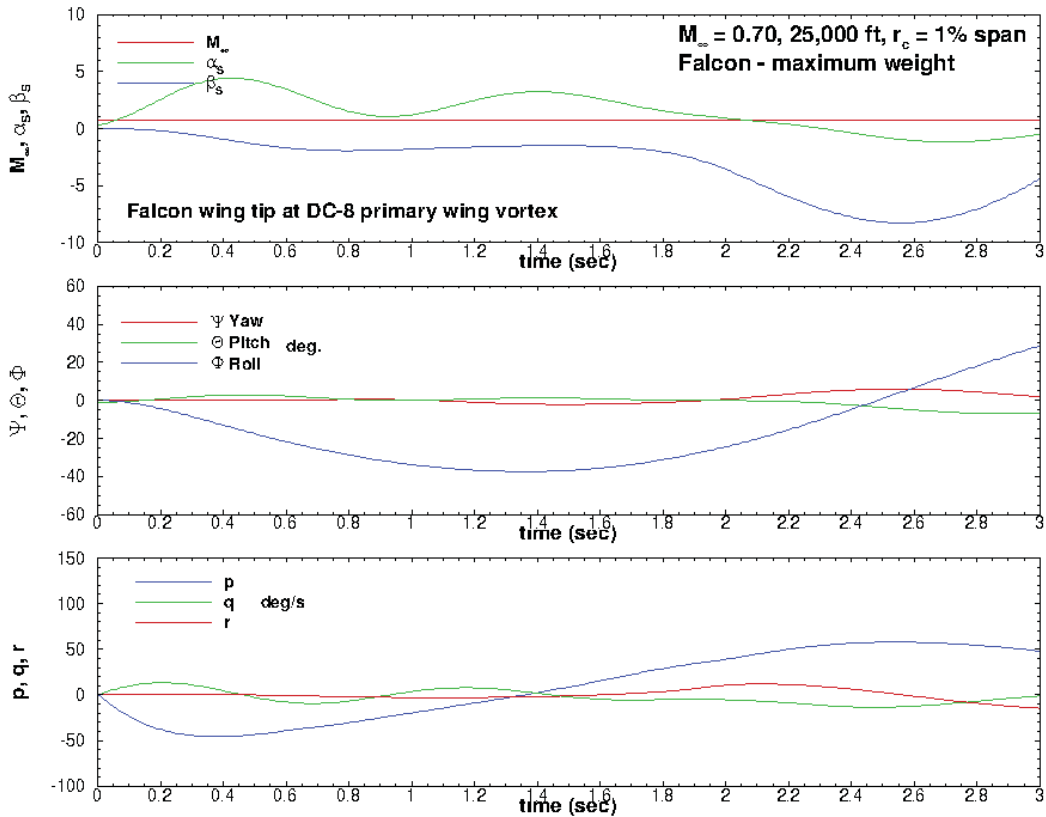


Figure 7.2-33. Response Data for Heavy Falcon Released with Wingtip in Vortex

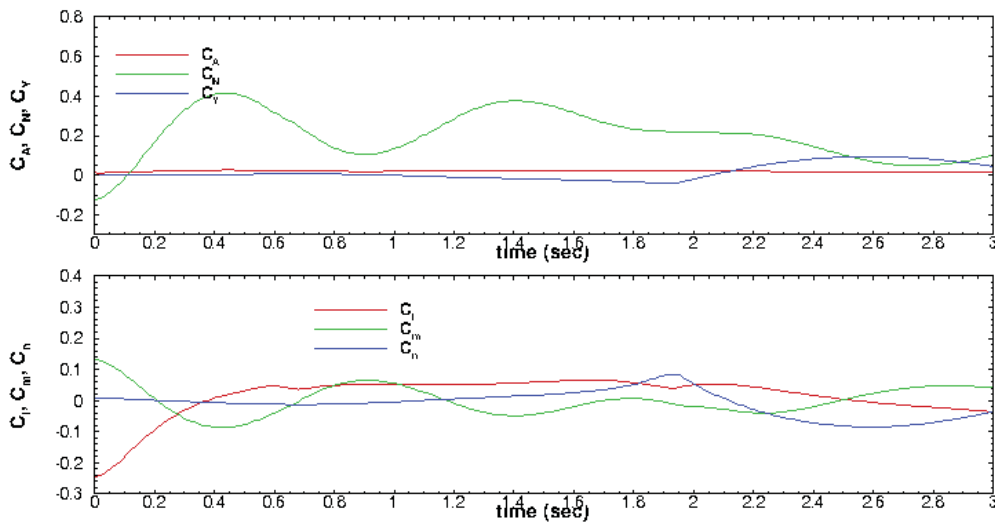



Figure 7.2-34. Force Data for Heavy Falcon Released with Wingtip in Vortex

|  |   |   |                        |
|--|---|---|------------------------|
|                 | <b>NASA Engineering and Safety Center<br/>Technical Assessment Report</b> | Document #:<br><b>NESC-RP-<br/>12-00822</b> | Version:<br><b>1.0</b> |
| Title:<br><b>Probing Aircraft Flight Test Hazard Mitigation<br/>for the ACCESS Research Team</b> |   | Page #:<br>91 of 118                        |                        |

### 7.3 Flight Test Hazards Mitigation

The NESC team discussed the structural failure, engine flameout, and loss of control hazards with a primary focus on the structural failure hazard. The NESC team developed findings, observations, and NESC recommendations to mitigate the hazards.

#### 7.3.1 Structural Failure Hazard

The NESC team considered information about the ACCESS flight test plans and the DC-8 and Falcon 20 aircraft (Section 6.1), lessons learned from similar previous flight tests (Section 6.2), physics of wake vortex behavior and evolution (Section 7.1), and results from its independent loads and simulations analyses (Section 7.2).

The team leveraged professional judgment based on engineering, flight testing, and aircraft operations experience, and developed five NESC recommendations for the ACCESS project team to mitigate structural failure hazards. The unifying theme of these five recommendations was to reduce the likelihood of inadvertent encounters with DC-8 wake vortices with the Falcon pilot practicing active avoidance. This would reduce the risks of loss of mission, damage to asset, loss of asset, and loss of personnel. The NESC team concluded that vortex avoidance must require vortex visibility and pilot practice; further, the project team could include instrumentation to enhance vortex visibility, vortex proximity awareness, and structural health; and the project team should review results from the independent loads and simulation analyses.


#### Vortex Detection

The NESC team discussed ways to detect vortex proximity:

1. Make vortex proximity visible to the Falcon pilot, via roll up with exhaust contrail or by generated smoke.
2. Make vortex proximity detectable to instrumentation (wingtip vanes, wingtip accelerometers) monitored in real time by personnel in radio contact with the pilot in command.
3. Make vortex proximity detectable to the pilot by training him to physically sense proximity (“seat of the pants”).

The NESC team concluded the optimal method to avoid inadvertent vortex encounter was for the vortices to be visible to the Falcon pilot in command. Instrumentation options were brainstormed, to be described later in this section. The third option was dismissed as a suboptimal primary means of detection but a satisfactory redundant means.



|  |   |   |                        |
|--|---|---|------------------------|
|                 | <b>NASA Engineering and Safety Center<br/>Technical Assessment Report</b> | Document #:<br><b>NESC-RP-<br/>12-00822</b> | Version:<br><b>1.0</b> |
| Title:<br><b>Probing Aircraft Flight Test Hazard Mitigation<br/>for the ACCESS Research Team</b> |   | Page #:<br>92 of 118                        |                        |

## Vortex Visibility

The NESC team found that DLR Falcon 20 pilots conducting similar experiments had adhered to a flight rule for approximately 20 years to only conduct flight tests when atmospheric conditions made leader aircraft engine exhaust plume contrails visible. The NESC team observed that visible contrails rolled up around wake vortices beyond about 1 wingspan aft of a leader aircraft, which made the primary wingtip vortices visible to the Falcon pilots. Vortices made visible in this way would provide unambiguous visual cues to permit ACCESS Falcon 20 pilots to avoid inadvertent encounters with a vortex while entering into, conducting sampling, or exiting from near- or far-field sampling areas. The NESC team noted that visible inboard engine exhaust plume contrails would also improve the ACCESS science mission success. The ACCESS project team acknowledged that such a flight rule would be best practice but discussed relaxing this requirement once vortex avoidance experience had been gained.

The NESC team's top recommendation was:

***R-1. Enforce as a mission rule that DC-8 wingtip vortices be made visible by rolled up exhaust contrail for all near- and far-field experiments.***

The NESC team considered the detailed sequential events that near- and far-field exhaust sampling operations might include, how these might relate to the near- and far-field geometry parameters the team developed (described in Sections 7.1.2 and 7.1.3), and implications for vortex avoidance.


## Near-Field Sampling Sequence

With the Falcon and the DC-8 flying at the altitude, speed, and direction desired for a sampling run, the Falcon pilot would ascertain from a position alongside the DC-8 near-field region that the DC-8 is producing engine exhaust contrails.

To enter into the near-field sample area, the NASA Falcon 20 pilot would likely climb from below and behind the DC-8 along its centerline, using military inflight refueling practices until in position between the DC-8's two inboard engine plumes. The pilot would target a zone *aft* of where the DC-8's outboard engine plumes appeared to have rolled up with the wingtip vortices but *forward* of where the inboard plumes appeared to roll up. During entry, the Falcon pilot would avoid lateral excursions.

To establish position to sample behind the DC-8's inboard engine plume, the Falcon pilot would slowly translate laterally from the extended DC-8 centerline into position behind an inboard engine. The pilot would use the contrail rolled up around the wake vortex as a visual cue to avoid overshooting the remaining lateral 4 ft (and unknown number of vertical ft) where the wingtip would encounter the vortex core.

The pilot would stabilize behind the inboard engine and hold position there for a period of seconds suitable to collect the research data. Roll and pitch inputs would be required to maintain position within the DC-8 wing downwash field. DLR pilots cautioned that they sometimes lost

|  |   |  |                        |
|--|---|--|------------------------|
|                 | <b>NASA Engineering and Safety Center<br/>Technical Assessment Report</b> | Document #:<br><b>NESC-RP-12-00822</b> | Version:<br><b>1.0</b> |
| Title:<br><b>Probing Aircraft Flight Test Hazard Mitigation<br/>for the ACCESS Research Team</b> |   | Page #:<br>93 of 118                   |                        |

outside visual references while flying inside the exhaust plume. They also noted that if the Falcon 20 wingtip approached the flow nearer the vortex, they “felt” the change.

To exit from the near-field sample area, the Falcon pilot would descend directly downward from the sampling location.

### **Near-Field Vortex Avoidance**

The NESC team concluded that near-field vortex avoidance was largely a geometry problem and that the specific roll-up behavior of engine exhaust plumes and vortices in the near field behind a four-engine heavy transport aircraft like a DC-8 in a clean wing configuration would be highly dependent on aircraft weight, geometry, altitude, and atmospheric conditions. Vortex behavior would be difficult to predict based on previous first-hand experience or the experience of others.


DLR Falcon 20 pilots recognized a near-field forward boundary of between 1 to 5 wingspans behind heavy four-engine transport aircraft, based on observations where clearly visible outboard engine plumes had been observed rolled up with wingtip vortices. The NESC team’s photometric analysis of 12 four-engine heavy transport aircraft contrail photographs revealed near-field roll-up distances consistent with the DLR observations. DLR pilots noted that their data were based on four four-engine aircraft types, including a DC-8, flying between 27,000 and 35,000 ft altitude at unspecified weights and in unspecified (but probably not turbulent per DLR practices) atmospheric conditions. The NESC team considered that this range must reflect the weight, geometry, and size differences between the four types, but in an unspecified manner, so that it was unclear where the DC-8 would fall in the range. The NESC team noted that the clearance between the Falcon 20 wingtip with the vortex when on station behind these various lead aircraft varied from essentially 0 to 32 ft. DLR Falcon 20 pilots reported they could “feel” when approaching wake vortices in the near field but were not specific as to which lead aircraft this subjective experience applied.

### **Far-Field Sampling Sequence**

With the Falcon and the DC-8 flying at the altitude, speed, and direction desired for a sampling run, the Falcon pilot would ascertain from a distance that the DC-8 is producing engine exhaust contrails visible in the far field and that the separation phenomenon is producing exhaust gases that ascend above the vortices at least 300 ft.

To enter into the far-field sample area, the NASA Falcon 20 pilot would descend from above and behind the target sample area (at least 300 ft above the vortices) into the visible, diffuse exhaust contrails. The pilot may lose clear visibility of the vortices during entry, hidden below the contrail. The vortices can be expected to behave chaotically depending on atmospheric conditions, the DC-8 weight, and the DC-8 engine thrust.

The Falcon pilot will level off and maintain position within the chaotic contrail for a period of seconds suitable to collect the research data. The pilot may lose outside visual references while flying inside the contrail. Once established in position to sample the contrail, the underside of

|  |   |  |                        |
|--|---|--|------------------------|
|                 | <b>NASA Engineering and Safety Center<br/>Technical Assessment Report</b> | Document #:<br><b>NESC-RP-12-00822</b> | Version:<br><b>1.0</b> |
| Title:<br><b>Probing Aircraft Flight Test Hazard Mitigation<br/>for the ACCESS Research Team</b> |   | Page #:<br>94 of 118                   |                        |

the Falcon might occasionally descend to less than 300 ft above the chaotically behaving vortices.

To exit from the far-field sample area, the Falcon 20 pilot will climb up from the sampling location and slide laterally upwind, as was the practice of the DLR Falcon pilots.

### **Far-Field Vortex Avoidance**

The team found that the far-field phenomenon described by the DLR pilots, where exhaust gases separate and rise above the vortices, was corroborated by other reports but was poorly characterized in technical literature. DLR Falcon 20 pilots recognized a far-field forward boundary of between 2 and 20 miles, based on observations where the separation phenomenon was clearly visible at these distances behind heavy transport aircraft flying at between 27,000 and 35,000 ft altitude at unspecified weights and in unspecified atmospheric conditions. The DLR pilots reported surveying the separated gases at distances greater than 300 ft above the vortices. They reported experiencing a partial to complete loss of visibility when immersed in the far-field separated exhaust contrail and feeling “washboard” buffeting.

### **Inadvertent Vortex Encounter**


The DLR Falcon 20 pilots reported an unspecified number of far-field vortex encounters in the 10- to 20-mile range that were all recovered with no apparent structural damage. Their reported excursions rates and extremes were consistent with the NESC team’s dynamic simulations. Their reports of the airplane’s response to the vortex encounter and its “natural” attitude recovery after the encounter were corroborated by other researched incidents and were consistent with the dynamic simulations.

If the Falcon should descend into a vortex at a shallow grazing angle (interpreted as less than 5 degrees), then the aircraft may deflect off the vortex. At such angles, it may be difficult or impossible to penetrate the core because the vortical flow forces overpower the airplane’s control authority [ref. 62]. This may be consistent with the DLR reports that on the occasions when pilots inadvertently encountered a vortex they experienced “graceful ejection.”

### **Pilot Proficiency Practice**

The NESC team observed that the NASA Falcon pilots’ experience in the NASA aircraft was limited to about 1 year, the time since the asset had been acquired by the Agency in November 2011. The team noted that through a period of 20 years, the DLR Falcon 20 pilots transferred “tribal knowledge” about wake vortex avoidance with each other verbally, without formal documentation. Finally, the team also considered that atmospheric conditions in the R-2508 airspace may yield results different than those reported by DLR pilots.

The NESC team concluded that the DLR Falcon 20 pilot experiences were applicable to the ACCESS experiment but carried limitations that necessitated the NASA Falcon 20 pilots to conduct their own dedicated training flights to gain experience in avoiding vortex encounters. Emulating the DLR Falcon 20 pilots’ near- and far-field wake vortex avoidance techniques,

|  |   |  |                        |
|--|---|--|------------------------|
|                 | <b>NASA Engineering and Safety Center<br/>Technical Assessment Report</b> | Document #:<br><b>NESC-RP-12-00822</b> | Version:<br><b>1.0</b> |
| Title:<br><b>Probing Aircraft Flight Test Hazard Mitigation<br/>for the ACCESS Research Team</b> |   | Page #:<br>95 of 118                   |                        |

practices, and procedures would not be equivalent to first-hand experience and alone would be insufficient to mitigate or reduce the risk of vortex encounter.


The NESC team concluded that the NASA pilots should conduct dedicated flight tests to develop pilot proficiency in avoiding vortex encounters. Based on the results and judgment, the NESC team brainstormed and developed the following candidate elements for these tests:

### Near-Field Practice Flight Tests

- Observe visible engine contrail (inboard) and visible wake vortex core (outboard) behavior from multiple angles before attempting entry.
- Turn autopilot and autothrottles OFF prior to initial entry.
- Do not use rudder pedal during approach or entry, while inside the near-field zone, or during nominal or unexpected exit from the near-field zone.
- Limit airspeed to at or below maneuvering speed ( $V_a$ ) to allow for full aileron deflection at all credible conditions that the aircraft could experience during flight; once experience is gained, consider increasing airspeed to be consistent with mission objectives.
- Observe the precautions as listed in Section 7.0 of the flight manual for entering severe turbulence/thunderstorm (except autopilot/autothrottle use); continue this practice unless it poses a greater hazard.
- Develop knock-it-off disengagement criteria based on crew observations (pilot judgment) and instrument indications.
- Develop knock-it-off disengagement criteria (red lines) for monitored wake vortex core proximity warning instrumentation (if any).

### Far-Field Practice Flight Tests

- Observe visible engine contrail (separated upper) and visible wake vortex core (separated lower) behavior from multiple angles before attempting entry.
- Turn autopilot and autothrottles OFF prior to entry; once established in position, evaluate use of autopilot in attitude hold, altitude hold, and turbulence settings to determine the optimal method of stabilization and sampling.
- Do not use rudder pedal during approach or entry, while inside the far-field zone, or during nominal or unexpected exit from the far-field zone.
- Limit velocity to at or below maneuvering speed to allow for full aileron deflection at all credible conditions that the aircraft could experience during flight; once experience is gained, consider increasing airspeed.

|  |   |  |                        |
|--|---|--|------------------------|
|                 | <b>NASA Engineering and Safety Center<br/>Technical Assessment Report</b> | Document #:<br><b>NESC-RP-12-00822</b> | Version:<br><b>1.0</b> |
| Title:<br><b>Probing Aircraft Flight Test Hazard Mitigation<br/>for the ACCESS Research Team</b> |   | Page #:<br>96 of 118                   |                        |

- Observe the precautions as listed in Section 7.0 of the flight manual for entering severe turbulence/thunderstorm; once experience is gained, enter using precautions as listed in Section 7.0 of the flight manual for entering moderate turbulence.
- Develop knock-it-off disengagement criteria based on crew observations (pilot judgment) and instrument indications.
- Develop knock-it-off disengagement criteria (red lines) for monitored wake vortex core proximity warning instrumentation (if any).
- Consider descending into the better visibility region just beneath the separated exhaust contrail and above the wake vortex; deliberately assume this risk posture to gain experience and feel for the aircraft response when approaching the wake vortex from above.

#### **Pre-Experiment Data Analysis**

- Develop overhead and rear-view maps of the near- and far-field zones with identified wake vortex core and engine plume zones, based on pilot experiences and on collected data (if any) to facilitate crew briefing, crew cross training, in-flight marking of discovered conditions, and mission debriefing and to improve crew situational awareness of DC-8 wake vortex core and engine exhaust behavior and Falcon wake vortex core encounters, as these will vary with density altitude and moisture content.

The second NESC recommendation was:


***R-2. Conduct pre-experiment flight tests in near- and far-field zones, dedicated to developing pilot proficiency in avoiding wake vortices. Consider the candidate methods, procedures, and activities above.***

#### **Structural Health Monitoring Instrumentation**

DLR did not have special systems or instrumentation on their Falcon 20 for go/no-go determination or for safety-of-flight assurance. The NESC team discussed candidate instrumentation strategies for vortex avoidance and for Falcon structural health monitoring. Some of the strategies required real-time data monitoring; others involved post-flight analysis or inspection. The list of strategies considered by the team included:

1. In-flight monitoring of the aircraft state (INS/GPS instrument used primarily for post-flight trajectory reconstruction of wake vortex encounters).
2. In-situ monitoring of the flow field around the aircraft to predict the Falcon 20's proximity to the wake vortex core (LIDAR, wingtip pressure measurements, or angle of attack and sideslip vanes).
3. Strain gages installed on critical aircraft structure (to allow either real-time or post-flight analysis of localized stress/strain and avoid or detect limit load exceedance).



|  |   |  |                        |
|--|---|--|------------------------|
|                 | <b>NASA Engineering and Safety Center<br/>Technical Assessment Report</b> | Document #:<br><b>NESC-RP-12-00822</b> | Version:<br><b>1.0</b> |
| Title:<br><b>Probing Aircraft Flight Test Hazard Mitigation<br/>for the ACCESS Research Team</b> |   | Page #:<br>97 of 118                   |                        |

4. Accelerometers mounted on wing, vertical tail, and/or horizontal tail (to monitor in-flight vibration of these structural elements).
5. Post-flight visual inspection of aircraft structure looking for indications of local yielding (e.g., popped rivets, skin wrinkles, bent structure) and excessive free play in the rudder control surface.

### **INU/GPS**

The first concept considered was adding an inertial navigation unit (INU) and GPS onto the Falcon, with a data acquisition system and an on-board recorder. This system could record Falcon inertial states (e.g., Euler angles or quaternions, angular rates, vehicle positions, linear velocities, accelerations) to facilitate post-flight state reconstruction in the event of an inadvertent vortex encounter. This concept could be used as a post-flight mitigation as part of a tool set that could later be used to predict Falcon aerodynamic and inertial loads. These anchored predictions could be compared with aircraft design limit loads to help develop or modify Falcon flight safety restrictions.

### **Flow-Field Measurement**

The team discussed instrumentation concepts that could characterize the flow-field experienced by the Falcon. The team observed that adding a LIDAR instrument to the Falcon, such as was used in the NASA Airborne Coherent LIDAR for Advanced In-Flight Measurements (ACLAIM) project [ref. 63], would be expensive and would require real-time monitoring to understand the aircraft's proximity to the wake vortex core. The team also considered the merits of adding one or more pressure transducers or angle of attack and sideslip vanes onto one Falcon wingtip, with a data acquisition system and an on-board recorder. Data from such a system could be monitored during pre-experiment flight tests to identify whether they could be used to identify vortex-proximity knock-it-off criteria. Once knock-it-off criteria were developed and calibrated, an automated warning system such as a cockpit indicator light could be added to alert the pilot of vortex proximity. The team recognized that a system of wingtip pressure sensors intended to measure flow-field changes would require the Falcon to have closer proximity to a wake vortex than would a LIDAR system. Figure 7.3-1 shows a representation of flow field vectors from a vortex on a wing tip.

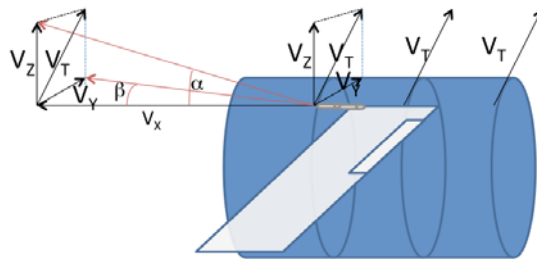


Title:

Probing Aircraft Flight Test Hazard Mitigation  
for the ACCESS Research Team

Page #:

98 of 118



$$\alpha = V_y / V_x \quad \& \quad \beta = V_z / V_x$$

$V_T$  = Tangential Flow Velocity of Vortex

$V_x$  = Forward Vehicle Velocity

$V_y, V_z$  = Lateral, Vertical Flow Velocities

Figure 7.3-1. Vane Directions and Velocity Vectors

### Strain Gages


The team also considered installing uncalibrated strain gages at strain sensitive locations on or near the Falcon's vertical tail root attachment that would be judged by project engineers (if not identified by the aircraft manufacturer) to be in the tail's primary load path. Unloaded strain ambient readings would be recorded on the ground between flights. If ambient strain shifts were observed, these could be considered a potential indication of yielded structure. A lack of strain shift would not conclusively mean no yield had occurred, but a strain shift would trigger more detailed visual structural inspections. This type of instrumentation would only support post-flight mitigation of structural failure.

### Accelerometers

The NESC team considered installing accelerometers on the Falcon wingtips, vertical tail tip, and horizontal tail tips, oriented normal to each surface, with a data acquisition system and an on-board recorder. These instruments could be monitored during pre-experiment flight tests to identify and, if possible, develop knock-it-off criteria for wake vortex core proximity. The team observed that such accelerometers could observe large response at dominant frequencies if the aerodynamic surface was in close proximity to a wake vortex core. The NESC team would need to perform a pre-flight impulse (hammer) response test to identify the first few wing and tail modes and their natural frequencies if this information was not available from the manufacturer. Post-flight analysis would be needed to develop in-flight knock-it-off criteria. Once knock-it-off criteria were developed and calibrated, an automated warning system such as a cockpit indicator light could be added to alert the pilot of vortex proximity.

### Post-Flight Visual Inspections

The easiest risk mitigation discussed by the NESC team was to perform inspections between flights to look for signs of aircraft structure localized yielding or other signs of structural failure

|   |   |  |                        |
|---|---|--|------------------------|
|  | <b>NASA Engineering and Safety Center<br/>Technical Assessment Report</b> | Document #:<br><b>NESC-RP-12-00822</b>   | Version:<br><b>1.0</b> |
|   |   | <b>Probing Aircraft Flight Test Hazard Mitigation<br/>for the ACCESS Research Team</b> |                        |


including popped rivets, skin wrinkles, etc. More extensive and time-consuming inspections of internal components with panels and covers removed could also be conducted between flights.

### Prioritized Instrumentation List

The NESC team observed that the ACCESS project’s schedule and budget may not allow for installation of unplanned additional instrumentation on either aircraft before the planned February 2103 tests. Likewise, the expected pace of the tests may not allow the addition of time-consuming inspections or data reduction activities. As options for project team consideration, the assessment team developed a prioritized list of seven candidate instrumentation items that could improve vortex avoidance or allow structural health monitoring. Table 7.3-1 shows these candidate instrumentation items. An eighth candidate instrumentation item is included on this list to improve engine flameout avoidance; see Section 7.3.2 for the narrative background for this hazard. If not adopted during the 2013 flight test campaign, these items could be considered for an anticipated 2014 ACCESS flight test campaign.

**Table 7.3-1. Candidate Instrumentation Items for Vortex Avoidance, Structural Health Monitoring, or Engine Flameout**

| Reason for Instrumentation   | ITEM     | Candidate Instrumentation  |
|------------------------------|----------|--|
| Vortex Avoidance             | <b>1</b> | Smoke generators weighing less than 100 lb on the DC-8 outboard wing pylons, or oil injection system behind both outboard DC-8 engines. Real-time mitigation.  |
| Vortex Avoidance             | <b>2</b> | An alpha and a beta vane on the Falcon 20 left wingtip, and a data acquisition system and recorder, monitored during pre-experiment flight tests to identify if useful as a wake vortex proximity knock-it-off disengagement parameter. Post-flight analysis would be needed to develop in-flight knock-it-off criteria.   |
| Vortex Avoidance             | <b>3</b> | Accelerometers on the Falcon 20 left wingtip, vertical tail tip, and horizontal tail tip, oriented normal to each surface, and a data acquisition system and recorder, monitored during pre-experiment flight tests to identify if useful as a wake vortex proximity knock-it-off disengagement parameter; if large response at dominant frequencies is observed, could be deductively associated with the first few modes of vibration and may require follow-up conversations with the aircraft manufacturer; conduct a pre-flight impulse (hammer) response test to identify simple modes and their natural frequencies. Post-flight analysis would be needed to develop in-flight knock-it-off criteria. |
| Structural Health Monitoring | <b>4</b> | Uncalibrated strain gages at locations near the root attachment of the vertical tail judged by project engineers (if not identified by the aircraft manufacturer) to be in primary load path and to have potential for high strain; to be interrogated between flights in an unloaded condition and assessed for strain shifts that might be indicative of yielded structure. Lack of strain shift would not conclusively mean no yield has occurred, but a strain shift would compel structural inspections. Post-flight mitigation.  |

|  |   |                         |            |
|--|---|-------------------------|------------|
|       | <b>NASA Engineering and Safety Center<br/>Technical Assessment Report</b> | Document #:             | Version:   |
|  |   | <b>NESC-RP-12-00822</b> | <b>1.0</b> |
| Title:   |   | Page #:                 |            |
| <b>Probing Aircraft Flight Test Hazard Mitigation<br/>for the ACCESS Research Team</b> |   | 100 of 118              |            |

| Reason for Instrumentation   | ITEM     | Candidate Instrumentation  |
|------------------------------|----------|--|
| Vortex Avoidance             | <b>5</b> | Strain gages at locations near the root attachment of the vertical tail judged by project engineers (if not identified by the aircraft manufacturer) to be in primary load path, and install a data acquisition system and recorder, monitored during pre-experiment flight tests to identify if useful as a wake vortex proximity knock-it-off disengagement parameter; recorded for post flight analysis; conduct a pre-flight calibration exercise that applies a known load to the vertical tail (need not be elaborate). Post-flight analysis would be needed to develop in-flight knock-it-off criteria. |
| Structural Health Monitoring | <b>6</b> | An INU/GPS and a data acquisition system and recorder to allow recording of Falcon 20 Euler angles, angular rates, positions, linear velocities, and accelerations to facilitate post-flight reconstructions and loads computations in the event of inadvertent wake vortex encounter. Post-flight mitigation.   |
| Vortex Avoidance             | <b>7</b> | Pressure transducer on the Falcon 20 left wingtip, and a data acquisition system and recorder, monitored during pre-experiment flight tests to identify if useful as a wake vortex proximity knock-it-off disengagement parameter; recorded for post flight analysis. Post-flight analysis would be needed to develop in-flight knock-it-off criteria.   |
| Engine Flameout Avoidance    | <b>8</b> | An alpha and a beta vane on the Falcon 20 fuselage, and a data acquisition system and recorder, monitored during pre-experiment flight tests to identify if useful as a “distorted flow in engine” knock-it-off disengagement parameter. Post-flight analysis would be needed to develop in-flight knock-it-off criteria.  |

The third NESC recommendation was:


**R-3.** *Consider adding instrumentation to the Falcon 20 or the DC-8 to improve vortex detection and avoidance or to monitor structural health. Consider the candidate items listed in Table 7.3-1.*

### Falcon Static Loads

The NESC team found that Falcon 20 empennage strength margins could not be firmly determined because aircraft design envelope condition data were not available from the manufacturer. The team compared computed vortex-encounter loads with maximum loads condition data found documented in a manufacturer report that had apparently inadvertently become public. The NESC team conservatively assumed these conditions represented limit conditions.

The NESC team computed static induced load coefficients and peak loads using a conservative vortex strength with a tool of higher fidelity than that used by the project team (Tables 7.2-4 and 7.2-5). Summary findings included:

- Maximum wing and vertical tail shear and root bending moments remained below 100-percent design limit load (79.6 and 92.7 percent, respectively).

|  |   |  |                        |
|--|---|--|------------------------|
|                 | <b>NASA Engineering and Safety Center<br/>Technical Assessment Report</b> | Document #:<br><b>NESC-RP-12-00822</b> | Version:<br><b>1.0</b> |
| Title:<br><b>Probing Aircraft Flight Test Hazard Mitigation<br/>for the ACCESS Research Team</b> |   | Page #:<br>101 of 118                  |                        |

- Maximum horizontal tail differential shear and differential bending moment exceeded 100-percent DLL (144 and 109 percent, respectively).

These static results contained no inertial relief. The NESC team planned but did not enact a contingency to pay the Falcon manufacturer to assess computed loads data against proprietary design envelopes and provide a “pass or fail” disposition.

The team conducted a sensitivity study, computing results in the same manner for 2.0- and 3.5-percent vortex core sizes. No loads exceeded 100-percent limit load. The resulting data were a data deliverable that will allow the project team to assess structural risk using their own vortex decay model assumptions.


**R-4. Consider the provided independent static loads results and maps calculated for 1-, 2-, and 3.5-percent core sizes. (Tables 7.2-4 and 7.2-5)**

### Falcon Simulations

The NESC team conducted 6-DOF independent simulations of the Falcon 20 dynamic response beginning at various locations in the flow field behind the DC-8.

- The stick-fixed dynamic simulation of an EOW Falcon beginning at the location of maximum rolling moment exhibited a maximum rate of 170 deg/sec, reaching a roll attitude of 190 degrees.
- The stick-fixed dynamic simulation of an MTOW Falcon beginning at the location of maximum rolling moment exhibited a maximum rate of 140 deg/sec, reaching a roll attitude of 140 degrees. *This response mimicked reports from DLR Falcon pilots who had inadvertently descended into vortices in the far field.*
- The stick-fixed dynamic simulation of an EOW Falcon beginning at the inboard engine sampling location shows the Falcon aircraft rolling toward the vortex and then reversing the roll from 40 degrees one wing down to 40 degrees the other wing down in about 1 second as it traversed just above the vortex core.
- The stick-fixed dynamic simulation of an MTOW Falcon beginning at the inboard engine sampling location shows the Falcon aircraft rolling toward the vortex, descending, and then passing benignly beneath the vortex.
- The stick-fixed dynamic simulation of an EOW Falcon beginning with its wingtip inside the vortex core shows the Falcon aircraft rolling toward the vortex and then reversing roll from 35 degrees one wing down to 45 degrees the other wing down in 1.5 seconds as the aircraft traverses just above the vortex core. The NESC team examined the predicted tail loads from this simulation as the Falcon traversed a vortex and found that adverse phasing of flight rates could cause inertial effects to increase loads rather than just decrease them as had been presumed.



|  |   |  |                        |
|--|---|--|------------------------|
|                 | <b>NASA Engineering and Safety Center<br/>Technical Assessment Report</b> | Document #:<br><b>NESC-RP-12-00822</b> | Version:<br><b>1.0</b> |
| Title:<br><b>Probing Aircraft Flight Test Hazard Mitigation<br/>for the ACCESS Research Team</b> |   | Page #:<br>102 of 118                  |                        |

- The stick-fixed dynamic simulation of an MTOW Falcon beginning with its wingtip inside the vortex core shows the Falcon aircraft rolling toward the vortex, descending, and passing benignly beneath the vortex.

**R-5.** *Consider the independent dynamic simulation results of the Falcon 20 response to a wake vortex encounter when assessing the Falcon 20 near- and far-field structural risks from an inadvertent wake vortex encounter. Make note of the assumptions and limitations of the provided results.*

### 7.3.2 Engine Flameout Hazard

Incidentally during the course of this assessment, the NESC team discussed the risks of engine compressor stall or over-temperature due to distorted engine inlet flow. This hazard was identified in slide 11 of the ACCESS SRR briefing. (Appendix B).

The NESC team considered information about the DC-8 and Falcon 20 aircraft (Section 6.1) and other information and leveraged professional judgment based on engineering, flight testing, and aircraft operations experience to develop one NESC recommendation to the ACCESS project team to mitigate engine flameout hazards.

The NESC team considered reports from DLR pilots that during the course of their exhaust-sampling experiments they experienced one single-engine flameout, caused by wake vortex ingestion into an engine (unspecified if near or far field). The engine was restarted in flight, the aircraft landed without incident, and post-flight inspection revealed no engine damage.

To mitigate the risk of engine flameout, DLR observed a rule that a suitable runway must be within gliding distance of the Falcon aircraft. To begin testing, they also required all installed Falcon aircraft systems to be operable, a minimum of 10,000-ft visual meteorological conditions, and a visible horizon below the mission altitude.

The NESC team also discussed the possibility that aircraft with aft-mounted, over-wing engine configurations may be susceptible to engine compressor stalls or engine over-temperatures at high angles of attack or high sideslip angles, because flow separation on the inboard wing section at high angles of attack and flow separation from the fuselage at high sideslip angles can partially blank the engine fan face.

The NESC team considered a USAF research program [ref. 64] involving a Fairchild Republic A-10 Thunderbolt close air support military aircraft.

The research showed adverse engine inlet flow distortion could occur with flight conditions that included a combination of high angle of attack and high sideslip angle. The A-10 had twin engines mounted on its aft fuselage, positioned over its wing trailing edge in a configuration similar to that of the Falcon 20.

The team noted that the Falcon 20's engines were mounted at the 3- and 9-o'clock positions on its fuselage, as compared with the 2- and 10-o'clock positions for the A-10, as can be seen in


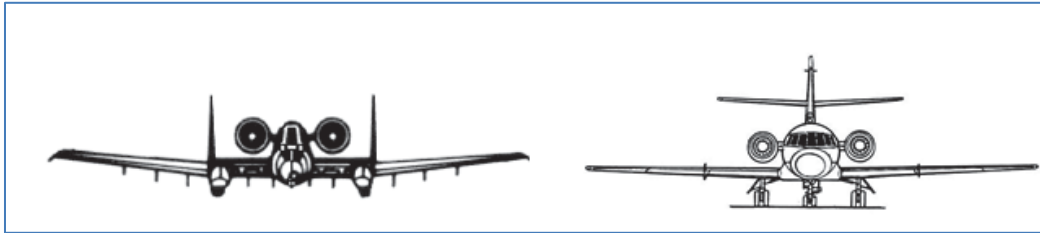
|  |   |                         |            |
|--|---|-------------------------|------------|
|       | <b>NASA Engineering and Safety Center<br/>Technical Assessment Report</b> | Document #:             | Version:   |
|  |   | <b>NESC-RP-12-00822</b> | <b>1.0</b> |
| Title:   |   | Page #:                 |            |
| <b>Probing Aircraft Flight Test Hazard Mitigation<br/>for the ACCESS Research Team</b> |   | 103 of 118              |            |

Figure 7.3-2. This geometric factor was thought to potentially make the Falcon 20 more prone to flow distortion due to sideslip than the Thunderbolt. The NESC team concluded that an engine flameout risk could arise not just from wake vortex flow ingestion but also from adverse flow patterns around the Falcon 20 in the DC-8 wake.



*Figure 7.3-2. Approximately Scaled Comparison of A-10 and Falcon 20 showing Engine Layout*

The NESC team recognized that relevant data were not available from the engine or aircraft manufacturers and that analytical characterization of flow tolerance was impracticable.


For this reason, the NESC team included angle of attack and sideslip instrumentation in a compiled list of hazard mitigation instrumentation recommendations (See item 8 in Table 7.3-1), with the intent that these be monitored real-time during pre-experiment flight tests.

The NESC team considered too that a build-up technique for near-field operations could include gradually reducing the distance aft from the DC-8 and vertical distance of separation from the wake vortex while monitoring angle of attack and sideslip excursions. In this manner, as angle of attack and sideslip limits were approached, limitations on aft separation and vertical distance could be established. If adverse engine events were experienced during this build up, angle of attack and sideslip limitations could be established based on these events.

The NESC team discussed project plans to conduct, on an opportunity basis prior to beginning experimental flight tests, far-field exhaust data collection en route from Hampton, VA, to Edwards Air Force Base, CA. Although not directly in scope, the NESC team concluded that such enroute sampling trials should not be conducted because they were planned to occur prior to completion of the recommended pre-experiment flight tests intended to develop pilot proficiency in avoiding wake vortices.

The NESC team assessed the principal unaddressed risk that, even at FAA-approved far-field distances beyond 5 miles, the Falcon's engines could flameout while enroute cross country over a region lacking a suitable reachable airfield; the DLR experience shows Falcon 20 flameout risk from wake vortex ingestion is "not zero."

***R-6. Do not conduct far-field sampling behind "target of opportunity" commercial transport aircraft in controlled airspace prior to conduct of pre-experiment flight tests due to uncharacterized risk of inadvertent wake vortex encounter.***

|  |   |  |                        |
|--|---|--|------------------------|
|                 | <b>NASA Engineering and Safety Center<br/>Technical Assessment Report</b> | Document #:<br><b>NESC-RP-12-00822</b> | Version:<br><b>1.0</b> |
| Title:<br><b>Probing Aircraft Flight Test Hazard Mitigation<br/>for the ACCESS Research Team</b> |   | Page #:<br>104 of 118                  |                        |

### 7.3.3 Loss of Control Hazard

The NESC team considered Falcon 20 inadvertent vortex encounter resulting in inadvertent loss of control, because a recovery maneuver from an upset could become a cause of subsequent structural failure. The NESC team researched information and leveraged professional judgment based on engineering, flight testing, and aircraft operations experience to develop recommendations and provide them the ACCESS project team to mitigate loss of control hazards.

The NESC team examined the Falcon 20 Flight Manual [ref. 3], and discussed airspeed limitations and aircraft flight control system configuration mitigation ideas. The NESC team also discussed anecdotal data from other wake vortex encounter programs and data from flight programs involving the Falcon 20 aircraft, including:

- DLR measurements of DC-8 emissions
- DLR\_CONCERT Project--acp-10-9039-2010
- DLR\_FAA\_near\_field\_encounter\_assessment\_v11
- HU-25A\_AIREYE\_HandlingQualities
- HU-25A\_AIREYE\_Loads\_Flutter


The NESC team also examined videos:

- NASA SUCCESS Field Mission using T-39 (1996)
- B-737 Wake Encounter Flight Test (date unknown)
- DLR Contrails Behind A-380 (2008)

The NESC team discussed aircraft roll and yaw responses during inadvertent vortex encounters. The team's Falcon 20 simulations indicated that some stick-free upsets were self-limited and recovered automatically.

The NESC team discussed the potential for large sideslip (beta) buildup following a near-field upset. The NESC team reviewed a National Transportation Safety Board conclusion that an operational cause of a 2001 Airbus-300 aircraft crash [ref. 65] in New York City was overuse of the rudder mechanism. This aircraft's first officer made a rudder pedal input in response to a far-field wake vortex encounter and then made a series of alternating full rudder inputs that led to increasingly higher sideslip angles and increasingly higher aerodynamic loads, until the aircraft's vertical tail separated from the aircraft resulting in loss of control. From this review, the NESC team observed that rudder reversals can result in vertical tail loads in excess of design capability, applicable to near-field and far-field vortex encounters.

The NESC team also discussed but could not establish conclusively whether the Falcon 20 roll-axis artificial feel unit (with its Arthur Q variable-length bell crank) would prevent wing

|  |   |  |                        |
|--|---|--|------------------------|
|                 | <b>NASA Engineering and Safety Center<br/>Technical Assessment Report</b> | Document #:<br><b>NESC-RP-12-00822</b> | Version:<br><b>1.0</b> |
| Title:<br><b>Probing Aircraft Flight Test Hazard Mitigation<br/>for the ACCESS Research Team</b> |   | Page #:<br>105 of 118                  |                        |

overload if a pilot were to conduct a robust roll input during an inadvertent vortex entry. The team observed that DLR required all aircraft systems to be operable to begin an exhaust sampling mission, so any indication of an Arthur Q unit or artificial feel unit failure for them would have been an abort criterion.


***R-7. Enforce as a mission rule, Falcon 20 pilots to minimize control inputs if an inadvertent wake vortex encounter appears imminent or is indicated to be imminent by instrumentation (if any); allow the vortex wake to move the Falcon naturally out of the vortex flow and then stabilize the aircraft.***

The team’s review of a U.S. Air Force Flight Test Center (AFFTC) test report [ref. 66] revealed a description of a 1983 Falcon 20 (HU-25A) upset and recovery. Within 10 seconds of an inadvertent upset, the aircraft rolled to one direction through inverted flight and continued for approximately one and one-half full rolls with several intermediate roll rate reversals. The aircraft was rolled about 100 degrees when control was regained. The report cited similarities of this rolling departure with those experienced by some fighter aircraft and noted that past experiences indicated that the best recovery technique was a rapid and positive centering of the flight controls. This was said to help minimize excursions in sideslip and angle of attack and to reduce the likelihood of the aircraft transitioning into a spin through inertial coupling. This action would allow the aircraft to recover itself “or transition to a recognizable out of control mode, at which time the appropriate recovery controls could be applied.”

***R-8. ACCESS Falcon 20 pilots, after an inadvertent wake vortex encounter, once clear of the vortex perform a rapid and positive centering of the flight controls to minimize excursions in sideslip and angle of attack and to reduce the likelihood of spin entry through inertial coupling.***

The NESC team discussed submitting loads to the Falcon manufacturer for evaluation against DLL and pass/fail disposition. The NESC assessment lead and MTSO Project Analyst explored an option to leverage an existing contract between the U.S. Coast Guard and the manufacturer on behalf of the project team but never enacted the plan. The NESC team’s analyses results were sufficient to develop hazard-mitigating recommendations for the 2013 flight test campaign. The NESC team concluded that the project team should pursue this lead prior to an expected 2014 test campaign.

***R-9. Pursue the request for quote from the Falcon 20 manufacturer to assess project and NESC loads analyses results against aircraft design load limits prior to an expected 2014 test campaign.***


|  |   |  |                        |
|--|---|--|------------------------|
|                 | <b>NASA Engineering and Safety Center<br/>Technical Assessment Report</b> | Document #:<br><b>NESC-RP-12-00822</b> | Version:<br><b>1.0</b> |
| Title:<br><b>Probing Aircraft Flight Test Hazard Mitigation<br/>for the ACCESS Research Team</b> |   | Page #:<br>106 of 118                  |                        |

## 8.0 Findings, Observations, and NESC Recommendations


### 8.1 Findings

- F-1.** DLR Falcon pilots, conducting near- and far-field flight tests behind leader aircraft similar to the planned ACCESS tests, adhered for 20 years to an informal flight rule requiring visible engine exhaust contrails because visible contrails provide unambiguous vortex proximity and sampling area geometry cues.
- F-2.** During flight-test planning discussions, the ACCESS project team considered beginning testing requiring visible engine exhaust contrails but relaxing the requirement after vortex avoidance experience was gained.
- F-3.** Data were insufficient to determine a *near-field* structural safe operating envelope, but a near-field target zone 750 ft aft of the DC-8 was identified where it would be likely that the Falcon pilot would be able to see and avoid DC-8 wingtip vortices.
- F-4.** The near-field wake vortex and exhaust roll-up behavior behind the DC-8 is poorly understood, and the near-field zone is dependent on aircraft weight, altitude, geometry, and atmospheric conditions, making the vortex location position difficult to predict.
- F-5.** Data were insufficient to determine a *far-field* structural safe operating envelope, but DLR pilot observations that far-field exhaust gases can rise to a vertical separation distance of about 300 ft at 2 miles aft of a leader aircraft was corroborated by an independent means.
- F-6.** The far-field contrail/core separation phenomenon described by DLR Falcon 20 pilots is poorly characterized.
- F-7.** Instrumentation was identified that may improve pilot ability to avoid wake vortex encounters or provide structural health data.
- F-8.** Falcon empennage margins of safety could not be determined because strength capability information was not available from the manufacturer at a cost or on a schedule that was practicable for the project or with NESC assistance.
- F-9.** Falcon 20 vertical-tail normal force and root bending moment from a wake vortex encounter with no inertial relief was computed by independent analysis to remain below 100-percent DLL (79.6 and 92.7 percent, respectively).
- F-10.** Falcon 20 horizontal-tail differential load from a wake vortex encounter with no inertial relief was computed by independent analysis to exceed 100-percent DLL (144 and 109 percent, respectively).
- F-11.** Falcon 20 wing loads from a wake vortex encounter with no inertial relief were computed by independent analysis to be less than 100-percent DLL; asymmetric effects from jet efflux were not assessed.



|  |   |  |                        |
|--|---|--|------------------------|
|                 | <b>NASA Engineering and Safety Center<br/>Technical Assessment Report</b> | Document #:<br><b>NESC-RP-12-00822</b> | Version:<br><b>1.0</b> |
| Title:<br><b>Probing Aircraft Flight Test Hazard Mitigation<br/>for the ACCESS Research Team</b> |   | Page #:<br>107 of 118                  |                        |


- F-12.** Computed results from a parametric study of loads versus core size using an independent analysis tool can be applied with project assumptions regarding decay models to assess structural risk.
- F-13.** The empirically validated NEAR DC-8 wake flow-field model produced results sufficient enough that a contingency plan to collect new DC-8 wake data using a DFRC fighter aircraft asset was not necessary.
- F-14.** The stick-fixed dynamic simulation of an EOW Falcon beginning at the location of maximum rolling moment exhibited a maximum rate of 170 deg/sec, reaching a roll attitude of 190 degrees.
- F-15.** The stick-fixed dynamic simulation of an MTOW Falcon beginning at the location of maximum rolling moment exhibited a maximum rate of 140 deg/sec, reaching a roll attitude of 140 degrees.
- F-16.** The stick-fixed dynamic simulation of an EOW Falcon beginning at the inboard engine sampling location showed the Falcon aircraft rolling toward the vortex, then reversing roll from 40 degrees one wing down to 40 degrees the other wing down in about 1 second as it traversed just above the vortex core.
- F-17.** The stick-fixed dynamic simulation of an MTOW Falcon beginning at the inboard engine sampling location showed the Falcon aircraft rolling toward the vortex, descending, and passing benignly beneath the vortex.
- F-18.** The stick-fixed dynamic simulation of an EOW Falcon beginning with its wingtip inside the vortex core showed the Falcon aircraft rolling toward the vortex and then reversing roll from 35 degrees one wing down to 45 degrees the other wing down in about 1.5 seconds as it traversed just above the vortex core.
- F-19.** The stick-fixed dynamic simulation of an MTOW Falcon beginning with its wingtip inside the vortex core showed the Falcon aircraft rolling toward the vortex, descending, and passing benignly beneath the vortex.
- F-20.** Simulation results suggest that adverse phasing of flight rates while traversing a vortex could cause inertial effects to increase rather than decrease loads when compared with static computed loads.
- F-21.** NASA Falcon 20 pilots will gain knowledge by practicing avoiding wake vortex encounters that is not possible to obtain by listening to DLR Falcon 20 pilot reports from similar flight tests.
- F-22.** Pre-experiment *near-field* flight test elements or activities detailed in this report could reduce the risk of inadvertent wake vortex encounter.
- F-23.** Pre-experiment *far-field* flight test elements or activities detailed in this report could reduce the risk of inadvertent wake vortex encounter.

|  |   |   |                        |
|--|---|---|------------------------|
|                 | <b>NASA Engineering and Safety Center<br/>Technical Assessment Report</b> | Document #:<br><b>NESC-RP-<br/>12-00822</b> | Version:<br><b>1.0</b> |
| Title:<br><b>Probing Aircraft Flight Test Hazard Mitigation<br/>for the ACCESS Research Team</b> |   | Page #:<br>108 of 118                       |                        |

- F-24.** Developing overhead view and rear-view maps of the near-field and far-field zones with identified wake vortex core and engine plume zones based on pre-experiment activity could improve crew situational awareness of DC-8 wake vortex core and engine exhaust behavior.
- F-25.** A Falcon 20 single-engine flameout caused by wake vortex ingestion into an engine is possible based on an event reported by the DLR Falcon 20 pilots (unspecified whether near field or far field).
- F-26.** NASA numerical simulations consistent with DLR pilot reports indicate that upsets are self-limited and self-recovery is likely.
- F-27.** An AFFTC investigation of the safe recovery of a Falcon 20 from a 1983 rolling upset concluded that a rapid and positive centering of the flight controls to minimize excursions in sideslip and angle of attack was an effective recovery technique because it decreases the aircraft's likelihood to transition to a spin through inertial coupling.
- F-28.** The Falcon structural risk cannot be quantified without knowledge of aircraft limit load capability. Other objective evidence suggests the risk of Falcon 20 structural overload and failure is acceptable.

## **8.2 Observations**

- O-1.** Pilots gain hazard avoidance skills through personal practice that are superior to those learned by listening to lessons learned by other pilots.
- O-2.** A mission rule that requires far-field contrail visibility would provide for science mission success.
- O-3.** The short scheduled time between instrumentation installation, which began in November 2012, and the beginning of experimental flight tests in February 2013 may impact programmatic risk assessment decisions involving adding safety-of-flight instrumentation for the 2013 test campaign.
- O-4.** Following an aircraft upset, rudder reversals can result in large beta buildup and vertical tail loads in excess of design capability, which caused the 2001 American Airlines Flight 587 aircraft accident.
- O-5.** It was not clear whether Falcon 20 (HU-25) artificial feel units in combination with variable-length bell cranks (Arthur Q units) were adequate to prevent wing structure overload from pilot control inputs countering a wake vortex entry.
- O-6.** Arthur-Q and artificial feel units were likely required for all DLR Falcon 20 tests because DLR observed a flight rule that all systems must be operable for missions.
- O-7.** Load conditions can be submitted to the manufacturer for assessment against design envelopes in the near field prior to an expected 2014 test campaign.


|  |   |  |                        |
|--|---|--|------------------------|
|                 | <b>NASA Engineering and Safety Center<br/>Technical Assessment Report</b> | Document #:<br><b>NESC-RP-12-00822</b> | Version:<br><b>1.0</b> |
| Title:<br><b>Probing Aircraft Flight Test Hazard Mitigation<br/>for the ACCESS Research Team</b> |   | Page #:<br>109 of 118                  |                        |

**O-8.** Project team cooperation with the NESC team was professional and respectful, and requests for information were acted upon fully and timely.

### **8.3 NESC Recommendations**

The following NESC recommendations to mitigate structural hazard are directed to the ACCESS Integration Manager, unless otherwise noted.

- R-1.** Enforce as a mission rule that DC-8 wingtip vortices be made visible by rolled-up exhaust contrail for all near-field and far-field experiments. *(F-1, F-8, O-2)*
- R-2.** Conduct pre-experiment flight tests in near- and far-field zones, dedicated to developing pilot proficiency in avoiding wake vortices. *(F-2, F-3, F-4, F-5, F-6, F-21, F-22, F-23, F-24, O-1)*
- Candidate methods, procedures, and activities are listed in Section 7.3.1.
- R-3.** Consider adding instrumentation to the Falcon 20 and/or the DC-8 to improve vortex detection and avoidance or to monitor structural health. *(F-7, O-3)*
- Candidate items are listed in Table 7.3-1.
- R-4.** Consider the independent static loads results and maps calculated for 1-, 2-, and 3.5-percent core sizes. *(F-9, F-10, F-11, F-12, F-13)*
- Results are summarized in Tables 7.2-4 and 7.2-5.
- R-5.** Consider the independent dynamic simulation results, with identified assumptions and limitations, of the Falcon 20 response to a wake vortex encounter when assessing the aircraft near-field and far-field structural risks from an inadvertent wake vortex encounter. *(F-14, F-15, F-16, F-17, F-18, F-19, F-20)*
- R-6.** Do not conduct far-field sampling behind “target of opportunity” commercial transport aircraft in controlled airspace prior to conducting pre-experiment flight tests due to the uncharacterized risk of inadvertent wake vortex encounter. *(F-25)*
- R-7.** Enforce as a mission rule that Falcon 20 pilots minimize control inputs if an inadvertent wake vortex encounter appears imminent or is indicated to be imminent by instrumentation (if any); allow the vortex wake to move the Falcon naturally out of the vortex flow and then stabilize the aircraft. *(F-26, O-4, O-5, O-6)*
- R-8.** ACCESS Falcon 20 pilots, after an inadvertent wake vortex encounter, once clear of the vortex perform a rapid and positive centering of the flight controls to minimize

|  |   |  |                        |
|--|---|--|------------------------|
|                 | <b>NASA Engineering and Safety Center<br/>Technical Assessment Report</b> | Document #:<br><b>NESC-RP-12-00822</b> | Version:<br><b>1.0</b> |
| Title:<br><b>Probing Aircraft Flight Test Hazard Mitigation<br/>for the ACCESS Research Team</b> |   | Page #:<br>110 of 118                  |                        |

excursions in sideslip and angle of attack and to reduce the likelihood of spin entry through inertial coupling. (*F-27*)

- R-9.** Pursue the request for quote from the Falcon 20 manufacturer to assess project and NESC loads analyses results against aircraft DLLs prior to an expected 2014 test campaign. (*F-8, F-28, O-3, O-7*)

## 9.0 Alternate Viewpoint

There were no alternate viewpoints identified during the course of this assessment by the NESC team or the NRB quorum.

## 10.0 Other Deliverables

- Vortex-induced aerodynamic coefficients and component loads, summarized in Appendix E, with data delivered in Microsoft Excel spreadsheets.
- Tabulated aerodynamic coefficients and component loads for the simulations, summarized in Appendix F, with data provided in Microsoft Excel spreadsheets.
- Six simulation animation files.

## 11.0 Lessons Learned

No applicable lessons learned were identified for entry into the NASA Lessons Learned Information System as a result of this assessment.

## 12.0 Recommendations for NASA Standards and Specifications


No recommendations for NASA standards and specifications were identified as a result of this assessment.

## 13.0 Definition of Terms

**Corrective Actions** Changes to design processes, work instructions, workmanship practices, training, inspections, tests, procedures, specifications, drawings, tools, equipment, facilities, resources, or material that result in preventing, minimizing, or limiting the potential for recurrence of a problem.

**Finding** A relevant factual conclusion and/or issue that is within the assessment scope and that the team has rigorously based on data from their independent analyses, tests, inspections, and/or reviews of technical documentation.

**Lessons Learned** Knowledge, understanding, or conclusive insight gained by experience that may benefit other current or future NASA programs and projects.


|  |   |                         |            |
|--|---|-------------------------|------------|
|       | <b>NASA Engineering and Safety Center<br/>Technical Assessment Report</b> | Document #:             | Version:   |
|  |   | <b>NESC-RP-12-00822</b> | <b>1.0</b> |
| Title:   |   | Page #:                 |            |
| <b>Probing Aircraft Flight Test Hazard Mitigation<br/>for the ACCESS Research Team</b> |   | 111 of 118              |            |

|                      |   |
|----------------------|---|
|                      | The experience may be positive, as in a successful test or mission, or negative, as in a mishap or failure.   |
| Observation          | A noteworthy fact, issue, and/or risk, which may not be directly within the assessment scope, but could generate a separate issue or concern if not addressed. Alternatively, an observation can be a positive acknowledgement of a Center/Program/Project/Organization’s operational structure, tools, and/or support provided.  |
| Problem              | The subject of the independent technical assessment.  |
| Proximate Cause      | The event(s) that occurred, including any condition(s) that existed immediately before the undesired outcome, directly resulted in its occurrence and, if eliminated or modified, would have prevented the undesired outcome.   |
| Recommendation       | A proposed measurable stakeholder action directly supported by specific Finding(s) and/or Observation(s) that will correct or mitigate an identified issue or risk.   |
| Root Cause           | One of multiple factors (events, conditions, or organizational factors) that contributed to or created the proximate cause and subsequent undesired outcome and, if eliminated or modified, would have prevented the undesired outcome. Typically, multiple root causes contribute to an undesired outcome.   |
| Supporting Narrative | A paragraph, or section, in an NESC final report that provides the detailed explanation of a succinctly worded finding or observation. For example, the logical deduction that led to a finding or observation; descriptions of assumptions, exceptions, clarifications, and boundary conditions. Avoid squeezing all of this information into a finding or observation |


## 14.0 Acronyms List

|                 |   |
|-----------------|---|
| ACCESS          | Alternative Fuel Effects on Contrails & Cruise Emissions    |
| ACLAIM          | Airborne Coherent LIDAR for Advanced In-Flight Measurements |
| AFF             | Autonomous Formation Flight                                 |
| AFFTC           | Air Force Flight Test Center                                |
| ARMD            | Aeronautics Research Mission Directorate                    |
| CAPS            | Cloud, Aerosol, and Precipitation Spectrometer              |
| CDP             | Cloud Droplet Probe   |
| CFD             | Computational Fluid Dynamics                                |
| CO              | Carbon Monoxide   |
| CO <sub>2</sub> | Carbon Dioxide  |
| CONCERT         | Contrail and Cirrus Experiment                              |




|  |   |  |                        |
|--|---|--|------------------------|
|                 | <b>NASA Engineering and Safety Center<br/>Technical Assessment Report</b> | Document #:<br><b>NESC-RP-12-00822</b> | Version:<br><b>1.0</b> |
| Title:<br><b>Probing Aircraft Flight Test Hazard Mitigation<br/>for the ACCESS Research Team</b> |   | Page #:<br>112 of 118                  |                        |

|                  |   |
|------------------|---|
| CPC              | Condensation Particle Counter   |
| CRDS             | Cavity Ring-down (Spectroscopy)   |
| DLH              | Diode Laser Hygrometer  |
| DLL              | Design Limit Load   |
| DLR              | Deutsches Zentrum für Luft- und Raumfahrt (German Aerospace Center)     |
| DFRC             | Dryden Flight Research Center   |
| DOF              | Degrees of Freedom  |
| EOW              | Empty Operating Weight  |
| FAA              | Federal Aviation Administration   |
| GPS              | Global Positioning System   |
| GRC              | Glenn Research Center   |
| H <sub>2</sub> O | Water   |
| ICAO             | International Civil Aviation Organization                               |
| INS              | Inertial Navigation System  |
| INU              | Initial Navigation Unit   |
| IRS              | Inertial Reference System   |
| KTAS             | knots true airspeed   |
| LaRC             | Langley Research Center   |
| LIDAR            | Laser Imaging Detection and Ranging                                     |
| MTOW             | Maximum Takeoff Weight  |
| NDIR             | Nondispersive Infrared  |
| NEAR             | Nielsen Engineering and Research  |
| NESC             | NASA Engineering and Safety Center                                      |
| nm               | nautical miles  |
| NO               | Nitric Oxide  |
| NO <sub>2</sub>  | Nitrogen Dioxide  |
| NRB              | NESC Review Board   |
| O <sub>3</sub>   | Ozone   |
| OEW              | Operating Empty Weight  |
| PIM              | Project Integration Manager   |
| PMS              | Particle Measurement System   |
| POLINAT          | Pollution from Aircraft Emissions in the North Atlantic Flight Corridor |
| SP2              | Single Particle Soot Photometer   |
| SRR              | Systems Requirements Review   |
| SURF             | Sky Surfing for Fuel Economy  |
| TCAS             | Traffic Alert and Collision Avoidance System                            |
| UHSAS            | Ultra-high Sensitivity Aerosol Spectrometer                             |
| U.S.             | United States   |
| USAF             | United States Air Force   |
| VFR              | Visual Flight Rules   |


|  |   |   |                        |
|--|---|---|------------------------|
|                 | <b>NASA Engineering and Safety Center<br/>Technical Assessment Report</b> | Document #:<br><b>NESC-RP-<br/>12-00822</b> | Version:<br><b>1.0</b> |
| Title:<br><b>Probing Aircraft Flight Test Hazard Mitigation<br/>for the ACCESS Research Team</b> |   | Page #:<br>113 of 118                       |                        |

## 15.0 References


1. *Douglas DC-8 Maintenance Manual*, Douglas Aircraft Company, Long Beach, CA, 1959.
2. "HU-25 Weight and Balance Manual," U.S. Coast Guard, CGTO 1U-25-5, September 15, 2007.
3. "Flight Manual, U.S. Coast Guard Series HU-25 Aircraft," CGTO 1U-25A-1, Change 1, May 11, 2009.
4. "Maintenance Manual, U.S. Coast Guard Model HU-25A Falcon Jet," CGTO 1U-25A-2, Change 2, August 15, 2011.
5. "Structural Repair Manual, U.S. Coast Guard Model HU-25 Falcon Jet," CGTO 1U-25A-3, December 1, 2009.
6. Brown, A. P. and Bastian, M. "A Feasibility Study on the Inflight Measurement of Enroute Wake Vortex Characteristics," AIAA-2004-5366, August 2004.
7. Proctor, F. H.: "Model for Wind Distribution in the Wake of a DC-8 Presentation," July 2, 2012.
8. Proctor, F. H., Ahmad, N. N., Switzer, G. S., Limon Duparcmeur, F. M.: "Three-Phased Wake Vortex Decay," AIAA 2010-7991, August 2010.
9. Vicroy, D.: "Aerodynamic Loads Presentation," August 14, 2012.
10. "Falcon HU-25 Stabilizer and Fin Analysis Study Presentation," Mike Pagnotta, August 13, 2012.
11. Breitsamter, C.: "Wake Vortex Characteristics of Transport Aircraft," *Progress in Aerospace Sciences*, Vol. 47, 2011, pp. 89–134.
12. "Aircraft Wake Turbulence," Federal Aviation Administration, U.S. Department of Transportation, Report: AC90-23E, October 1, 1991.
13. Rossow, V.: "Lift-Generated Vortex Wakes of Subsonic Transport Aircraft," *Progress in Aerospace Sciences*, Vol. 35, 1999, pp. 507–660.
14. Gerz, T., Holzaphel, F., and Darracq, D.: "Commercial Aircraft Wake Vortices," *Progress in Aerospace Sciences*, Vol. 38, 2002, pp. 181–202.
15. Delisi, D. P., Greene, G. C., Robins, R. E., Vicroy, D. C., Wang, F. Y.: "Aircraft Wake Vortex Core Size Measurements," AIAA-2003-3811, June 2003.
16. Proctor, F., Ahmad, N., Switzer, G., and Duparcmeur, F.: "Three-Phased Wake Vortex Decay," Presented at the AIAA Guidance, Navigation, and Control Conference, Toronto, Canada, Augusts 2–5, 2010.

|  |   |   |                        |
|--|---|---|------------------------|
|                 | <b>NASA Engineering and Safety Center<br/>Technical Assessment Report</b> | Document #:<br><b>NESC-RP-<br/>12-00822</b> | Version:<br><b>1.0</b> |
| Title:<br><b>Probing Aircraft Flight Test Hazard Mitigation<br/>for the ACCESS Research Team</b> |   | Page #:<br>114 of 118                       |                        |

17. Holzapfel, F.: “Probabilistic Two-Phase Wake Vortex Decay and Transport Model,” *Journal of Aircraft*, Vol. 40, No. 2, March–April 2003.
18. De Visscher, I., Winckelmans, G., Lonfils, T., Bricteux, L., Duponcheel, M., and Bourgeois, N.: “The Wake4D Simulation Platform for Predicting Aircraft Wake Vortex Transport and Decay: Description and Examples of Application,” Presented at the AIAA Guidance, Navigation, and Control Conference, Toronto, Canada, August 2–5, 2010.
19. Rossow, V. and Brown, A.: “Effect of Jet-Exhaust Streams on Structure of Vortex Wakes,” *Journal of Aircraft*, Vol. 47, No. 3, May–June 2010, pp. 1076–1083.
20. Economon, T.: “Effects of Wake Vortices on Commercial Aircraft,” AME 48491, Department of Aerospace and Mechanical Engineering, Notre Dame University, December 6, 2006.
21. Gerz, T. and Schwarz, C.: “The DLR Project Wetter & Fliegen (Weather & Flying),” DLR Research Centres, Oberpfaffenhofen, Braunschweig, Gottingen, and Hamburg, Germany, ISSN 1434-8454, 2012.
22. Rossow, V. and Brown, A.: “Separation of Lift-Generated Vortex Wakes Into Two Diverging Parts,” NASA TM-2010-216400, 2010.
23. Rossow, V. J.: Initiation of Long-Wave Instability of Vortex Pairs at Cruise Altitudes, NASA TM–2011-216420, February 2011.
24. Rose, W. C. and Cooley, J. M.: “Data Analysis for Wake Turbulence Measurements behind an A-3 Aircraft,” Final report prepared in support of Contract N00014-85-C-2639, Rose Engineering & Research, Inc., February 1987.
25. “C-130 Wake Encounter Flight Tests,” National Aeronautics and Space Administration video, 1991.
26. “Encounter with Wake Turbulence: Air Canada Airbus A-319-114 C-GBHZ, Washington State, United States, 10 January 2008,” Report Number A08W0007, Transportation Safety Board of Canada, 2008.
27. Hohne, G., Fuhmann, M., and Luckner, R.: “Critical Wake Vortex Encounter Scenarios,” *Aerospace Science and Technology*, Vol. 8, 2004, pp. 689–701.
28. “The Wings of the Web: airliners.net,” URL: <http://www.airliners.net/>, accessed September 2012.
29. “747-400 Airplane Characteristics for Airport Planning,” Boeing Commercial Airplanes, D6-58326-1, December 2002.
30. “A340-500/-600 Airplane Characteristics for Airport Planning,” Airbus S.A.S., January 2012.
31. “An-124-100 Russian,” URL: <http://an124.com/>, accessed September 2012.


|  |   |   |                        |
|--|---|---|------------------------|
|                 | <b>NASA Engineering and Safety Center<br/>Technical Assessment Report</b> | Document #:<br><b>NESC-RP-<br/>12-00822</b> | Version:<br><b>1.0</b> |
| Title:<br><b>Probing Aircraft Flight Test Hazard Mitigation<br/>for the ACCESS Research Team</b> |   | Page #:<br>115 of 118                       |                        |

32. Andrews, W. H., Robinson, G. H., and Larson, R. R.: "Exploratory Flight Investigation of Aircraft Response to the Wing Vortex Wake Generated by Jet Transport Aircraft," NASA TN D-6655, March 1972.
33. Lesieutre, D. J. and Perkins, S. C., Jr.: "Store Separation Prediction Program *STRLNCH*, Version December 2008, NEAR TR 655, Nielsen Engineering & Research, Inc., Mountain View, CA, December 2008.
34. Dillenius, M. F. E., Love, J. F., Hegedus, M. C., and Lesieutre, D. J.: "Program *STRLNCH* for Simulating Missile Launch from a Maneuvering Parent Aircraft at Subsonic Speed," NEAR TR 509, Nielsen Engineering & Research, Mountain View, CA, 1996.
35. Dillenius, M. F. E., Goodwin, F. K., and Nielsen, J. N.: "Analytical Prediction of Store Separation Characteristics from Subsonic Aircraft," *Journal of Aircraft*, Vol. 12, No. 10, October 1975, pp. 812-818.
36. Dillenius, M. F. E., Goodwin, F. K., and Nielsen, J. N.: "Extension of the Method for Predicting Six-Degree-of-Freedom Store Separation Trajectories at Speeds up to the Critical Speed to Include a Fuselage with Noncircular Cross Section, Volume I - Theoretical Methods and Comparisons with Experiment," AFFDL-TR-74-130, AF Flight Dynamics Lab., Wright-Patterson AFB, OH, March 1974.
37. Lesieutre, D. J.: "Detailed Aerodynamic Prediction Program MISDL, Code User's Manual, Version July 2008," NEAR TR 654, Nielsen Engineering & Research, Inc., Mountain View, CA, November 2008.
38. Lesieutre, D. J., Dillenius, M. F. E., and Lesieutre, T. O.: "Multidisciplinary Design Optimization of Missile Configurations and Fin Planforms for Improved Performance," 7th Symposium on Multidisciplinary Analysis and Optimization, St. Louis, MO, September 1998.
39. Lesieutre, D. J., Dillenius, M. F. E., Love, J. F., and Perkins, S. C., Jr.: "Nonlinear Engineering-Level Missile Aerodynamics Prediction Methods *MISL3*, *MISDL*, and *NEARZEUSIN/ZEUSBL*," CEAS Aerospace Aerodynamics Research Conference, London, UK, June 10-12, 2003.
40. Lesieutre, D. J., Love, J. F., and Dillenius, M. F. E.: "Prediction of the Nonlinear Aerodynamic Characteristics of Tandem-Control and Rolling-Tail Missiles," AIAA 2002-4511, August 2002.
41. "Mystère (Falcon) 20 Series with Fairings, Calculation of Loads, DTX-37713," Parts 1 and 2, Dassault Aviation, April 1966.


|  |   |  |                        |
|--|---|--|------------------------|
|                 | <b>NASA Engineering and Safety Center<br/>Technical Assessment Report</b> | Document #:<br><b>NESC-RP-12-00822</b> | Version:<br><b>1.0</b> |
| Title:<br><b>Probing Aircraft Flight Test Hazard Mitigation<br/>for the ACCESS Research Team</b> |   | Page #:<br>116 of 118                  |                        |

42. Hallberg, E., Cenko, A., and Dillenius, M. F. E.: "Store Separation Trajectory Simulation for the High Speed Anti-Radiation Demonstrator (HSAD) from the F-4 Aircraft," AIAA 2008-6381, 2008.
43. Lesieutre, D. J., Dillenius, M. F. E., and Gjestvang, J. A.: "Store Separation Simulation of the Penguin Missile from Helicopters," Paper Number 9, Presented at NATO-RT0 Symposium on Innovative Missile Systems, Amsterdam, The Netherlands, May 2006, RTO-MP-AVT-135.
44. Love, J. F., Perkins, S. C., Jr., Lesieutre, D. J., and Dillenius, M. F. E.: "F-18C/D Input Models for Use With STRLNCH Store Separation Code Updated With Automated Wing Camber and Thickness Calculation Procedure," NEAR TR 585, Nielsen Engineering & Research, Inc., Mountain View, CA, February 2003.
45. Hegedus, M. C., Love, J. F., and Dillenius, M. F. E.: "Enhancements/ Modifications to Supersonic Portion of STRLNCH Store Separation Program for Application to F-22 Aircraft," NEAR TR 573, Nielsen Engineering & Research, Inc., Mountain View, CA, May 2002.
46. Dillenius, M. F. E., Lesieutre, D. J., Perkins, S. C., Jr., and Love, J. F.: "Prediction of Nonlinear Missile Aerodynamics with Applications Including Store Separation," RTO-MP-5, Missile Aerodynamics, November 1998.
47. Dillenius, M. F. E., Perkins, S. C., Jr., and Lesieutre, D. J.: "Engineering Level Methods for Carriage Loads, High-Alpha Launch from Pitching Aircraft, and Submunition Aerodynamics," AGARD CP-570, Aerodynamics of Store Integration and Separation, February 1996, pp. 10-1-10-9.
48. Mendenhall, M. R., Lesieutre, T. O., Lesieutre, D. J., and Dillenius, M. F. E.: "Carriage and Release Aerodynamics of the Pegasus Air-Launched Space Booster," AGARD CP-570, Aerodynamics of Store Integration and Separation, February 1996, pp. 11-1-11-12.
49. Dillenius, M. F. E., Lesieutre, D. J., Whittaker, C. H., and Lesieutre, T. O.: "New Application of Engineering Level Missile Aerodynamics and Store Separation Prediction Methods," AIAA 94-0028, January 1994.
50. Dillenius, M. F. E., Perkins, S. C., Jr., Johnson, D. L., and Lesieutre, D. J.: "Engineering Level Predictions for External Store Separation and Submunition Aerodynamics," *Store Carriage, Integration, and Release Proceedings*, Royal Aeronautical Society, April 1990, pp. 18.1-18.21.
51. Mendenhall, M. R., Lesieutre, D. J., Caruso, S. C., Dillenius, M. F. E., and Kuhn, G. D.: "Aerodynamic Design of Pegasus - Concept to Flight with CFD," AIAA 91-0190, January 1991.



|  |   |   |                        |
|--|---|---|------------------------|
|                 | <b>NASA Engineering and Safety Center<br/>Technical Assessment Report</b> | Document #:<br><b>NESC-RP-<br/>12-00822</b> | Version:<br><b>1.0</b> |
| Title:<br><b>Probing Aircraft Flight Test Hazard Mitigation<br/>for the ACCESS Research Team</b> |   | Page #:<br>117 of 118                       |                        |

52. Dillenius, M. F. E., Johnson, D. L., and Torres, T. O.: "Support for Analysis of Store Release from the F-14A Aircraft," NEAR TR 409, Nielsen Engineering & Research, Mountain View, CA, December 1989.
53. Smith, Charles A.: "Theoretical Separation Characteristics of the FACC Advanced Medium Range Air to Air Missile (AMRAAM) from the F-15 Aircraft," NEAR TR 162, Nielsen Engineering & Research, Mountain View, CA, 1978.
54. Dillenius, M. F. E., Lesieutre, D. J., Perkins, S. C., Jr., Jeter, E. L., and Schulz, J. C.: "Methodology for Aerostructural Analysis of a Missile Attached to a Maneuvering Aircraft," AIAA 89-0480, January 1989.
55. Perkins, S. C., Jr., Mendenhall, M. R., and Dillenius, M. F. E.: "Analytical Investigation of Two Subsonic Store/ Aircraft Configurations," NEAR TR 378, Nielsen Engineering & Research, Mountain View, CA, April 1987.
56. Lesieutre, D. J. and Dillenius, M. F. E.: "AV-8B Aircraft Mathematical Model for NEAR Subsonic Six-Degree-of-Freedom (6-DOF) Store Separation Code," NEAR TR 368, Nielsen Engineering & Research, Mountain View, CA, October 1986.
57. Goodwin, F. K. and Smith, C. A.: "Theoretical Separation Characteristics of Two Conceptual Solid Rocket Booster Parachute Test Units from the B-52 Aircraft," NEAR TR 114, Nielsen Engineering & Research, Mountain View, CA, August 1976.
58. Lesieutre, D. J.: "MISL3 Aerodynamic Analysis for Finned Vehicles with Axisymmetric Bodies," NEAR TR 654, Nielsen Engineering & Research, Inc., Mountain View, CA, November 2008.
59. Lesieutre, D. J., Love, J. F., and Dillenius, M. F. E.: "Recent Applications and Improvements to the Engineering-Level Aerodynamic Prediction Software MISL3," AIAA 2002-0275, January 2002.
60. Roskam, J.: *Airplane Design Part V: Component Weight Estimation*, Roskam Aviation and Engineering Corporation, Lawrence, KS, USA, 1985.
61. *Jane's All the World's Aircraft: 2008-2009*, Paul Jackson, Ed., Jane's Information Group Limited, Cambridge University Press, Great Britain, UK, 2008.
62. Brandon, J. M., Jordan, F. L., Jr., Stuever, R. A., and Buttrill, C. W.: "Application of Wind Tunnel Free-Flight Technique for Wake Vortex Encounters," NASA TP-3672, November 1997.
63. Burken, J. J., Maine, T. A., Burcham, F. W., Jr., Kahler, J. A.: "Longitudinal Emergency Control System using Thrust Modulation Demonstration on an MD-11 Airplane," NASA TM 104318, July 1996.

|  |   |  |                        |
|--|---|--|------------------------|
|                 | <b>NASA Engineering and Safety Center<br/>Technical Assessment Report</b> | Document #:<br><b>NESC-RP-12-00822</b> | Version:<br><b>1.0</b> |
| Title:<br><b>Probing Aircraft Flight Test Hazard Mitigation<br/>for the ACCESS Research Team</b> |   | Page #:<br>118 of 118                  |                        |

64. Yechout, T. R., Buscher, A. J., Rosza, J. D., and Rolling, A. J.: “Wind Tunnel Investigation of A-10 Engine/Airframe Compatibility,” U.S. Air Force Academy, Department of Aeronautics, USAFA DFAN TR 1109, December 2011 (For Official Use Only).
65. “In-Flight Separation of Vertical Stabilizer American Airlines Flight 587 Airbus Industrie A300-605R, N14053 Belle Harbor, New York November 12, 2001,” Aircraft Accident Report, National Transportation Safety Board, NTSB/AAR-04/04, PB2004-910404, Notation 7439B, October 26, 2004.
66. Roth, D. and Small, J., Jr.: “HU-25A AIREYE Safety of Flight Test Program Performance and Flying Qualities Evaluation,” AFFTC-TR-84-1, April 1984.

## **16.0 Volume II. Appendices (separate volume)**

- Appendix A. Initial Evaluation
- Appendix B. ACCESS System Requirements Review (June 2012)
- Appendix C. NESC Team Kickoff
- Appendix D. ACCESS Project Analyses Inbriefing: Proctor, Vicroy, and Pagnatta Analyses
- Appendix E. Tabulated Vortex-Induced Aerodynamic Coefficients and Component Loads
- Appendix F. STRLNCH Simulations Component Loads Results
- Appendix G. DLR Teleconference Q&A
- Appendix H. Preliminary Stakeholder Outbrief
- Appendix I. ACCESS Pre-Experiment Technical Briefing (To DFRC Independent Review Team), February 8, 2013
- Appendix J. 2013 Pilot Proficiency Practice Flight Tests Lessons Learned

**REPORT DOCUMENTATION PAGE**

*Form Approved  
OMB No. 0704-0188*

The public reporting burden for this collection of information is estimated to average 1 hour per response, including the time for reviewing instructions, searching existing data sources, gathering and maintaining the data needed, and completing and reviewing the collection of information. Send comments regarding this burden estimate or any other aspect of this collection of information, including suggestions for reducing this burden, to Department of Defense, Washington Headquarters Services, Directorate for Information Operations and Reports (0704-0188), 1215 Jefferson Davis Highway, Suite 1204, Arlington, VA 22202-4302. Respondents should be aware that notwithstanding any other provision of law, no person shall be subject to any penalty for failing to comply with a collection of information if it does not display a currently valid OMB control number.  
**PLEASE DO NOT RETURN YOUR FORM TO THE ABOVE ADDRESS.**

|  |                    |                     |   |                            |   |  |
|--|--------------------|---------------------|---|----------------------------|---|--|
| <b>1. REPORT DATE (DD-MM-YYYY)</b><br>01-05 - 2013   |                    |                     | <b>2. REPORT TYPE</b><br>Technical Memorandum |                            | <b>3. DATES COVERED (From - To)</b><br>August 2012 - April 2013                 |  |
| <b>4. TITLE AND SUBTITLE</b><br>Probing Aircraft Flight Test Hazard Mitigation for the Alternative Fuel Effects on Contrails & Cruise Emissions (ACCESS) Research Team   |                    |                     |   |                            | <b>5a. CONTRACT NUMBER</b>  |  |
|  |                    |                     |   |                            | <b>5b. GRANT NUMBER</b>   |  |
|  |                    |                     |   |                            | <b>5c. PROGRAM ELEMENT NUMBER</b>   |  |
| <b>6. AUTHOR(S)</b><br>Kelly, Michael J.   |                    |                     |   |                            | <b>5d. PROJECT NUMBER</b>   |  |
|  |                    |                     |   |                            | <b>5e. TASK NUMBER</b>  |  |
|  |                    |                     |   |                            | <b>5f. WORK UNIT NUMBER</b><br>869021.05.07.08.03                               |  |
| <b>7. PERFORMING ORGANIZATION NAME(S) AND ADDRESS(ES)</b><br>NASA Langley Research Center<br>Hampton, VA 23681-2199  |                    |                     |   |                            | <b>8. PERFORMING ORGANIZATION REPORT NUMBER</b><br><br>L-20268 NESC-RP-12-00822 |  |
| <b>9. SPONSORING/MONITORING AGENCY NAME(S) AND ADDRESS(ES)</b><br>National Aeronautics and Space Administration<br>Washington, DC 20546-0001   |                    |                     |   |                            | <b>10. SPONSOR/MONITOR'S ACRONYM(S)</b><br><br>NASA                             |  |
|  |                    |                     |   |                            | <b>11. SPONSOR/MONITOR'S REPORT NUMBER(S)</b><br>NASA/TM-2013-217995/Volume I   |  |
| <b>12. DISTRIBUTION/AVAILABILITY STATEMENT</b><br>Unclassified - Unlimited<br>Subject Category 03 Air Transportation and Safety<br>Availability: NASA CASI (443) 757-5802  |                    |                     |   |                            |   |  |
| <b>13. SUPPLEMENTARY NOTES</b>   |                    |                     |   |                            |   |  |
| <b>14. ABSTRACT</b><br>The Alternative Fuel Effects on Contrails & Cruise Emissions (ACCESS) Project Integration Manager requested in July 2012 that the NASA Engineering and Safety Center (NESC) form a team to independently assess aircraft structural failure hazards associated with the ACCESS experiment and to identify potential flight test hazard mitigations to ensure flight safety. The ACCESS Project Integration Manager subsequently requested that the assessment scope be focused predominantly on structural failure risks to the aircraft empennage (horizontal and vertical tail). This report contains the outcome of the NESC assessment. |                    |                     |   |                            |   |  |
| <b>15. SUBJECT TERMS</b><br>ACCESS; NASA Engineering and Safety Center; Wake vortices; Engine exhaust plumes; Near field; Far field  |                    |                     |   |                            |   |  |
| <b>16. SECURITY CLASSIFICATION OF:</b>   |                    |                     | <b>17. LIMITATION OF ABSTRACT</b>             | <b>18. NUMBER OF PAGES</b> | <b>19a. NAME OF RESPONSIBLE PERSON</b>  |  |
| <b>a. REPORT</b>   | <b>b. ABSTRACT</b> | <b>c. THIS PAGE</b> |   |                            | STI Help Desk (email: help@sti.nasa.gov)  |  |
| U  | U                  | U                   | UU  | 123                        | <b>19b. TELEPHONE NUMBER (Include area code)</b><br>(443) 757-5802              |  |